

# A window on infrared QCD with small expansion parameters

Marcela Peláez,<sup>1</sup> Urko Reinosa,<sup>2</sup> Julien Serreau,<sup>3</sup> Matthieu Tissier,<sup>4</sup> and Nicolás Wschebor<sup>1</sup>

<sup>1</sup>*Instituto de Física, Facultad de Ingeniería, Universidad de la República, J.H.y Reissig 565, 11000 Montevideo, Uruguay.*

<sup>2</sup>*Centre de Physique Théorique, CNRS, Ecole polytechnique, IP Paris, F-91128 Palaiseau, France.*

<sup>3</sup>*Université de Paris, CNRS, Astroparticule et Cosmologie, F-75013 Paris, France.*

<sup>4</sup>*LPTMC, Laboratoire de Physique Théorique de la Matière Condensée, CNRS UMR 7600, Sorbonne Université, boîte 121, 4 pl. Jussieu, 75252 Paris Cedex 05, France.*

(Dated: June 9, 2021)

Lattice simulations of the QCD correlation functions in the Landau gauge have established two remarkable facts. First, the coupling constant in the gauge sector remains finite and moderate at all scales, suggesting that some kind of perturbative description should be valid down to infrared momenta. Second, the gluon propagator reaches a finite nonzero value at vanishing momentum, corresponding to a gluon screening mass. We review recent studies which aim at describing the long-distance properties of Landau gauge QCD by means of the perturbative Curci-Ferrari model. The latter is the simplest deformation of the Faddeev-Popov Lagrangian in the Landau gauge that includes a gluon screening mass at tree-level. There are, by now, strong evidences that this approach successfully describes many aspects of the infrared QCD dynamics. In particular, several correlation functions were computed at one- and two-loop orders and compared with *ab-initio* lattice simulations. The typical error is of the order of ten percent for a one-loop calculation and drops to few percents at two loops. We review such calculations in the quenched approximation as well as in the presence of dynamical quarks. In the latter case, the spontaneous breaking of the chiral symmetry requires to go beyond a coupling expansion but can still be described in a controlled approximation scheme in terms of small parameters. We also review applications of the approach to nonzero temperature and chemical potential.

## Contents

<b>I. The ultraviolet Dr. Jekyll and the infrared Mr. Hyde</b>	2
<b>II. QCD and gauge fixing</b>	5
A. The QCD lagrangian	5
B. Gauge fixing	5
C. The Gribov ambiguity	7
<b>III. Yang-Mills correlation functions: previous results</b>	7
A. Correlation functions from continuum approaches	8
B. Lattice results: propagators and three-point vertices	9
<b>IV. The Curci-Ferrari model</b>	11
A. The Curci-Ferrari Lagrangian	11
B. Symmetries and renormalisability	12
C. Unitarity	12
D. A minimal deformation of the Faddeev-Popov Lagrangian	13
<b>V. Yang-Mills Correlation functions in the vacuum</b>	14
A. Renormalisation and renormalisation group	14
B. Fitting procedure	16
C. Yang-Mills propagators	17
D. Yang-Mills three-point functions	19
1. The three-gluon vertex	20
2. The ghost-gluon vertex	21
<b>VI. Dynamical quarks</b>	23
A. Propagators.	24
B. The quark-gluon vertex	26
C. The rainbow-improved perturbative expansion and the spontaneous breaking of chiral symmetry.	28

D. Hadronic observables	31
<b>VII. Nonzero temperature and density: The confinement-deconfinement transition</b>	<b>32</b>
A. The Landau-DeWitt gauge	32
B. The background-field effective potential in perturbation theory	34
C. The issue of massless unphysical modes in the confined phase	36
D. Center-symmetric background field approach	37
E. Dynamical quarks	38
F. Propagators	39
<b>VIII. Results in the Minkowskian domain</b>	<b>41</b>
<b>IX. Open questions</b>	<b>42</b>
<b>X. Conclusions</b>	<b>43</b>
<b>Acknowledgments</b>	<b>44</b>
<b>References</b>	<b>44</b>

## I. THE ULTRAVIOLET DR. JEKYLL AND THE INFRARED MR. HYDE

Since the discovery of asymptotic freedom in the early 70’s [Pol73, GW73], a plethora of experimental and theoretical works have firmly established quantum chromodynamics (QCD) as the fundamental theory of strong interactions. QCD seems paradoxical at first sight, however, being a description of physically observable objects (the hadrons) in terms of unobservable ones (the quarks and the gluons). The former are the relevant excitations at length scales larger than about a Fermi whereas the latter appear to be the relevant degrees of freedom at smaller distances [Wei96]. As is well-known, the coexistence of these two, infrared (IR) and ultraviolet (UV) faces of the theory poses a major difficulty for the detailed understanding of the properties and interactions of hadrons. On the theory side, the dichotomy takes the form of an essentially perturbative regime at short distances and/or UV momenta versus a nonperturbative IR regime. This picture actually extends to a wide class of QCD-like theories with various quark contents, including the pure Yang-Mills (YM) case, with no dynamical quarks, known as the quenched limit. It is based, on the one hand, on the phenomenon of asymptotic freedom at UV scales and, on the other hand, on the fact that standard perturbation theory predicts its own failure at IR momenta in the form of a Landau pole, a finite energy scale  $\Lambda_{\text{QCD}} \sim 300$  MeV at which the coupling constant diverges.

Some essential aspects of the IR regime can be tackled from first principles using numerical simulations based on lattice gauge theory. In the QCD case, for instance, these simulations are able to reproduce the hadron spectrum with great accuracy using only the coupling constant and the quark masses as input parameters [FH12]. More generally, lattice simulations give strong theoretical support in favor of two fundamental phenomena at IR scales, namely confinement—the fact that the physical excitations of the theory are massive colourless objects—and the dynamical breaking of the chiral symmetry for theories with not too many light quark flavours, including QCD [D<sup>+</sup>14]. Lattice simulations also study the rich phase structure of such theories under extreme conditions of temperature [BFH<sup>+</sup>14, B<sup>+</sup>14] and density [Sex14, Sco16, GL16, AAJS16]—relevant for quark-gluon plasma physics in high-energy nuclear collisions, astrophysics of ultra compact stars, or early-Universe cosmology—with, in particular, the possibility of a confinement-deconfinement transition and of a restoration of the chiral symmetry, depending on the details of the quark content.

Although lattice simulations are by far the most powerful tool to explore the IR sector of such theories, they remain limited in at least two ways. First, they are based on the Monte Carlo sampling technique, which requires a positive definite measure of the (discretized) functional integral. They are thus essentially limited, so far, to the calculation of static quantities, that can be accessed from the Euclidean action when the latter is real. Typical dynamical quantities, which involve Minkowskian momenta (cross sections, transport coefficients, etc.), or cases where the Euclidean action is complex (for instance for some theories—including QCD—at nonzero chemical potential<sup>1</sup>) are still largely out of reach to present-day lattice technology. The second important limitation is that Monte Carlo simulations are, to a

---

<sup>1</sup> This problem is usually known in the literature as the “sign problem”.

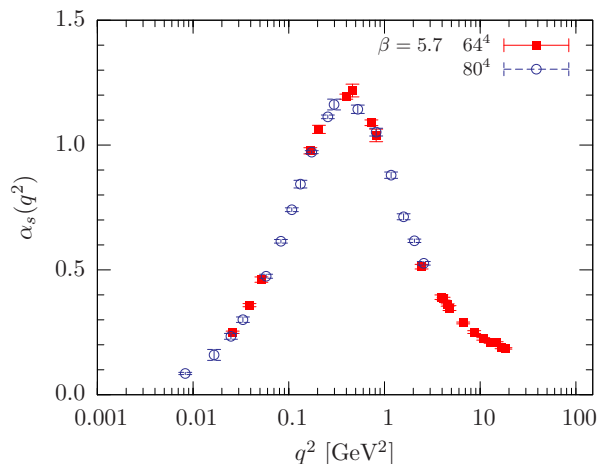


FIG. 1: Lattice results for the Landau gauge Taylor coupling  $\alpha_S(q^2)$  in the SU(3) YM theory. Figure from Ref. [BIMPS09].

large extent, a black box from which it is not easy to pinpoint which are the fundamental phenomena at play. For instance, the basic dynamics of confinement remains, to date, largely unknown.

Alternatives to lattice methods typically involve functional quantum field theory techniques, such as Dyson-Schwinger equations (DSE) [vSAH97, AB98, AvS01, LvS02, FA02, FP07, FMP09, CFM<sup>+</sup>16], the functional renormalisation group (FRG) [EHW98, PLNvS04, FG04, FMP09, CFM<sup>+</sup>16], and the variational Hamiltonian approach (VHA) [SLR06]. Although those, in principle, do not suffer from the limitations mentioned above for lattice simulations, they come with their own caveats. First, they necessarily rely on some approximations which are often difficult to control in a systematic way in the nonperturbative regime. Second, contrarily to lattice techniques, which can directly access the physical observables of the theory, the continuum approaches<sup>2</sup> are formulated in terms of the quark and gluon degrees of freedom and it is often quite involved to extract information for physically observable quantities such as, *e.g.*, hadron masses.

Having brushed this broad panorama, let us now draw the main contours of this review article. The above paradigmatic picture of a weakly coupled high-energy regime versus a strongly coupled one in the IR essentially relies on the Faddeev-Popov (FP) approach to perturbation theory [FP67], whose predictions are, however, in contradiction with some *ab-initio* results. In particular, the aforementioned Landau pole is most probably spurious. Indeed, numerical calculations of pure YM theories in the Landau gauge show that, in the UV, the coupling<sup>3</sup> increases with decreasing momentum scale as predicted by the FP perturbation theory, but it remains finite at all scales and even decreases in the deep IR [BIMPS09], see Fig. 1. Even more, one observes that the actual loop-expansion parameter—that is, in  $d = 4$  dimensions,  $N_c \alpha_S / (4\pi)$ , with  $N_c = 3$  the number of colours—never exceeds moderate values, of the order of 0.3, thus potentially opening a novel perturbative way in the IR regime. This does not imply that the IR sector is fully perturbative—spontaneous chiral symmetry breaking is one among many examples of phenomena that is not captured by a coupling expansion at any finite order—but this indicates that it is neither genuinely nonperturbative and that, at least in the Landau gauge, some aspects of the IR dynamics may admit a perturbative description. This stunning observation has, surprisingly, never reached to the broad audience it deserves and remains largely unknown even to the QCD community. It is one goal of the present article to advertise it to its full merit and to discuss in detail its far-reaching consequences.

Because the FP theory predicts a Landau pole, an IR perturbative approach necessarily involves a modified starting point. One famous possibility is the Gribov-Zwanziger (GZ) quantization scheme [Gri78, Zwa89], which aims at tackling the Gribov-Singer ambiguity [Gri78, Sin78] that plagues the FP theory in the IR. The approach reviewed in this article follows a different, more phenomenological route which exploits another important result of lattice simulations in the Landau gauge, namely, the fact that the gluon propagator reaches a finite nonzero value at vanishing momentum, corresponding to a nonzero screening mass, as shown in Fig. 2. This massive-like behaviour is of the

<sup>2</sup> In this article, for simplicity, we shall use the denomination “continuum” to encompass all theoretical approaches, except for lattice simulations.

<sup>3</sup> To be precise, the present statements concern the Taylor coupling, which characterizes the ghost-antighost-gluon vertex at vanishing ghost momentum [Tay71]; see Section III A. For a review of the strong coupling constant, see Ref. [DBdT16].

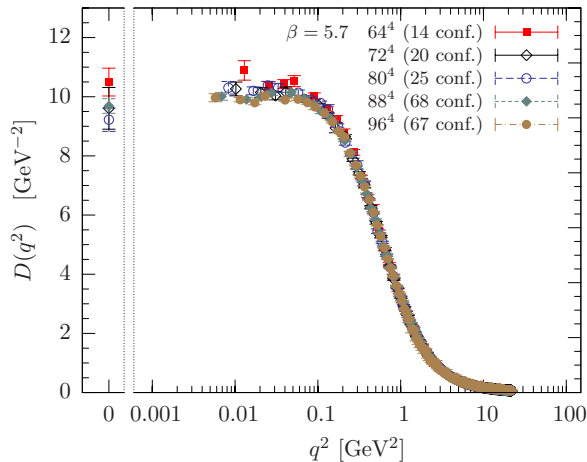


FIG. 2: Lattice results for the gluon propagator in the SU(3) YM theory in the Landau gauge. Figure from Ref. [BIMPS09]. In this reference,  $D(q)$  stands for the gluon propagator, denoted  $G(q)$  in the present article.

utmost importance but, surprisingly again, has remained largely unknown even in the QCD community.

This suggests a simple massive deformation of the Landau gauge FP Lagrangian, with a tree-level gluon mass term [TW10], which actually corresponds to a particular case of the Curci-Ferrari (CF) Lagrangian [CF76a].<sup>4</sup> Note that the gluon mass is introduced in a gauge-fixed setting and thus does not, *per se*, break the gauge invariance of the theory.<sup>5</sup> Among the interesting properties of this model let us mention i) its perturbative renormalisability in four dimensions; ii) the fact that one recovers the standard FP theory together with the associated phenomenology in the UV regime; and iii) the key observation [TW11] that the mass term suffices to screen the IR divergences responsible for the Landau pole of the FP theory, thereby allowing for a well-defined perturbative expansion all the way from the UV to the deep IR.

In this context, the working hypothesis is that the CF model provides a good starting point for an efficient perturbative description of various IR aspects of QCD-like theories. This is to be viewed as an effective description, where essential aspects of the IR dynamics (in the Landau gauge) are efficiently captured by a simple gluon mass term—which has to be fitted against some (*e.g.*, lattice or experimental) data—and where the residual interactions can then be treated perturbatively. This idea has been first put forward in Refs. [TW10, TW11], where the Euclidean ghost and gluon propagators of YM theories in the Landau gauge were computed at one-loop order in the CF model and successfully compared to lattice data for different gauge groups and different spacetime dimensions. This exciting observation has triggered systematic studies of modified (IR) perturbative descriptions based on the CF model. This includes the genuine CF model, viewed as a phenomenological proxy of a—yet to be found—IR completion of the FP Lagrangian [PTW13, RSTW14, PTW14, RSTW15b, RSTW15a, PTW15, RSTW16, RST15, RSTT17, PRS<sup>+</sup>17, RSTW17, GPRT19, PRS<sup>+</sup>21, Rei20, BPRW20, Ser20, BGPR21, HK19, HK20, Kon15, KWH<sup>+</sup>20, Web12, DW20, KS21, SBHK19, SK19], as well as the screened perturbation theory approach [Sir15a, Sir15b, Sir16b, Sir16a, Sir17, CS18, CS20], where the gluon mass term is added and subtracted to the FP Lagrangian and where the subtracted mass is treated, together with the coupling, in a perturbative expansion around the CF Lagrangian. A large number of quantities of physical interest have been computed, either in the vacuum or at nonzero temperature and density, including propagators, three-point vertex functions, phase diagrams, etc. at one-loop order and, by now, also at two-loop order in many cases [GPRT19, BPRW20, BGPR21]. The results compare very well with the available lattice data, thereby confirming the above perturbative picture. The approach is also used to investigate quantities which are not directly accessible with lattice techniques. The present article aims at summarising these results and advertising them to a broad audience.

The article is organised as follows. In Section II, we introduce our notations and discuss some aspects of the gauge fixing in nonAbelian gauge theories that motivate the model studied in this review. Section III presents an overview of the status of the YM propagators in the Landau gauge. In Section IV, we briefly review the CF model and in Section V, we present the results of perturbative calculations of propagators and three-point vertex functions of YM

<sup>4</sup> A possible relation between the gluon mass term and the Gribov-Singer ambiguity problem has been investigated in [ST12, RSTT21].

<sup>5</sup> The more subtle question of the Becchi-Rouet-Stora-Tyutin symmetry of the gauge-fixed theory is discussed in Sect. IV B.

theories in this model at one- and two-loop orders and their comparison to lattice results. Similar calculations in the case of dynamical quarks are reviewed in Section VI, including the case of light quarks, where the dynamical breaking of chiral symmetry plays a key role. We discuss the results of the perturbative CF model for the propagators and the phase diagram of the theory at nonzero temperature and chemical potential in Section VII. Section VIII reviews some results in the Minkowskian domain and Section IX briefly discusses some of the open questions. Finally, we summarise and conclude in Section X.

## II. QCD AND GAUGE FIXING

### A. The QCD lagrangian

The aim of this section is mainly to fix our notations. QCD is a field theory which involves fermionic (Dirac bispinor) fields  $\psi$  for the quarks and a gluon field  $A_\mu$  which takes values in the Lie algebra of the SU(3) gauge group. In this review, we mainly focus on Euclidean properties and it is therefore convenient to work with the Wick-rotated Lagrangian density  $\mathcal{L}$ , which can be written as the sum of a pure gauge term  $\mathcal{L}_{\text{YM}}$  and a matter term  $\mathcal{L}_\psi$ . The first one is the YM Lagrangian

$$\mathcal{L}_{\text{YM}} = \frac{1}{2} \text{tr} F_{\mu\nu}^2. \quad (1)$$

It involves the field strength  $F_{\mu\nu} = \partial_\mu A_\nu - \partial_\nu A_\mu - ig_b[A_\mu, A_\nu]$ , where  $g_b$  is the bare coupling constant. The matter term involves a sum over the quark flavours:

$$\mathcal{L}_\psi = \sum_{i=1}^{N_f} \bar{\psi}_i (\not{D} + M_{b,i}) \psi_i, \quad (2)$$

where the covariant derivative acting on a fermion is  $D_\mu \psi = (\partial_\mu - ig_b A_\mu) \psi$ , the Feynman notation is used ( $\not{D} = \gamma_\mu D_\mu$  with  $\gamma_\mu$  the Euclidean Dirac matrices whose anticommutator is diagonal,  $\{\gamma_\mu, \gamma_\nu\} = 2\delta_{\mu\nu} \mathbb{1}$ ), and  $M_{b,i}$  are the bare masses of the different quark flavours. For completeness, we recall that the covariant derivative acting on a field  $X$  which takes values in the Lie algebra reads  $D_\mu X = \partial_\mu X - ig_b[A_\mu, X]$ .

QCD involves, in principle, six quark normalisations. For the present applications, the three heavier ones,  $c$ ,  $b$ , and  $t$ , can be safely neglected and one considers only the three lighter ones,  $u$ ,  $d$ , and  $s$ . It is however, interesting, for methodological purposes, to consider other gauge groups, different number of quark flavours and even change the space(time) dimension. The QCD-like theories considered here are based on the gauge groups SU( $N_c$ ) and involve  $N_f$  quark normalisations with various masses. The case  $N_f = 0$  is interesting by its simplicity and because it is expected to exhibit several key properties of QCD. This pure YM or quenched limit can be viewed as QCD with all quark masses so large that there are no contribution from fermionic fluctuations.

Under a gauge transformation, the fields transform as

$$A_\mu \rightarrow A_\mu^U = U A_\mu U^\dagger + \frac{i}{g_b} U \partial_\mu U^\dagger, \quad \psi \rightarrow \psi^U = U \psi, \quad (3)$$

where  $U(x)$  is a field which takes value in the gauge group. This causes the field strength and the covariant derivatives to transform as  $F_{\mu\nu} \rightarrow U F_{\mu\nu} U^\dagger$  and  $D_\mu \psi \rightarrow U D_\mu \psi$ , which in turn implies that the QCD lagrangian is gauge invariant.

In actual calculations, it is often convenient to decompose a field  $X$  taking values in the Lie algebra (such as the gluon field) on a basis  $\{t^a\}$  of the Lie algebra:  $X = X^a t^a$ . We choose the normalisation of the generators  $t^a$  such that  $\text{tr} t^a t^b = \frac{1}{2} \delta^{ab}$  so that the YM lagrangian reads (sum over indices implicit)

$$\mathcal{L}_{\text{YM}} = \frac{1}{4} (F_{\mu\nu}^a)^2. \quad (4)$$

In this basis, the components of the covariant derivative,  $(D_\mu X)^a = \partial_\mu X^a + g_b f^{abc} A_\mu^b X^c$ , and of the field strength,  $F_{\mu\nu}^a = \partial_\mu A_\nu^a - \partial_\nu A_\mu^a + g_b f^{abc} A_\mu^b A_\nu^c$ , involve the structure constants  $f^{abc}$  of the gauge group.

### B. Gauge fixing

Gauge invariance is a very powerful concept that highly constrains the possible physical theories but it also comes with important drawbacks. In particular, it implies that the propagator for the gluon field, one of the building blocks

of continuum quantum field theory approaches, is not well defined. Technically, gauge invariance imposes that the second derivative of the YM action is transverse,  $q_\mu \delta^2 S_{\text{YM}} / \delta A_\mu^a(q) \delta A_\nu^b(-q) = 0$ , and thus noninvertible, which makes apparent that there is no tree-level gluon propagator associated to the YM action.

To overcome this difficulty, the strategy used in virtually all continuum approaches consists in fixing the gauge. The underlying idea consists in dividing the space of all gauge configurations in equivalence classes, called gauge orbits: two gauge configurations belong to the same equivalence class if they are related by a gauge transformation. Gauge invariance stipulates that all the field configurations within a gauge orbit bear the same physical content. In the path integral version of quantum field theory, summing over all gauge field configurations is redundant and it is enough to retain one representative per gauge orbit. The procedure which consists in restricting the path integral to one field configuration per gauge orbit is called gauge fixing and the representative is chosen according to a given gauge condition. The Landau gauge, defined by the condition

$$\partial_\mu A_\mu^a = 0, \quad (5)$$

is a very convenient and widely used choice, in particular, for what concerns nonperturbative approaches. This whole review concerns the Landau gauge.<sup>6</sup>

In continuum approaches, the gauge-fixing procedure is, most often, implemented through the famous FP procedure [FP67]. It boils down to adding to the Lagrangian density a gauge-fixing part expressed in terms of ghost fields  $c$  and  $\bar{c}$  (which are Grassmann variables) and a Lagrange multiplier  $h$  (known as the Nakanishi-Lautrup field). For the Landau gauge, it reads

$$\mathcal{L}_{\text{FP}} = \partial_\mu \bar{c}^a (D_\mu c)^a + ih^a \partial_\mu A_\mu^a. \quad (6)$$

The YM and FP actions are invariant under the Becchi-Rouet-Stora-Tyutin (BRST) symmetry [BRS75, BRS76, Tyu75], whose generator  $s$  is characterized by

$$sA_\mu^a = (D_\mu c)^a, \quad sc^a = -\frac{g^b}{2} f^{abc} c^b c^c, \quad s\bar{c}^a = ih^a, \quad s(ih)^a = 0. \quad (7)$$

The BRST symmetry is a crucial property of the FP gauge fixing procedure which is heavily used to prove renormalisability and discuss the unitarity of the theory (we will come back on these issues below). It has several interesting properties. First, the symmetry is nonlinearly realized (the variations of the fields are not linear in the fields). It is actually a supersymmetry, which transforms bosonic fields to Grassmann ones, and reciprocally. This implies that  $s$  *anticommutes* with the Grassmann quantities. Finally, it is nilpotent,  $s^2 = 0$ .

Once the gauge is fixed, it becomes meaningful to compute averages of quantities which are *not* gauge invariant. In fact, the determination of physical observables in this context relies inevitably on the previous evaluation of such quantities: the correlation functions of the fundamental fields appearing in the Lagrangian. In the last two decades, an important activity has been devoted to characterize the basic QCD correlation functions by various methods, including lattice simulations. We stress though that it is by no means necessary to fix the gauge on the lattice in order to extract physical observables. Still, the calculation of correlation functions by means of gauge-fixed lattice simulations provides a very important insight.

The results obtained by lattice simulations are described in Sect. IIIB, but before embarking on this discussion, let us recall why the Landau gauge is particularly useful in lattice simulations. In principle, fixing the gauge on the lattice requires to find the gauge transformation  $U$  such that the gauge constraint  $\partial_\mu A_\mu^U(x) = 0$  is fulfilled. This represents a large set of nonlinear equations (there are  $(N_c^2 - 1)$  such equations per lattice site) and this problem is highly nontrivial numerically. In the case of the Landau gauge, an alternative approach consists in extremising the functional [Wil80, MO87, MO90]

$$f[A, U] = \int d^d x \text{tr} [A_\mu^U(x) A_\mu^U(x)] \quad (8)$$

with respect to the gauge transformation  $U$  at fixed  $A$ . It can easily be shown that such an extremum fulfills the Landau gauge condition. This extremisation problem is still quite intricate because  $f$  involves many variables but very powerful numerical methods are available if one restricts to local minima. In any case, it is way easier to address than the original root-finding problem.

---

<sup>6</sup> We mention that the screened perturbation theory approach has also been applied to the case of linear covariant gauges [SC18, Sir19b], which have recently also been investigated with lattice techniques [CMS09, BBC<sup>+</sup>15, CDM<sup>+</sup>18].

### C. The Gribov ambiguity

The general philosophy behind the idea of gauge fixing presented in section II B suffers from a major issue. As first pointed out by Gribov [Gri78], the procedure of retaining one representative per gauge orbit is in practice more intricate than it may seem. Indeed, there exist distinct gauge-field configurations that fulfil the gauge condition (5) but that are the gauge transforms of one another. In other words, the functional (8) admits many extrema. These are called Gribov copies. Later on, Singer [Sin78] proved that this ambiguity is not restricted to the Landau gauge only but exists for a large class of gauge conditions. Moreover, Neuberger [Neu87, Neu86] studied the influence on the Gribov copies on the gauge-fixing property *à la* FP. He showed that, on a lattice of finite size, the FP procedure is ill defined because physical observables are given by an undetermined 0/0 ratio. The status of this gauge-fixing procedure is therefore questionable at a nonperturbative level.

In a first attempt to overcome this ambiguity, Gribov [Gri78] proposed to limit the domain of functional integration over the gluon field to what is now called the first Gribov region, characterised by minima of the functional (8). Later, Zwanziger [Zwa89] proposed a local, renormalisable field theory (the GZ theory) which implements this restriction of the domain of integration at the expense of adding a collection of auxiliary fields. It was clear from the seminal work of Gribov that the restriction to the first region successfully eliminates the infinitesimal Gribov copies, *i.e.*, copies that are infinitesimally close to one another. Unfortunately, it was also pointed out that this may not be sufficient to fully resolve the Gribov ambiguity, that is, to completely fix the gauge. In fact, Van Baal [vB92] proved that there exist Gribov copies within the first Gribov region. An unambiguous gauge fixing, called the absolute Landau gauge, would consist in restricting to gauge configurations belonging to the fundamental modular region, which corresponds to absolute minima of the functional (8). This is however a very difficult numerical task and no continuum or lattice technique exists to implement this constraint in an efficient way. Nonetheless, some geometric characterisations of the fundamental modular region lead to the conclusion that constraining the path integral to such field configurations would modify correlation functions in the UV by exponentially small contributions  $\propto \exp(-a/g_6^2)$  with some constant  $a$ . Taking into account the running of the coupling constant, it is therefore expected that Gribov copies have no role in the UV but may influence the IR properties of QCD.<sup>7</sup>

Another strategy for tackling the Gribov ambiguity consists in summing over *all* Gribov copies—be they minima, maxima or saddle points of the functional (8)—with a non-flat weight function that lifts the degeneracy between the (equivalent) Gribov copies and compensates their multiple counting in the path integral [ST12]; see also [STT14, STT15, Tis18, RSTT21]. By properly choosing the weight function, the gauge-fixed theory can be written in terms of a local, renormalisable action using standard auxiliary fields techniques.

Several other proposals have been put forward to address the Gribov issue in continuum approaches, none of which is completely satisfactory, and we refer the reader to the literature for a more detailed description [PJJ90, Zwa90, FP91, Sch99, vSGW08, Maa10]. Finally, we stress that the Gribov-Singer ambiguity is easily resolved in lattice calculations, for instance by arbitrarily choosing only one of the numerous extrema (in practice a minimum) of the discrete version of the functional (8) [MO87, MO90]. Other choices are possible as well [Maa10].

The existence of the Gribov-Singer ambiguity has far-reaching consequences. In particular, the textbook FP construction described above is justified only as long as there exists only one representative per gauge orbit but is *a priori* invalid when there are more. Consequently, predictions based on the FP action must be taken with a grain of salt. For instance, the aforementioned Landau pole could be the consequence of an ill-defined gauge-fixing procedure. A second example concerns the BRST symmetry described by Eq. (7) which is indeed a symmetry of the FP action but whose status is questionable at a nonperturbative level [Neu86, Neu87].

### III. YANG-MILLS CORRELATION FUNCTIONS: PREVIOUS RESULTS

Computing gauge-invariant quantities in continuum approaches heavily relies on the knowledge of correlation functions which do depend on the gauge condition. Here, we focus on the Landau gauge, which has been the most studied in this context. We first describe the results from semi-analytical methods and, in the following section, the results from lattice Monte-Carlo simulations.

---

<sup>7</sup> This is indeed what is observed in lattice simulations [SIMPS05, MS14]. It was also argued that the constant  $a$  in the exponential above tends to 0 in the IR, which explains why the copies cannot be neglected in this range [DZ89].

### A. Correlation functions from continuum approaches

The Landau gauge condition (5) imposes a transversality condition: any correlation function vanishes if the Lorentz index of an external gluon leg is contracted with the corresponding momentum. This drastically reduces the number of tensorial structures that may appear in a given correlation function. For instance, the gluon propagator in the Landau gauge is transverse with respect to the gluon momentum. In the Euclidean domain, it reads

$$G_{\mu\nu}^{ab}(q) = \delta^{ab} P_{\mu\nu}^{\perp}(q) G(q) \quad \text{with} \quad P_{\mu\nu}^{\perp}(q) = \delta_{\mu\nu} - \frac{q_{\mu}q_{\nu}}{q^2}, \quad (9)$$

where  $G(q)$  is a scalar function of  $q^2$ . In general (*e.g.*, in linear gauges), the gluon propagator also involves a longitudinal part, proportional to  $P_{\mu\nu}^{\parallel} = \delta_{\mu\nu} - P_{\mu\nu}^{\perp}$ .

The pioneering semi-analytical studies [Man79, BG80, BP88, BP89] for the IR behaviour of QCD were guided by the idea of “IR slavery” and were based on the conjecture of a gluon propagator with a singular IR behaviour

$$G^{\text{IR slavery}}(q) \sim \frac{1}{q^4}, \quad (10)$$

that, in a one-gluon exchange approximation, could justify the existence of a confining linear potential between static quarks. This behaviour was indeed obtained as a solution of the DSE for the gluon propagator in a very simple approximation.

However, the analysis of more elaborate truncations within the DSE, the FRG, and the VHA, including not only the gluon but, also, the ghost propagator, led to the discovery of solutions with a completely different IR behaviour [AvS01] where the gluon propagator tends to zero at small momentum

$$G^{\text{scaling}}(q) \sim q^{\alpha}, \quad \text{with} \quad \alpha > 0, \quad (11)$$

while the ghost propagator is more singular than the bare one in the IR regime [vSAH97, AB98, AvS01, LvS02, FA02, PLNvS04, FG04, FP07, SLR06, HAFS08, FMP09, FP09, HMvS12, HvS13, QRH14, QR15, Hub16, CFM<sup>+</sup>16, Hub20],

$$G_{c\bar{c}}^{\text{scaling}}(q) \sim \frac{1}{q^{2+\beta}}, \quad \text{with (in } d=4) \quad \beta = 1 + \frac{\alpha}{2}. \quad (12)$$

These two correlation functions behave as power laws in the long-distance regime, hence the name “scaling” solution.<sup>8</sup>

Another class of solutions, referred to as “decoupling”, was identified some years later, where the gluon propagator saturates in the IR (it tends to a strictly positive constant at small momentum) and the ghost correlation function behaves just as its tree-level expression, up to nonsingular corrections [AN04, AP06, BBL<sup>+</sup>06, AP08, ABP08, BLY<sup>+</sup>08, BLLY<sup>+</sup>08, HvS13]:

$$G^{\text{decoupling}}(q) \sim cst., \quad (13)$$

$$G_{c\bar{c}}^{\text{decoupling}}(q) \sim \frac{1}{q^2}. \quad (14)$$

In the Landau gauge, the coupling constant can be defined as the ghost-antighost-gluon vertex at vanishing ghost momentum. This choice, called the Taylor scheme, is particularly interesting because it receives no loop corrections [Tay71]. As a consequence it is essentially determined from the ghost and gluon propagators:

$$\alpha_S(q^2) = \frac{g_0^2}{4\pi} D(q^2) F^2(q^2), \quad (15)$$

where we have introduced the gluon and the ghost dressing functions

$$D(q) = q^2 G(q) \quad \text{and} \quad F(q) = q^2 G_{c\bar{c}}(q), \quad (16)$$

and where  $g_0$  is the renormalised coupling defined at the same renormalisation point as  $D(q)$  and  $F(q)$ . Both the scaling and the decoupling solutions show a regular coupling constant in the IR, which tends to a constant in the former case and decreases to zero in the latter.

---

<sup>8</sup> A nonsingular solution for the gluon propagator was observed even before in Ref. [EHW98] but the authors considered this behaviour as an artefact of their approximations.

The IR behaviour of correlation functions has also been studied at leading order in the GZ approach. The early implementations of the original GZ model gave a scaling solution [Gri78, Zwa89, Zwa94]. However, it was soon realized that nontrivial condensates can naturally appear in this model, which, when included in a refined version of the model [DGS<sup>+</sup>08, VZ12], led to a decoupling solution.

An important property of the scaling and the decoupling solutions is that they are both incompatible with the existence of a Källén-Lehmann representation with a positive spectral density for transverse gluons [AvS01, CMT05, CFM<sup>+</sup>16]. It was argued that such positivity violations are somehow related to confinement and to the presence of negative norm states which cannot appear in the physical spectrum of a unitary theory [AvS01]. This will be discussed in more detail in Sec. V C.

These positivity violations were then observed in first-principle Monte-Carlo simulations [CMT03, CMT05, CM08b, BHL<sup>+</sup>07, Maa07, BIMPS09] and there is no doubt of their existence. However, their interpretation is far from settled. In particular, it is clear that a *nonpathological* model with negative norm states must necessarily include some form of confinement. That is, there must exist, within the set of possible states, a subspace of physical states with positive definite norm with an  $S$ -matrix that involves only such states. This effective decoupling of negative (and null) norm states must occur either because there is some set of symmetries that allows to characterise a physically acceptable subspace and/or due to some selection rule of purely dynamical origin. Proving the existence of a physical space with these characteristics and the unitarity of the  $S$ -matrix in this space is as hard as proving confinement. What is clear, in the present state of affairs, is that, just as positivity violations cannot be invoked as an indication of confinement, neither can a model be ruled out on the sole basis of their existence. It could happen that we simply do not know the true physical subspace with positive norm and unitary  $S$ -matrix.

Both the scaling and decoupling solutions unveiled a remarkable surprise: far from being very strong (not to mention with Landau pole-type singularities), the featured correlations stay modest in the IR. Surprisingly, these results were initially received with some indifference by the QCD community. This may be due to various reasons. First, initial studies focused on correlations functions which are not directly physical observables. Second, these solutions were found on the basis of approximation schemes that did not rely on a small parameter that would ensure their robustness. In fact, these were considered *nonperturbative* but the criterion used to retain or neglect a vertex was similar to what would be done in perturbation theory. Typically, two-point correlation functions were initially computed with either bare three- or four-point vertices or with dressed expressions based on educated guesses. Higher-order vertices were systematically neglected. More recently, richer approximations have been considered and the results have shown to be reasonably robust (see, for example, [Hub20]) but, again, the vertices of order greater than four have always been neglected, which still bears similarities in spirit to a higher-order perturbative analysis.

At this point, we mention that a plausible simple explanation of the success of approximations which, although considered as nonperturbative, closely resemble perturbation theory is the existence of a relatively moderate coupling constant. This idea actually underlies the work reviewed in this article.

## B. Lattice results: propagators and three-point vertices

The development of the semi-analytical methods presented in the previous section stimulated an important activity in computing correlation functions by means of lattice Monte-Carlo techniques. Using the gauge-fixing procedure described in Sect. II B, various two- and three-point correlation functions have been simulated in YM theory [MO87, BBLW00, BBL<sup>+</sup>01, CM08a, BIMPS09, BMMP10, ISI09, BLY<sup>+</sup>12, Maa13, OS12] and in QCD [BHL<sup>+</sup>04, BHL<sup>+</sup>05, SO10] (see Sect. VI). Once the gauge has been properly fixed, the computation of gluon correlators is straightforward. It is also possible to compute correlation functions involving ghosts, assuming that the terms in the gauge-fixed action that depend on these fields have the form of the FP Lagrangian. The (Gaussian) functional integration over the ghost field can be carried out exactly, which results in a nonlocal functional measure in the gauge fields. An explicit expression given by Wick's theorem for Grassmann variables is obtained that involves products of the inverse of the FP operator times the determinant of that same operator. The same holds for correlators involving quark fields.

The results of lattice simulations have confirmed the essential features obtained from the continuum approaches, in particular, the absence of strong correlations in the IR. Moreover, they allowed to resolve, on a first-principle basis, the controversy about the scaling versus decoupling solutions in YM or in QCD.

Simulations of the gluon and ghost two-point correlators have become very precise and clearly show a decoupling type solution in  $d = 3$  and  $d = 4$  dimensions both for pure YM and for QCD [BBLW00, BBL<sup>+</sup>01, CM08a, BIMPS09, BMMP10, ISI09, Maa13, OS12]. This is illustrated in Figs. 1, 2, and 3, which show the lattice results of Ref. [BIMPS09] for the Taylor coupling (15), the gluon propagator, and the ghost dressing function in  $d = 4$  for the SU(3) YM theory. Concomitantly to the saturation of the gluon propagator at small momenta, the ghost propagator behaves as that of a massless excitation in this limit, that is, the dressing function remains finite in the deep IR. Simulations have also been made for other values of the number of colours  $N_c$  and of the number of quark flavours  $N_f$  with similar results.

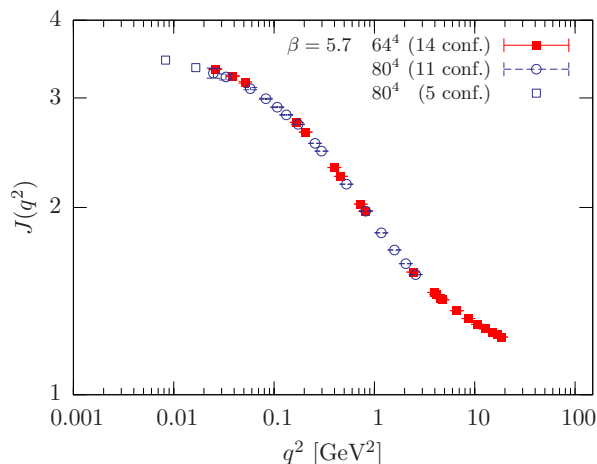


FIG. 3: The ghost dressing function—the propagator multiplied by  $q^2$ —in the SU(3) YM theory in the Landau gauge. Figure from Ref. [BIMPS09]. In that reference,  $J(q)$  stands for the ghost dressing function, denoted  $F(q)$  in the present article; see Eq. (16).

In  $d = 2$  dimensions, instead, the lattice results show a scaling solution [CM08a, Maa13]. Furthermore, as already mentioned, the detailed analysis of the gluon propagator reveals, with no ambiguity, that, if it admits a Källén-Lehmann representation, then the spectral function cannot be positive definite [CMT05, BHL<sup>+</sup>07] (see Sect. VC for a detailed discussion of this point).

As already mentioned, the relevant perturbative expansion parameter is not  $\alpha_S(q)$  but, in  $d = 4$ , [Wei95]

$$\lambda(q) = \frac{N_c g^2(q)}{16\pi^2} = \frac{N_c \alpha_S(q)}{4\pi}. \quad (17)$$

Since the Taylor coupling  $\alpha_S(q)$  never exceeds 1.3, see Fig. 1, the expansion parameter  $\lambda(q)$  is bounded by 0.3. This is a remarkable observation.<sup>9</sup> In the absence of any prejudice, it indicates that some sort of perturbation theory should apply in the IR, at least in the SU(3) YM theory. In the context of YM theories and QCD, this natural conclusion, however, came at odds with the common wisdom of a genuinely nonperturbative IR regime and has remained largely unknown. This is the seed of a new paradigm.

Three-point correlators have also been simulated on the lattice and bring important information despite the fact that the statistical and systematic errors are much larger than for the propagators. One of the most important results is that the various coupling constants that can be extracted from the ghost-gluon vertex (in various configurations of momenta) take, again, moderate values for all momenta, including the IR limit, where they typically show a slow decrease towards zero [IMPS<sup>+</sup>07, Ste06, CMM08, BIMPS09, BLY<sup>+</sup>12, Maa20, ADSF<sup>+</sup>21]. Remarkably, the smallness of the couplings is compatible with a perturbative expansion. These observations include, as a particular case, the configuration of momenta corresponding to the Taylor scheme shown in Fig. 1.

As for the three-gluon vertex, lattice results clearly show a “zero-crossing” in  $d = 3$  [CMM08, MV20] and, although not as clearly, also in  $d = 4$  dimensions [CMM08, BBDS<sup>+</sup>14, BDRQZ17, SBK<sup>+</sup>17, MV20]. That is, for the various configurations of momenta studied, there always seems to be a sufficiently small momentum at which the correlation function changes sign and becomes negative. In the regime in which all momenta tend to zero the correlation function seems to diverge towards minus infinity for  $d = 3$ . However, the coupling constant that can be extracted from this vertex also remains rather small for all momenta.<sup>10</sup>

Lattice simulations of correlators involving quarks have been performed both in the quenched limit  $N_f = 0$  and in the presence of dynamical quarks  $N_f > 0$  [BHL<sup>+</sup>04, BHL<sup>+</sup>05, SMMPvS12, OSSS19]. The most important result observed in these simulations is that the quark propagator shows a significant dynamical mass generation, which is a signature of the spontaneous breaking of the chiral symmetry. That is, even in cases where the running mass is very

<sup>9</sup> Similarly, the coupling is bounded in  $d = 3$  and  $d = 2$ , with a moderate although slightly larger value in  $d = 3$  than in  $d = 4$  and significantly larger value in  $d = 2$ .

<sup>10</sup> The couplings constant must be extracted, in general, from combinations of three- or four-point functions and propagators.

small at the microscopic level (of the order of a few MeV), its zero momentum limit—the constituent mass—is of the order of several hundred MeV.

Finally, the quark-gluon vertex has been simulated in Refs. [SK02, SBK<sup>+</sup>03, SKB<sup>+</sup>04, KLSW07]. Among the more striking results, the associated coupling constant can get up to two-to-three times larger than the one in the pure gauge sector. This has far-reaching consequences as it indicates that, unlike the YM sector, the dynamics of light quarks is strongly coupled. This is consistent with the early observation [AJ88] that spontaneous chiral symmetry breaking requires a sufficiently large quark-gluon coupling in the IR.

#### IV. THE CURCI-FERRARI MODEL

One of the striking features of the studies reported in the previous section is the saturation of the gluon propagator in the IR, which shows the dynamical generation (in the Landau gauge) of what is called a screening mass—not to be confused with a pole mass, as discussed in Sec. IV C below. This phenomenon is, by now, well established. As already mentioned, the FP perturbation theory is unable to describe the generation of this screening mass and the simplest deformation of the FP Lagrangian that includes it is a particular case of a class of Lagrangians known as the CF Lagrangians. We review the latter and their main properties, including symmetries and renormalisability, in the present section.

##### A. The Curci-Ferrari Lagrangian

In the 70's, Curci and Ferrari proposed an alternative to the Higgs mechanism that would provide a consistent theory of massive vector bosons in the presence of nonAbelian symmetries [CF76a]. Although this original motivation has been abandoned (mainly for reasons related to the issue of unitarity, see Sec. IV C below), the model has received a renewed interest in the context of IR QCD [TW10, TW11]. In this section, we consider the original model, which goes beyond the case of the Landau gauge, for completeness. The Lagrangian density<sup>11</sup> reads

$$\mathcal{L} = \mathcal{L}_{\text{YM}} + \mathcal{L}_{\text{CFDJ}} + \mathcal{L}_m, \quad (18)$$

where  $\mathcal{L}_{\text{YM}}$  is the YM Lagrangian density (1) and where the gauge-fixing and mass contributions read, respectively,

$$\mathcal{L}_{\text{CFDJ}} = \frac{1}{2} \partial_\mu \bar{c}^a (D_\mu c)^a + \frac{1}{2} (D_\mu \bar{c})^a \partial_\mu c^a + \frac{\xi_b}{2} h^a h^a + i h^a \partial_\mu A_\mu^a - \xi_b \frac{g_b^2}{8} (f^{abc} \bar{c}^b c^c)^2, \quad (19)$$

and

$$\mathcal{L}_m = m_b^2 \left[ \frac{1}{2} (A_\mu^a)^2 + \xi_b \bar{c}^a c^a \right]. \quad (20)$$

Here,  $g_b$ ,  $\xi_b$ , and  $m_b$  are the bare coupling, gauge-fixing parameter, and gauge boson mass, respectively. The Lagrangian (19) is the first example in the literature of a nonlinear gauge fixing *à la* FP, sometimes referred to as the Curci-Ferrari-Delbourgo-Jarvis gauge [DJ82]. An important technical aspect is that the mass term (20) is introduced at tree level in a gauge-fixed version of the Lagrangian density, which, notably, guarantees its perturbative renormalisability (see Sect. IV B). The principal reason is that the tree-level gluon propagator  $G_0(p)$  decreases as  $1/p^2$  at large momentum. This is at odds with what happens when a gauge boson mass is directly added to the YM Lagrangian, where  $G_0(p) \sim \text{const}$ .

We present here the Euclidean version of the model with the notations that are most commonly used nowadays and which differ slightly from those originally employed in [CF76a]. In particular, we consider the model in the presence of a Nakanishi-Lautrup field  $h^a$  that simplifies the writing of the (modified) BRST symmetry (see Sect. IV B). We do not consider matter fields for now, but their inclusion is straightforward, see Sect. VI. The main interest of the CF lagrangian in the form (19) is that the ghost-antighost exchange symmetry is simple and that it preserves the linear realization of some continuous symmetries [CF76b, DJ82, TW09]. This is not the case in the nonsymmetric version of the model:

$$\mathcal{L}_{\text{GF}}^{\text{ns}} = \partial_\mu \bar{c}^a (D_\mu c)^a + \frac{\xi_b}{2} h^a h^a + i h^a \partial_\mu A_\mu^a - i \frac{\xi_b}{2} g_b f^{abc} h^a \bar{c}^b c^c - \xi_b \frac{g_b^2}{4} (f^{abc} \bar{c}^b c^c)^2, \quad (21)$$

<sup>11</sup> In their original article [CF76a], Curci and Ferrari considered a more general model. We will limit ourselves here to the subset of parameters that are compatible with a massive renormalisable model.

which is obtained from Eq. (19) by the field redefinition  $ih^a \rightarrow ih^a + \frac{g_b}{2} f^{abc} \bar{c}^b c^c$  and which proves more convenient for actual calculations. The case  $\xi_b = 0$ , where the ghost mass and the four-ghost interaction are absent, corresponds to the simple massive extension of the Landau gauge considered in this review.

## B. Symmetries and renormalisability

In their original work, Curci and Ferrari observed that the Lagrangian (21) is invariant under the following generalisation of the—at the time recently discovered—BRST transformation

$$sA_\mu^a = (D_\mu c)^a, \quad sc^a = -\frac{g_b}{2} f^{abc} c^b c^c, \quad s\bar{c}^a = ih^a, \quad s(ih^a) = m_b^2 c^a. \quad (22)$$

In the massless case,  $m_b = 0$ , the symmetry (22) is the standard nilpotent BRST symmetry, see Eq. (7). In the massive case, the Lagrangian (19) can be seen as a deformation of the standard FP Lagrangian and the transformation (22) as the corresponding deformation of the BRST symmetry. These deformations modify the behaviour of the model for momenta comparable to or smaller than the renormalised gluon mass.

In Ref. [CF76a], Curci and Ferrari proved the renormalisability of the theory by making use of the symmetries of the model, in particular, the modified BRST symmetry (22). Later, de Boer *et al.* [dBSvNW96] computed the renormalisation factors at one-loop order, considering the five renormalisation factors

$$A^{\mu,a} = \sqrt{Z_A} A_R^{\mu,a}, \quad c^a = \sqrt{Z_c} c_R^a, \quad \bar{c}^a = \sqrt{Z_{\bar{c}}} \bar{c}_R^a, \quad g_b = Z_g g, \quad m_b^2 = Z_{m^2} m^2, \quad \xi_b = \frac{Z_A}{Z_\xi} \xi \quad (23)$$

as independent. The symmetries of the model imply that the divergent part of the renormalisation factors are constrained by the relations

$$\sqrt{Z_A} Z_c Z_g = Z_\xi^2, \quad Z_A Z_c Z_{m^2} = Z_\xi^2, \quad (24)$$

which reduces the number of independent renormalisation factors to three, which can all be extracted only from the two-point correlation functions. The first relation generalizes Taylor's nonrenormalisation theorem [Tay71], previously known in the particular case of the standard Landau gauge ( $\xi_b = 0$ ,  $m_b = 0$ ). The constraints (24), first conjectured in Refs. [BG02, Gra03], have been proven to all orders of perturbation theory [Wsc08] and were, in fact, shown to be direct consequences of gauged supersymmetries of the Lagrangian (20) [TW09]. The Landau gauge condition  $\xi = 0$  is stable under renormalisation, *i.e.*,  $Z_\xi(\xi = 0) = 1$  to all orders of perturbation theory,<sup>12</sup> so the number of independent renormalisation factors is further reduced to two.

## C. Unitarity

Despite the interesting properties described above, the CF model was soon discarded as a pertinent description of a massive Higgs boson because of issues related with unitarity. The aim of this section is to give a critical overview of this topic and discuss the possibility of a unitary CF model for describing strong interactions. We first recall the standard proof of unitarity, in the framework of the (massless) FP gauge fixing [BRS76, BRS75, ZJ75, KO78b, KO79a].

One of the main goals of a field theory is to describe the scattering amplitudes between in- and out-states. In the simple cases (*e.g.* for the  $\phi^4$  theory), the space of in-states is obtained by applying the creation operator  $a_{\text{in}}^\dagger(\vec{q})$  to the vacuum. It can be checked that these states have a positive norm, a necessary property for the state space to be a *bona fide* Hilbert space of a quantum theory. The situation is more involved when considering a (Lorentz-covariant) gauge-fixed field theory because some of the states obtained in this procedure have negative norm (this is the case of gluons with a polarization in the time direction and of the ghosts). Such a field theory makes sense at a quantum level only if one can define a subspace (called the physical subspace), which a) contains only states with a positive norm and b) is stable under the time evolution. Within this physical subspace, the theory has all the necessary ingredients to represent a quantum theory.

In order to impose condition b), a natural idea is to characterize the physical subspace by using symmetry arguments. The standard strategy consists in considering the kernel of the BRST symmetry. One however finds by inspection

<sup>12</sup> For  $\xi_b = 0$ , the FP lagrangian Eq. (19) is invariant under  $c \rightarrow c + \text{Cst}$ . The four-ghost interaction proportional to  $\xi_b$  breaks this symmetry. This is at the heart of the nonrenormalisation theorem  $Z_\xi(\xi = 0) = 1$ .

that there exist states with null norm, all of them belonging to the image of BRST [KO78b, KO78a, KO79b].<sup>13</sup> To account for these states, one defines the physical space as the cohomology of BRST, that is, the kernel of the BRST transformation modulo any element in the image. One must then explicitly check that the cohomology only involves states of positive norm, hence ensuring property a). It has been shown to be the case at all orders of perturbation theory for the FP Lagrangian.<sup>14</sup> This textbook construction is, however, not completely satisfactory for QCD because, as such, the physical subspace would contain coloured states, while confinement implies that only colour-neutral states should appear as acceptable states. An extra restriction, yet to be uncovered, should be used to define a physical subspace with only hadronic states.

How could this discussion be adapted to the CF model? A first difficulty is that the BRST symmetry is not nilpotent anymore ( $s^2 \neq 0$ ). It is, nevertheless, possible to work in the kernel of  $s^2$ , which is a symmetry of the CF action. In this subspace, the BRST symmetry is again nilpotent and we can adapt the procedure described above. There is, however, a more thorny issue: It has been shown that this subspace contains negative-norm states [Oji82, dBSvNW96]. On this basis, the CF model was discarded as being non-unitary. This conclusion is valid if the gauge field is associated with an observable particle (*e.g.*, in the context of weak interactions). However, it should be mitigated if one considers the CF model as a theory for strong interactions. Indeed, it could very well be that the CF model is, in fact, confining. More precisely, there could exist a subspace, yet to be found, in which properties a) and b) listed above hold. We recall that, even in the standard FP case, the construction of a satisfactory physical subspace, composed of singlet states, is yet to be built and it is conceivable that a fix to this issue could also resolve the unitarity problem in the CF model.<sup>15</sup> This intuition is based on the observation that the states of negative norm unveiled in [Oji82, dBSvNW96] are coloured. If all the negative norm states would be coloured, building a subspace where these states are removed would kill two birds with one stone: we would define a physical subspace consistent with confinement and where unitarity would be ensured. To date, the issue is still open and the CF model cannot be discarded on the basis of unitarity arguments.

The issue of unitarity discussed in this section has strong connections with the property of positivity violation discussed above. Indeed, a theory with only positive norm states would admit a Källén-Lehmann representation with a positive spectral density. Positivity violation for the transverse gluons indicates that (at least some of) these modes are unphysical and should be removed from the physical subspace.

#### D. A minimal deformation of the Faddeev-Popov Lagrangian

To conclude this section, we stress that the CF model in the Landau gauge is the simplest extension of the FP Lagrangian that:

- preserves standard perturbation theory in the UV, in particular, remains renormalisable;
- maintains the linearly realised symmetries of the FP Lagrangian;
- has the same field content as the FP Lagrangian;
- renounces to the standard, nilpotent BRST symmetry (that, anyway, seems to be broken beyond perturbation theory [Gri78, Sin78, Neu87]).

Indeed, in order to keep standard perturbation theory and linearly realised symmetries in the UV, the strictly renormalisable couplings must be identical to those of the FP Lagrangian and the only admissible modifications involve couplings with positive mass dimensions. Such deformations, which do not modify the UV, are called “soft”. In the Landau gauge, the only possibility is the gluon mass term.<sup>16</sup> In this sense, the Landau gauge CF model is the minimal extension of the FP approach with a soft breaking of the BRST symmetry in the IR.

Here, we want to warn the reader against a common misinterpretation of the CF model in the QCD context. The gluon mass term is not meant as an explicit modification of the theory—as the resemblance of the FP and CF Lagrangians might wrongly suggest—but, rather, as an effective way to capture actual features of Landau gauge QCD that are missed by the FP perturbative approach. Although such an effective deformation of the gauge-fixed

<sup>13</sup> Note that, since the standard BRST symmetry is nilpotent,  $s^2 = 0$ , the image of BRST belongs to the kernel.

<sup>14</sup> The proof consists in considering the axial gauge which is not Lorentz covariant but for which both the positivity of the state space and unitarity are explicit; see *e.g.* [Wei96].

<sup>15</sup> An attempt in this direction has been undertaken in the context of the GZ model [SZ14].

<sup>16</sup> Of course, the class of possible soft deformations is much larger if the field content of the model is enlarged as, *e.g.*, in the GZ approach.

Lagrangian may induce actual modifications of the original theory, the latter must remain under control if the model is to be a good description. In the remainder of this article, we review large pieces of evidence demonstrating that the CF model indeed captures many features of the YM and QCD-like theories at a relatively low computational cost.

## V. YANG-MILLS CORRELATION FUNCTIONS IN THE VACUUM

The working hypothesis underlying the use of the CF model in the Landau gauge is that it provides an efficient starting point for a reliable and controllable perturbative approach to the IR dynamics of the YM fields. This hypothesis has been put to test, by now, in a large number of cases, by comparing the results of actual perturbative calculations at one- and two-loop orders to lattice data in the Landau gauge, when available. The present section reviews these results in the case of the YM correlation functions in the vacuum.

Before we proceed, a word of caution is in order, which applies in fact to the remainder of the review. Our primary aim is to review those works in the literature which actually postulate perturbation theory in the IR. The main line of investigation concerns a genuine perturbative expansion within the CF model [TW10, TW11, Kon15, HK19, Web12, SBHK19, SK19].<sup>17</sup> The latter is considered either as an actual candidate or as a proxy for an IR completion of the FP theory. In the former case, the gluon mass term is expected to be either related to the issue of gauge fixing and of the Gribov problem, or it is to be eventually self-consistently determined. In the latter case, the gluon mass is simply an additional, phenomenological input parameter which encodes some unknown aspects of the IR physics.

Another approach [Sir16b] that revives the original screened perturbation theory [KPP97] of finite temperature field theory and extends it to the vacuum case, postulates the validity of the FP Lagrangian at all scales and uses the CF Lagrangian simply as a shifted expansion point for perturbation theory. In this case, one adds and subtracts a gluon mass term and formally treats the subtracted mass together with the coupling in a (double) perturbative expansion around the CF Lagrangian.<sup>18</sup> So, although they rely on different hypothesis, the two approaches appear very similar in practice and they actually give similar results when it comes to comparing with lattice data. In order to avoid confusion in the present review, we focus on the strict perturbative CF model and we mention the results of the screened perturbation theory when appropriate.

### A. Renormalisation and renormalisation group

As discussed in Sect. IV B, the CF model is renormalisable in  $d \leq 4$ . The divergent parts of the renormalisation factors in  $d = 4$  dimensions are constrained by the two nonrenormalisation theorems (24), where  $Z_\xi$  can be set to 1 in the case of the Landau gauge. To fully determine the renormalisation factors and, in particular, their finite parts, it is necessary to choose a renormalisation scheme. In order to unify the presentation as much as possible in this review, we choose to focus on results obtained within a single scheme. We mention, though, that other schemes have been considered as well and that the scheme dependence of the results has been—in some cases thoroughly—investigated [TW11, Web12, DW20]. As noted previously, one important feature of the CF model is that one can devise IR-safe schemes,<sup>19</sup> for which the flow is regular at all scales [TW11, Web12, DW20]. We choose the one such scheme for which most of the existing CF model calculations have been performed, namely, the one originally proposed in Ref. [TW11], which we shall refer to as the IRS scheme for simplicity. It is defined by the conditions

$$G^{-1}(p = \mu) = m^2 + \mu^2, \quad F(p = \mu) = 1, \quad Z_g \sqrt{Z_A} Z_c = 1, \quad Z_{m^2} Z_A Z_c = 1, \quad (25)$$

where  $G(p)$  and  $F(p)$  are the (renormalised) scalar part of the gluon propagator and the ghost dressing function, defined in Eqs. (9) and (16), respectively. Note that the two last conditions in Eq. (25) apply to both the divergent parts and the finite parts of the renormalisation factors.

<sup>17</sup> We mention that in some publications, the CF model is sometimes called a “massive YM” model. We find this confusing because this terminology wrongly suggests that one adds a mass to the YM Lagrangian before gauge fixing (which is well-known to be nonrenormalisable). Note, first, that the gluon mass does not break the gauge symmetry of the theory because it is introduced in the gauge-fixed Lagrangian. Second, it does not result in an actual massive vector asymptotic state, even at a perturbative level. Instead, as reviewed here, loop effects lead to spectral positivity violations, already at one-loop order, which guarantee that the (massive) gluon cannot be part of the physical spectrum of the model. For these reasons, we refrain from using the terminology “massive YM” model and we prefer “massive Landau gauge”, or, simply, the CF model.

<sup>18</sup> One interesting aspect of this approach is that the gluon mass parameter could, in principle, be self-consistently determined [CS18, Sir19a].

<sup>19</sup> We call IR-safe those schemes where the flow remains regular at all scales without the need to introduce other parameters than those of the original Lagrangian.

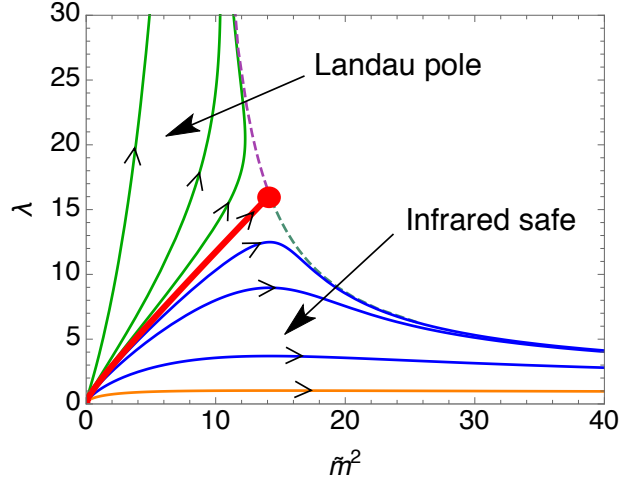


FIG. 4: The RG flow of the CF model in the plane  $(\lambda = N_c g^2 / (16\pi^2), \tilde{m}^2 = m^2 / \mu^2)$  in the IRS scheme for  $N_c = 3$  and  $d = 4$  at one-loop order. From Ref. [RSTW17]. The two-loop corrections have been computed in Ref. [GPRT19]. The green trajectories present a Landau pole, while the blue ones are IR safe. The separatrix (red curve) describes a scaling solution and ends at a nontrivial IR fixed point located at  $(\lambda^*, \tilde{m}^*) \sim (16.11, 3.77)$  at one loop and  $(\lambda^*, \tilde{m}^*) \sim (1.64, 0.6)$  at two loops. The orange line is the trajectory that describe well the lattice results for the propagators of the SU(3) YM theory. Figure from [RSTW17].

In order to correctly describe the logarithmic UV tails of the correlation functions, it is important to take into account renormalisation group (RG) effects. Indeed, although the coupling stays limited, its running is significant. We thus define the standard RG beta functions and anomalous dimensions as

$$\beta_g = \left. \frac{dg}{d \ln \mu} \right|_{g_b, m_b^2}, \quad \beta_{m^2} = \left. \frac{dm^2}{d \ln \mu} \right|_{g_b, m_b^2}, \quad \gamma_A = \left. \frac{d \ln Z_A}{d \ln \mu} \right|_{g_b, m_b^2}, \quad \gamma_c = \left. \frac{d \ln Z_c}{d \ln \mu} \right|_{g_b, m_b^2}, \quad (26)$$

where the  $\mu$ -derivatives are taken at fixed bare parameters. The renormalisation conditions (25) imply that the beta functions can be fixed in terms of the ghost and gluon anomalous dimensions as [TW11]

$$\beta_g = g \left( \frac{\gamma_A}{2} + \gamma_c \right) \quad \text{and} \quad \beta_{m^2} = m^2 (\gamma_A + \gamma_c). \quad (27)$$

The two-point correlation functions in the YM theory have been calculated in this model not only at one loop [TW10, TW11] but also at two loops [GPRT19]. An important point to be mentioned is that due to the gluon mass the model gives a well-behaved perturbative expansion. Not only is the model renormalisable but it also features no IR divergences for non-exceptional configurations of Euclidean momenta at all orders of perturbation theory (this applies to any vertex function for any  $d > 2$ , see Appendix B in Ref. [TW11]). This result is not entirely trivial due to the presence of massless ghost modes. In the case of exceptional configurations of Euclidean momenta, some IR divergences are present [TW11]. The case of Minkowskian momenta would require a separate analysis. The one-loop calculations are easily performed and already exhibit the main nontrivial features of the model [TW11, RSTW17]. In the IRS scheme (25), the one-loop anomalous dimensions read, for  $d = 4$ ,

$$\gamma_c = -\frac{g^2 N_c}{32\pi^2 t^2} [2(t+1)t - t^3 \ln t + (t+1)^2(t-2) \ln(t+1)], \quad (28)$$

$$\begin{aligned} \gamma_A = -\frac{g^2 N_c}{96\pi^2 t^3} & \left[ (17t^2 - 74t + 12)t - t^5 \ln t + (t-2)^2(2t-3)(t+1)^2 \ln(t+1) \right. \\ & \left. + t^{3/2} \sqrt{t+4} (t^3 - 9t^2 + 20t - 36) \ln \left( \frac{\sqrt{t+4} - \sqrt{t}}{\sqrt{t+4} + \sqrt{t}} \right) \right], \end{aligned} \quad (29)$$

where  $t = \mu^2 / m^2$ . The two-loop calculation is way more involved and requires the use of symbolic programming [GPRT19]. The RG flow is obtained by integrating the beta functions (27) with initial conditions  $m_0 = m(\mu_0)$  and

$g_0 = g(\mu_0)$  at a given scale  $\mu_0$ . The  $d = 4$  one-loop flow is shown in Fig. 4 in terms of the dimensionless mass  $\tilde{m}^2 = m^2/\mu^2 = 1/t$  and of the coupling (17). In the UV regime,  $t \gg 1$ , the beta functions behave as

$$\frac{\beta_g}{g} \sim -\frac{11}{3} \frac{N_c g^2}{16\pi^2} + \mathcal{O}(1/t) \quad \text{and} \quad \frac{\beta_{m^2}}{m^2} = -\frac{35}{6} \frac{N_c g^2}{16\pi^2} + \mathcal{O}(1/t). \quad (30)$$

All relevant trajectories start from the Gaussian fixed point  $g = t^{-1} = 0$  which is attractive in the UV. As anticipated, asymptotic freedom is recovered and the one-loop beta function for the coupling constant takes its universal form. As one flows towards the IR, three types of trajectories are observed. For a given coupling constant in the UV, if the gluon mass is large enough, the flow is driven towards a fully attractive IR fixed point, the vicinity of which is characterized by

$$\frac{\beta_g}{g} \sim \frac{1}{6} \frac{N_c g^2}{16\pi^2} + \mathcal{O}(t) \quad \text{and} \quad \frac{\beta_{m^2}}{m^2} \sim \frac{1}{3} \frac{N_c g^2}{16\pi^2} + \mathcal{O}(t). \quad (31)$$

In this case, the flow is IR safe (there is no Landau pole) and the propagators are regular for arbitrary momentum. As will be seen later, the trajectories that correctly describe the data from the numerical simulations are of this type. These trajectories correspond to the decoupling solutions described in Sect. III A. On the other hand, if the gluon mass is taken below a certain threshold the RG flow is singular and presents a Landau pole.<sup>20</sup> There is a limiting trajectory which separates these two behaviours. It connects the Gaussian fixed point in the UV to an IR nonGaussian fixed point. This corresponds to a scaling solution as described in Sect. III A, with, here,  $\alpha = \beta = d - 2$  (at all orders of perturbation theory [RSTW17]). This is called the Gribov scaling. The structure of the flow is robust against two-loop corrections, the main difference being the location of the IR scaling fixed point [GPRT19]. We stress that the latter involves large couplings for which the present perturbative analysis is not reliable. This, for instance, is reflected in the important change of the location of this fixed point from one to two loops. In contrast, the RG trajectory that describes best the lattice results is under perturbative control. Finally, the one-loop RG flow in the IRS scheme has also been studied for general dimensions [TW11, RSTW17]. Explicit expressions for the anomalous dimensions  $\gamma_A$  and  $\gamma_c$ , of similar complexity as above were obtained also for  $d = 3$  and  $d = 2$ . For  $d > 2$ , the structure of the flow is the same as the one described above in  $d = 4$ . Instead, the case  $d = 2$  is qualitatively different as there are no IR-safe trajectories, at one-loop order at least.

Once the running of the mass and coupling constant are determined, the RG-improved expressions for a vertex functions involving  $n_A$  gluon fields and  $n_c$  ghost fields are obtained, as usual, by solving the RG equation

$$\left( \mu \partial_\mu - \frac{n_A \gamma_A + n_c \gamma_c}{2} + \beta_g \partial_g + \beta_{m^2} \partial_{m^2} \right) \Gamma^{(n_A, n_c)} = 0, \quad (32)$$

whose solution relates the vertex function at different scales:

$$\Gamma^{(n_A, n_c)}(\{p_i\}, \mu, g(\mu), m^2(\mu)) = z_A^{n_A/2}(\mu) z_c^{n_c/2}(\mu) \Gamma^{(n_A, n_c)}(\{p_i\}, \mu_0, g_0, m_0^2). \quad (33)$$

This relations involves the  $z$  factors:

$$z_A(\mu) = \exp \int_{\mu_0}^{\mu} \frac{d\mu'}{\mu'} \gamma_A(\mu') = \frac{g_0^2}{g^2(\mu)} \frac{m^4(\mu)}{m_0^4} \quad (34)$$

$$z_c(\mu) = \exp \int_{\mu_0}^{\mu} \frac{d\mu'}{\mu'} \gamma_c(\mu') = \frac{g^2(\mu)}{g_0^2} \frac{m_0^2}{m^2(\mu)} \quad (35)$$

where we used Eq. (27) in the last equalities to relate these to the running coupling constant  $g(\mu)$  and mass  $m(\mu)$ , obtained by integrating the RG flow.

## B. Fitting procedure

The calculation of the RG-improved correlation functions relies on integrating the RG flow. In the standard FP theory, the initialisation of the coupling constant at some RG scale  $\mu_0$  is merely a scale-definition (this is the

---

<sup>20</sup> The general structure obtained here, with a regime of regular *vs.* singular solutions as a function of the gluon mass parameter at fixed coupling is also observed in nonperturbative continuum approaches [PLNvS04, FG04, FMP09] although the scaling exponents at the IR scaling fixed point are different than those obtained here in the IRS scheme [RSTW17].

phenomenon of dimensional transmutation). For a multidimensional flow, as in the CF model, the initialisation process has far-reaching consequences because it specifies one of the infinitely-many RG trajectories (see Fig. 4) and a change of initial condition is in general not a simple scale redefinition.

Now, following the philosophy that the gluon mass is a phenomenological parameter that we do not try to determine from first principles, its value should be fixed by using external information. The strategy is the following. One initialises the RG flow at some scale  $\mu_0$ , integrates it, compute the RG-improved correlation function by using Eq. (33) and compares it with available lattice data. One then changes the initialisation parameters so as to minimise an error function and obtain the best agreement with lattice simulations. In general, one uses the strategy of fitting simultaneously all available data. A less stringent test would consist in fitting independently different correlation functions. In this last situation, the minimum of the error function typically lies at different points in the parameter space for different correlation functions and one would obtain better agreement with lattice simulations for each one separately.

Finally, we mention that when comparing CF results with lattice data, yet another parameter must be fixed: the overall normalisation of the correlation function under study.<sup>21</sup> Consider the example of the YM propagators described in the next section. To obtain a set of curves, one needs to fix four parameters: the initial values  $g_0$  and  $m_0$  of the running coupling parameters as well as two multiplicative normalisation factors, for the gluon and for the ghost propagators.

### C. Yang-Mills propagators

The ghost and gluon propagators in YM theories have been computed at one-loop order in the perturbative CF approaches in Refs. [TW10, TW11, KWH<sup>+</sup>20, DW20] and in the screened perturbation approach in [Sir15a, Sir15b, Sir16b, Sir19a]. They give a good agreement with existing lattice data for appropriate values of the gluon mass and gauge coupling parameters. Recently, two-loop corrections have been computed [GPRT19], which clearly improve the agreement with lattice data and greatly strengthen the confidence in the validity of the CF perturbative approach. We review those latest results here.

Evaluating (33) for the two-point vertices at  $\mu = p$  and taking into account the renormalisation conditions (25), the gluon and ghost propagators can be expressed in terms of the running mass and coupling constant as

$$G(p) = \frac{m^4(p)}{m_0^4} \frac{g_0^2}{g^2(p)} \frac{1}{p^2 + m^2(p)}, \quad F(p) = \frac{g^2(p)}{g_0^2} \frac{m_0^2}{m^2(p)}. \quad (36)$$

The one- and two-loop gluon and ghost dressing functions are compared to lattice data in Fig. 5 in  $d = 4$  dimensions for  $N_c = 3$  and  $N_c = 2$ . The first remarkable point is that the comparison is very good already at one-loop order, with a global error of about 7% for  $N_c = 3$  and 10% for  $N_c = 2$  (and a maximal error of about 15%). For  $N_c = 3$ , the inclusion of the two-loop contributions clearly improves the agreement (with a global error of 4%), whereas the improvement is less significant (6%) for  $N_c = 2$  [BPRW20]. This can be understood from the fact that the coupling constant that controls the perturbative expansion is slightly larger for  $N_c = 2$  than for  $N_c = 3$ . We mention that these comparisons have also been done within other schemes and generically lead to similar results [TW11, GPRT19, DW20]. Interestingly, it is also possible to devise optimized IR safe schemes which give excellent agreement with the data already at one-loop order [DW20]. Finally, one observes that the scheme dependence is reduced when going from one to two loops and that the improvement is more pronounced in the SU(3) case, possibly for the reason mentioned above.

An important point, mentioned in Sect. III B, is that, as clearly seen from lattice simulations, the gluon propagator shows violations of positivity. To be precise, in a unitary, Lorenz-invariant theory with only positive norm states, one can prove the Källén-Lehmann representation, that is, the two following properties:

- the Euclidean propagator admits the integral representation

$$G(p) = \int_0^\infty \frac{d\mu}{2\pi} \frac{\rho(\mu)}{p^2 + \mu^2} \quad (37)$$

---

<sup>21</sup> The normalisation of correlation functions depends on both the regularisation and the renormalisation schemes and is thus different from one calculation to another, even from one lattice simulation to another. The relation between different normalisation factors could be computed in principle but this is a very difficult task in practice.

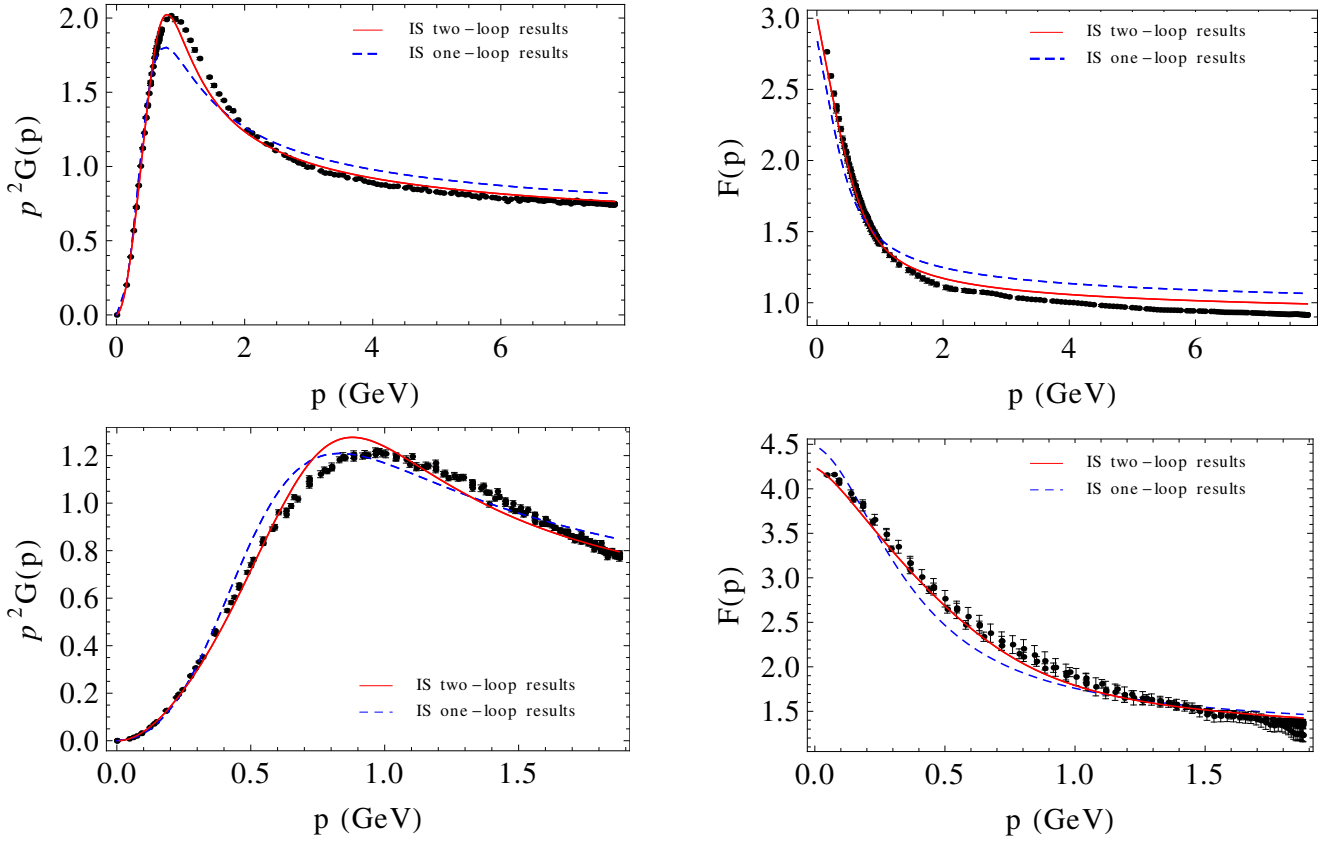


FIG. 5: The gluon (left) and ghost (right) dressing functions in  $d = 4$  for the SU(3) (top) and SU(2) (bottom) YM theories. The lines are the one- and two-loop results in the CF model. The squares are the lattice data from Ref. [DOS17] for SU(3) and from Ref. [CMM08] for SU(2). Figures from Ref. [GPRT19].

- the spectral density  $\rho(\mu)$  is positive or zero:

$$\rho(\mu) \geq 0 \quad (38)$$

It is difficult to test separately both properties by only having access to the Euclidean propagator. However, lattice simulations show that they cannot be satisfied simultaneously for the (transverse) gluon propagator. To test this, lattice simulations study the Fourier transform [CMT05, BHL<sup>+</sup>07]

$$C(t) = \int_{-\infty}^{+\infty} \frac{dp}{2\pi} e^{ipt} G(p) = \int_0^{\infty} \frac{d\mu}{2\pi} \frac{\rho(\mu)}{2\mu} e^{-\mu t} \quad (39)$$

where, in the last expression, the representation (37) was assumed. If, on top of (37), the inequality (38) is satisfied, then the function  $C(t)$  is *positive*. In Fig. 6 this function calculated in the lattice simulation [BHL<sup>+</sup>07] is compared to its one-loop expression in the CF model [TW10] for the  $N_c = 3$  case. One observes a good agreement and, clearly, the function is not positive. Similar lattice results were obtained for the  $N_c = 2$  case [CMT05]. The violation of this positivity condition on  $C(t)$  can have two origins. Either the propagator cannot be expressed in the form (37), or the representation (37) is valid, but with a density  $\rho(\mu)$  which takes negative values.

We also show, in Fig. 7, the Taylor coupling (15) as a function of momentum at one and two loops, compared to the lattice data for  $d = 4$  and  $N_c = 3$ . We find a good agreement with the lattice results and an apparent convergence of the successive perturbative orders. As mentioned before, a similar analysis can be made for  $N_c = 2$ , where, however, the maximum value of the coupling is slightly larger. Although the perturbative analysis is still valid, this seems to slow the apparent convergence [GPRT19, BPRW20].

The propagators have also been evaluated at one loop in  $d = 3$  dimensions [TW11, PTW13] and compared to existing numerical simulations for  $N_c = 2$ . Again, a fairly good agreement is obtained although the results are not as good as for  $d = 4$ . Finally, simulations have also been carried out for  $d = 2$  but, as mentioned previously, the

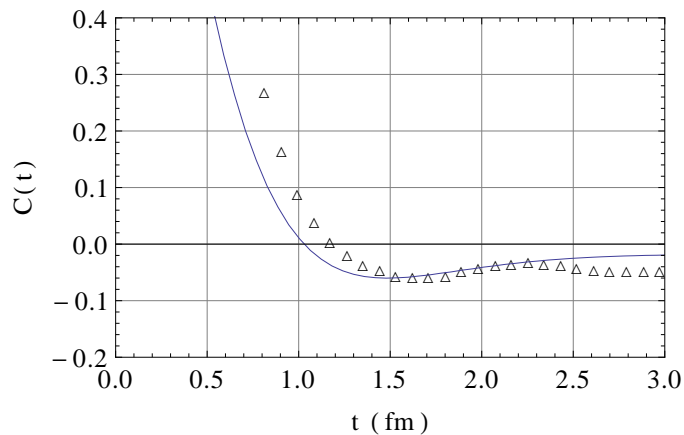


FIG. 6: The function  $C(t)$  defined in Eq. (39) as obtained from lattice simulations [BHL<sup>+</sup>07] (triangles) compared to CF result [TW10] (dots) in the  $N_c = 3$  case. The parameters are fixed by fitting the Euclidean propagators. A normalisation factor has been introduced to account for the multiplicative renormalisation of the lattice propagator.

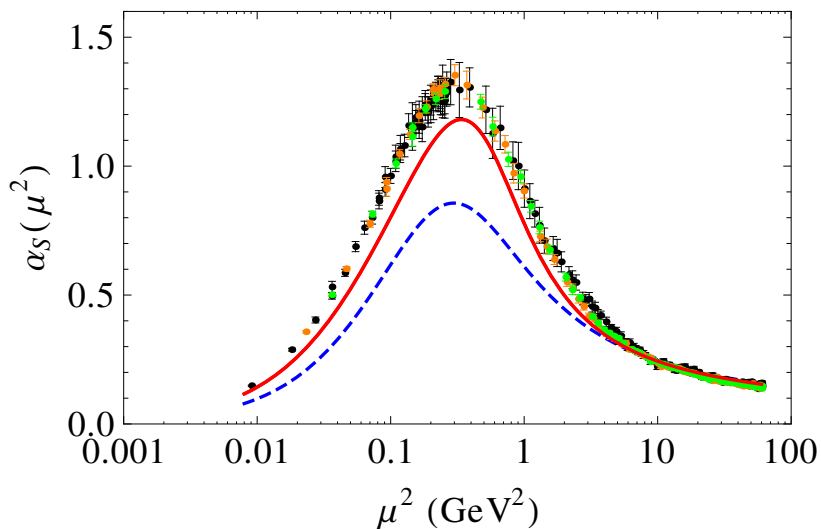


FIG. 7: The strong coupling constant in the Taylor scheme. The data points are those of Ref. [DOS16]. The dashed and plain lines correspond to the one-loop and two-loop CF results in the IRS scheme, respectively. In both cases, a normalisation factor is applied so that the value  $\alpha_S(\mu_0)$  agrees with the lattice result at  $\mu_0 = 10$  GeV; see Ref. [GPRT19] for details.

perturbative approach considered here is not applicable in that case. Also noteworthy is the fact that the positivity violations mentioned earlier are already produced at one-loop order in  $d > 2$  [TW10, TW11, RSTW17], thus implying that the tree-level mass term in the CF Lagrangian does not correspond to an actual massive excitation in the spectrum.

We thus see that a perturbative description is able to correctly describe nontrivial features of the YM propagators even at IR momenta. This validates—at the level of propagators for the moment—our working hypothesis concerning the perturbative CF model. This challenges the standard paradigm of the nonperturbative IR regime.

#### D. Yang-Mills three-point functions

In order to further test the ability of the CF model to reproduce the YM correlators, and now that the parameters have been fixed from the fits to two-point functions, the next natural step is to study the predictions of the model regarding higher correlation functions. In this section, we consider the three-gluon vertex and the ghost-gluon vertex, that have both been computed in lattice simulations for the YM theory in the Landau gauge for particular configu-

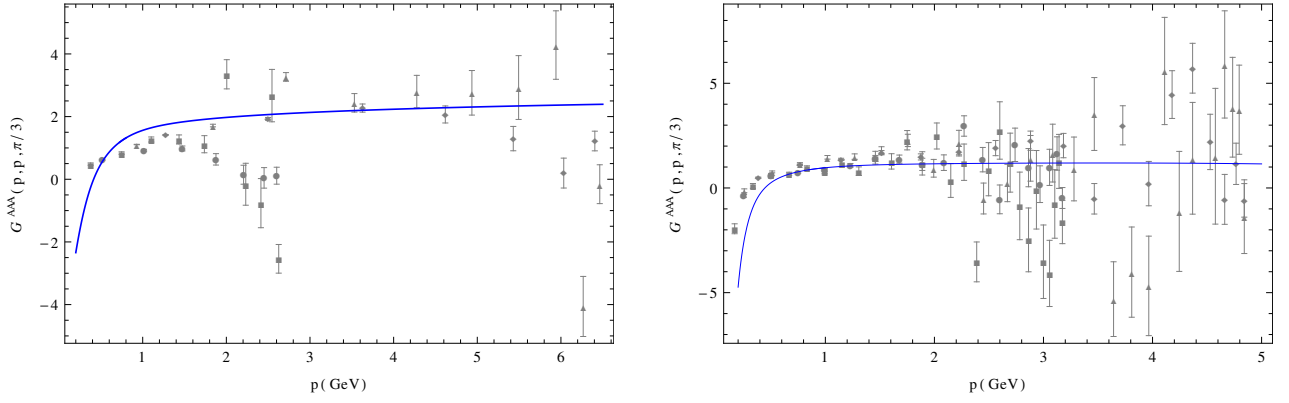


FIG. 8: Three gluon correlation function  $G^{AAA}(p, k, r)$  for  $p^2 = k^2 = r^2$  (employing the notations of Ref. [PTW13]) in  $d = 4$  (left) and  $d = 3$  (right). The blue curves correspond to the IRS scheme whereas the red dashed curves correspond to a vanishing momentum scheme. Lattice data from Ref. [CMM08, Maa20]. Figure extracted from Ref. [PTW13].

rations of momenta, for the SU(2) gauge group in  $d = 4$  and  $d = 3$  dimensions [CMM08, Maa20] and, more recently, also for the SU(3) gauge group in  $d = 4$  [IMPS<sup>+</sup>07, Ste06, SBK<sup>+</sup>17, BDSRQZ17, ZBDS<sup>+</sup>19, CZB<sup>+</sup>20, ADSF<sup>+</sup>20].<sup>22</sup>

### 1. The three-gluon vertex

In linear covariant gauges (including the Landau gauge), the colour structure of this vertex is proportional to the structure constants  $f^{abc}$  at all orders of perturbation theory [Smo82]. It can be decomposed in terms of six tensor components associated to the Lorentz group. We use the decomposition proposed by Ball and Chiu [BC80]:

$$\Gamma_{A_\mu^a A_\nu^b A_\rho^c}^{(3)}(p, k, r) = -ig_0 f^{abc} \Gamma_{\mu\nu\rho}(p, k, r). \quad (40)$$

with

$$\begin{aligned} \Gamma_{\mu\nu\rho}(p, k, r) = & A(p^2, k^2, r^2) \delta_{\mu\nu} (p - k)_\rho + B(p^2, k^2, r^2) \delta_{\mu\nu} (p + k)_\rho - C(p^2, k^2, r^2) (\delta_{\mu\nu} p \cdot k - p_\nu k_\mu) (p - k)_\rho \\ & + \frac{1}{3} S(p^2, k^2, r^2) (p_\rho k_\mu r_\nu + p_\nu k_\rho r_\mu) + F(p^2, k^2, r^2) (\delta_{\mu\nu} p \cdot k - p_\nu k_\mu) (p_\rho k \cdot r - k_\rho p \cdot r) \\ & + H(p^2, k^2, r^2) \left[ -\delta_{\mu\nu} (p_\rho k \cdot r - k_\rho p \cdot r) + \frac{1}{3} (p_\rho k_\mu r_\nu - p_\nu k_\rho r_\mu) \right] + \text{perm.}, \end{aligned} \quad (41)$$

where “perm.” stands for the simultaneously cyclic permutations of the momenta  $(p, k, r)$  and the indices  $(\mu, \nu, \rho)$ . The scalar functions  $A$ ,  $C$ , and  $F$  are symmetric under permutation of their first two arguments, whereas  $B$  is antisymmetric. The function  $H$  is completely symmetric and  $S$  is completely antisymmetric. All the tensorial components above have been computed at one-loop order in the CF model, for arbitrary momenta [PTW13]. It has been checked that the one-loop expressions reduce to the known ones in the FP model [DOT96] in the limit  $m \rightarrow 0$ . The expressions are rather cumbersome and we shall not reproduce them here. Instead, we focus on the comparison with lattice data.

It is worth emphasising that what is measured in lattice simulations are correlators, which involve a contraction of the external legs of the vertex (41) with (transverse) gluon propagators. It follows that the longitudinal structures, controlled by the functions  $B$  and  $S$ , are not accessible with the existing simulations. What has actually been calculated in the Monte-Carlo simulations for the SU(2) theory is the following quantity

$$G^{AAA}(p, k, r) = \frac{\lambda_{\mu\nu\rho}^{\text{tree}}(p, k, r) \Gamma_{\mu\nu\rho}(p, k, r)}{\lambda_{\mu\nu\rho}^{\text{tree}}(p, k, r) \lambda_{\mu\nu\rho}^{\text{tree}}(p, k, r)}. \quad (42)$$

<sup>22</sup> We mention that more precise data for the three-point correlators have been produced since then [ADSF<sup>+</sup>21].

where

$$\lambda_{\mu\nu\rho}^{\text{tree}}(p, k, r) = P_{\mu\alpha}^{\perp}(p)P_{\nu\beta}^{\perp}(k)P_{\rho\gamma}^{\perp}(r) [\delta_{\beta\gamma}(k-r)_{\alpha} + \delta_{\alpha\gamma}(r-p)_{\beta} + \delta_{\alpha\beta}(p-k)_{\gamma}]. \quad (43)$$

Eq. (42) corresponds to the transverse part of the three-gluon vertex projected along the tree-level tensorial component  $[\delta_{\beta\gamma}(k-r)_{\alpha} + \text{cyclic permutations}]$ , normalised by the same combination at tree level.

In Fig. 8, we show a comparison between the one-loop results in the CF model and the lattice data for the combination (42) for a particular configuration of momenta in both  $d = 4$  and  $d = 3$  dimensions. The overall agreement is satisfactory, although not as good as for the propagators. We stress that the lattice data show important statistical and (even larger) systematic uncertainties. This is clearly visible in Fig. 8 where the various lattice points are statistically incompatible among each other. For this reason, it is not obvious to assess the actual accuracy of the CF prediction. The one-loop expressions of Ref. [PTW13] have been compared to lattice data for all measured configurations of momenta, which yields a similar level of accuracy. The SU(3) case has also been treated in lattice simulations [BDSRQZ17] and compared to the one-loop predictions of the CF model [FP], with results of similar quality to those presented in Fig. 8. We recall that these comparison involve no fitting parameters except for an overall normalisation.<sup>23</sup>

In Fig. 8, one clearly observes, for  $d = 3$ , what has been referred to as a *zero crossing*: The vertex function becomes negative for small enough values of momenta. The same behaviour is observed also for other configurations of momenta. This feature, first observed in lattice simulations [CMM08], is a very simple prediction of the perturbative CF model at one-loop order.<sup>24</sup> It simply comes from the fact that, at very low momenta, the three-gluon vertex is dominated by the ghost-loop diagram which comes with the opposite sign as compared to the tree-level term. This implies, not only a zero crossing, but a divergence towards negative infinity when all momenta vanish. The same behaviour is also predicted in  $d = 4$  but for much smaller values of momenta, the divergence being only logarithmic [PTW13]. This explains why this is more difficult to see in lattice simulations [ADSF<sup>+</sup>21].

Finally, we note that the phenomenon of ghost dominance at low momenta, responsible for the above-mentioned zero crossing, is of a more general scope. For instance, it is also valid for other continuum approaches, such as the DSE or the FRG. It also plays a pivotal role for finite temperature physics, as discussed in Sec. VII. Finally, it provides a simple description of the dominant low momentum behaviour of vertex functions [TW11]. Let us describe this last point here. Characterizing correlation functions with more external legs becomes very involved because more and more Feynman diagrams must be computed and because the number of independent tensorial structures increases rapidly with the number of external legs. It is, however, possible to extract some information concerning the deep IR regime (that is, when all external momenta are small compared to the gluon mass) at a low computational cost [TW11]. In this regime, the vertex is dominated by the Feynman diagrams with the smallest number of (massive) gluon propagators. Moreover, at fixed number of external legs, the Feynman diagrams with more and more loops are suppressed for IR momenta. As a result, the leading IR behaviour is given by a one-loop diagram (barring an accidental compensation of diagrams). It is then possible to predict the leading IR behaviour of a vertex. For instance, the gluon self-energy is dominated by a one-ghost-loop diagram, which behaves, in  $d = 4$ , as  $\text{const.} + p^2 \ln(p^2/m^2)$  in the deep IR. Similarly, the three-gluon vertex behaves as  $p \ln(p^2/m^2)$ , which explains the zero crossing described in above. In general, the  $n$ -gluon vertex with  $n > 2$  behaves as  $p^{4-n}$  modulo logarithms.

## 2. The ghost-gluon vertex

The ghost-antighost-gluon vertex—usually dubbed ghost-gluon vertex for short—has a much simpler Lorentz structure than the three-gluon vertex. It can be decomposed in terms of two vectorial components as

$$\Gamma_{c\bar{a}bA_{\mu}^c}^{(3)}(p, k, r) = -ig_0 f^{abc} [k_{\mu}V(p^2, k^2, r^2) + r_{\mu}W(p^2, k^2, r^2)], \quad (44)$$

where  $p$ ,  $k$ , and  $r$  are the (incoming) momenta of the ghost, antighost and gluon, respectively. Only the scalar function  $V(p^2, k^2, r^2)$  is measurable in Landau gauge lattice simulations for it is the only term that contributes when the vertex is contracted with a (transverse) gluon propagator.

<sup>23</sup> The normalisation is not fixed by fitting the (renormalised) propagators because the data presented here [CMM08, Maa20] concern the bare three-point correlator.

<sup>24</sup> In fact, the zero crossing has been first explained in a continuum approach in the CF model calculation of [PTW13] and has later been observed in other continuum approaches [ABIP14, BHMvS14, EWAV14, ABB<sup>+</sup>16, BDSRQZ17].

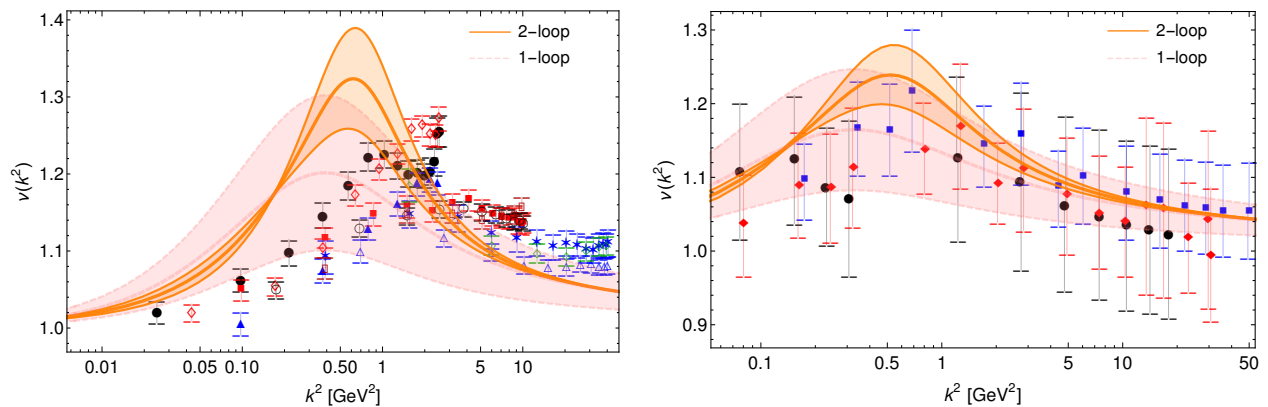


FIG. 9: The CF model prediction for the function  $v(k^2)$  in the SU(2) (left) and SU(3) case (right) in the IRS scheme, compared to the lattice data in the Taylor scheme from Ref. [Maa20] for SU(2) and from Ref. [IMPS<sup>+</sup>07, Ste06] for SU(3). The parameters  $m$  and  $g$  at the initial scale  $\mu_0$  where previously determined from the fits of the gluon and ghost propagators. Figures from Ref. [BGPR21].

Both vectorial components in Eq. (44) have been computed at one-loop order in the CF model for arbitrary momenta in  $d = 3$  and  $d = 4$  and for any  $N_c$  [PTW13]. The various symmetries of the model [TW09] give rise to (Ward and Slavnov-Taylor) identities that, first, constrain the three-gluon and the ghost-gluon vertices separately and, second, imply nontrivial relations between those. It has been checked that the one-loop CF expressions verify these identities and that they reduce to the known one-loop expressions in the FP model [DOT96] in the limit  $m \rightarrow 0$ .

The one-loop CF results have been compared to the existing lattice data. In a similar way as for the three-gluon vertex, what has been measured in the Monte-Carlo simulations is the following quantity:

$$G^{c\bar{c}A}(p, k, r) = \frac{k_\mu P_{\mu\nu}^\perp(r) [k_\nu V(p^2, k^2, r^2) + r_\nu W(p^2, k^2, r^2)]}{k_\mu P_{\mu\nu}^\perp(r) k_\nu} = V(p^2, k^2, r^2). \quad (45)$$

Again, this corresponds to the transverse part of the ghost-gluon vertex projected on the tree-level tensorial structure, normalised to the same combination at tree level. Thanks to Taylor's nonrenormalisation theorem, the expression (45) associated with the ghost-gluon vertex is UV finite and is identical to its tree-level form when the ghost momentum vanishes. This is to be contrasted with the quotient (42), which has a multiplicative UV divergence and needs to be renormalised.

On top of the full one-loop expressions of Ref. [PTW13], two-loop corrections to the ghost-gluon vertex have been calculated in Ref. [BPRW20]. The calculation is quite involved for general momentum configurations and the two-loop contribution has only been computed for the case of vanishing gluon momentum, namely,

$$v(k^2) = V(k^2, k^2, 0), \quad (46)$$

in  $d = 4$  and for both  $N_c = 2$  and  $N_c = 3$ . Even for this particular momentum configuration, the calculation requires the use of symbolic programming, similar to that used in the case of the two-loop propagators (see Sect. V C). It has been explicitly verified that the two-loops expressions fulfil several nontrivial consistency checks [BPRW20]:

- The divergent parts are compatible with the Taylor nonrenormalisation theorem.
- In the limit  $m \rightarrow 0$ , the expressions reduce to those of the FP theory, obtained for the same configuration of momenta in Ref. [DOT98].
- The one- and two-loops contributions vanish in the limit of zero ghost momentum, that is,  $v(k^2 = 0) = 1$ .

We stress that this last property which is clearly observed in lattice simulations is not retrieved from the usual (massless) calculations because of IR divergences which induce a nonanalytic behaviour at small momenta. Specifically, fixing first the gluon momentum to zero and later taking the limit of vanishing ghost momentum leads to a divergence of the vertex, at odds with the lattice data. The CF mass removes this IR divergence and yields the correct nonrenormalisation behaviour.

The one- and two-loop expressions of Refs. [PTW13, BPRW20] are compared with the lattice data from Refs. [Maa20] for  $N_c = 2$  and from Refs. [IMPS<sup>+</sup>07, Ste06] for  $N_c = 3$  in Fig. 9. It should be noted that this

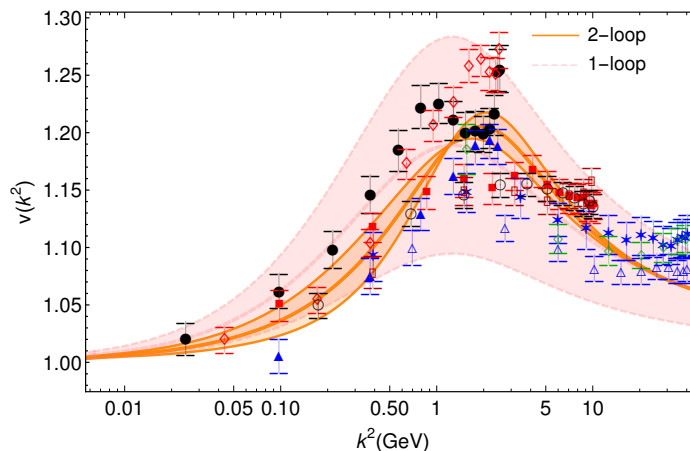


FIG. 10: The best fit for the vertex function  $v(k^2)$  in the SU(2) case at one- and two-loop orders [PTW13, BPRW20] in the IRS scheme, when compared to the lattice data in the Taylor scheme [Maa20]. Figure from Ref. [BGPR21].

comparison is done without any further parameter adjustment than the one used to fit the propagators (not even an overall normalisation factor). Because the fit of the latter for the SU(2) group is of lower quality than that for the SU(3) group, due, in part, to possible systematic errors in the lattice simulations, this can introduce a significant error in the parameter estimation. For this reason a second type of fit, including the ghost-gluon vertex together with the ghost and the gluon propagators, was considered in Ref. [BPRW20]. The corresponding results are shown in Fig. 10.

The first observation is that the one-loop results provide a good description of the data, although not as good as for the two-point functions. For both  $N_c = 2$  and  $N_c = 3$ , the quality of the comparison with the simulations improves when going from one loop to two loops. However, the improvement is significantly better for SU(3) as was already the case for the propagators.

To conclude, the perturbative results in the CF model are quite good. In fact, in the case of three-point vertices, it is not clear that, with the level of precision achieved, it is possible to completely neglect the errors coming from the lattice simulations. Put together, these results strongly indicate that the perturbative expansion of the CF model accurately describes the YM vacuum correlation functions in the Landau gauge. This is not only true for the two-point functions but also for three-point functions. Moreover, whenever tested, the precision improves when including higher orders of perturbation theory.

## VI. DYNAMICAL QUARKS

In the previous section, we put forward evidences which indicate that the IR regime of YM theory can be described within perturbation theory, the main nonperturbative ingredient being encapsulated in a phenomenological screening mass for the gluons. Focusing on a pure gauge theory is clearly simpler (it involves less Feynman diagrams, renormalisation factors, etc) and, at the same time, it is a first step for testing the working hypothesis under scrutiny. But, of course, these results are mainly methodological since the true QCD involves also light quarks with significant fluctuations. In this section, we discuss the attempts to include these particles to the perturbative scheme described in Section V.

Many physical phenomena occur in the presence of matter fields, which have no equivalent in the pure YM theory. Of utmost importance is the phenomenon of spontaneous chiral symmetry breaking. In a nutshell, the Dirac Lagrangian (2) for massless quarks is invariant under chiral transformations which rotate independently the left and right parts of the Dirac bispinor. This symmetry happens to be spontaneously broken by quantum fluctuations, which implies that, even if the valence quark mass (*i.e.*, the quark mass at a scale of the order of few GeV) is small, the constituent quark mass (the one defined at an IR scale, relevant, *e.g.*, for computing the mass of a hadron) is significantly larger.

At a technical level, dynamical quarks are taken into account by adding the Dirac Lagrangian (2) to the CF action. The theory is renormalisable and requires new renormalisation factors, for the quark field and masses,  $\psi = \sqrt{Z_\psi}\psi_R$ ,  $M_{b,i} = Z_{M,i}M_i$ .

In what follows, we describe the perturbative calculations of the propagators and the quark-antiquark-gluon vertex of the unquenched theory in the vacuum. For not too light quarks, they compare well with existing lattice data, as reviewed in Subsections VIA and VIB below. The dynamics of light quarks is strongly coupled and requires a more

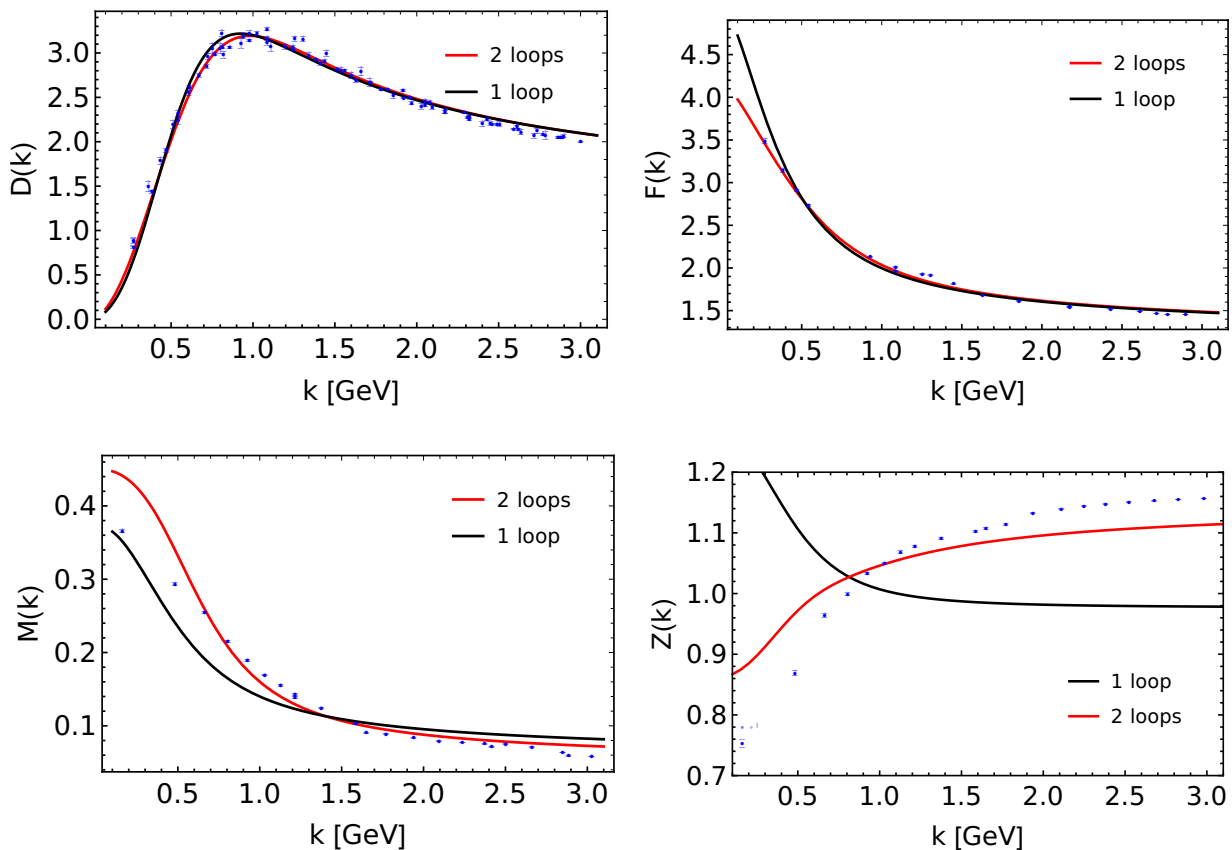


FIG. 11: The various propagators at one- and two-loop orders for  $N_f = 2$  degenerate normalis in  $d = 4$ . The upper plots present the gluon (left) and ghost (right) dressing functions whereas the lower plots show the quark mass (left) and dressing function (right). The parameters (defined at the scale  $\mu_0 = 1$  GeV) are  $g_0 = 4.53$ ,  $m_0 = 430$  MeV, and  $M_0 = 140$  MeV at one loop and  $g_0 = 4.10$ ,  $m_0 = 390$  MeV, and  $M_0 = 160$  MeV at two loops. The points are the lattice data of Ref. [OSSS19] for  $M_\pi = 426$  MeV. Figures from Ref. [BGPR21].

elaborate treatment, discussed in Subsection VIC.

### A. Propagators.

The calculation of the gluon, ghost, and quark propagators in perturbation theory is straightforward [PTW14, Sir16a, HK20, BGPR21]. At strict one-loop order, the ghost propagator is unchanged as compared to the quenched case whereas the gluon propagator receives an additional quark loop contribution. The RG running yields an additional source of normalis dependence which affects all propagators [PTW14, PTW15]. As in the quenched case, these calculations have been recently pushed to two-loop order, first, to assess the (apparent) convergence of the perturbative expansion and, second, to elucidate the case of the quark dressing function, which receives significant two-loop contributions [BGPR21]. The details of the calculations, with and without RG improvement can be found in the mentioned references. Here, we give a brief summary of the comparison of the perturbative results for the propagators with various lattice data for different flavour contents and different quark masses [BHL<sup>+</sup>04, BHL<sup>+</sup>05, ABB<sup>+</sup>12, SMMPvS12, OSSS19].

The first observation is that the sensitivity of the unquenched ghost and gluon propagators to the normalis content of the theory is well described by the one-loop results. One observes though that, for a given normalis content, these propagators are rather insensitive to the precise values of the quark masses in the range of at most a few hundred MeV. The renormalised quark propagator

$$S(p) = \frac{Z(p)}{-i\not{p} + M(p)} = Z(p) \frac{i\not{p} + M(p)}{p^2 + M^2(p)} \quad (47)$$

has two independent components, the (RG invariant) mass function  $M(p)$  and the dressing function  $Z(p)$ , which are

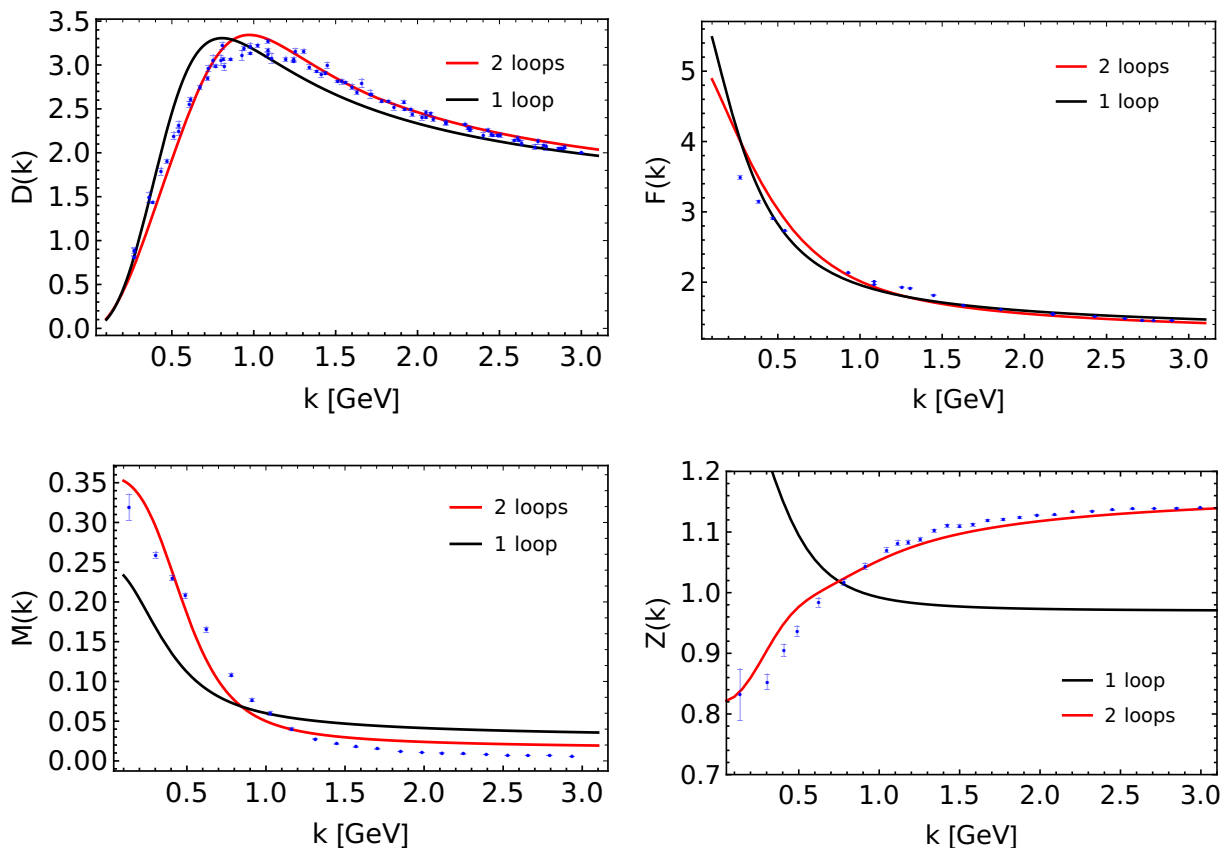


FIG. 12: The various propagators at one- and two-loop orders for  $N_f = 2$  degenerate normalised in  $d = 4$ . The upper plots present the gluon (left) and ghost (right) dressing functions whereas the lower plots show the quark mass (left) and dressing function (right). The parameters (defined at the scale  $\mu_0 = 1$  GeV) are  $g_0 = 4.29$ ,  $m_0 = 350$  MeV, and  $M_0 = 60$  MeV at one loop and  $g_0 = 4.35$ ,  $m_0 = 360$  MeV, and  $M_0 = 50$  MeV at two loops. The points are the lattice data of Ref. [OSSS19] for  $M_\pi = 150$  MeV. Figures from Ref. [BGPR21].

both well measured on the lattice. One can easily find values of the parameters for which the former is well reproduced by the one-loop results, in particular, if one only fits this function, independently of the others. Of course, fitting only one function can lead to artificially good results and, in order to obtain a realistic estimate of the quality of the one-loop approximation, one should fit all possible data with a single set of parameters. This is shown in Figs. 11 and 12, for the lattice data of Refs. [SMMPvS12, OSSS19], corresponding to  $N_f = 2$  and two values of the pion mass  $M_\pi$  (or, equivalently, of the bare quark mass). One observes that the one-loop results indeed give a satisfactory description of the data, including the quark mass function. Instead, the one-loop quark dressing function compares badly to lattice data. As anticipated in Ref. [PTW14], this is because the one-loop contribution to this function is abnormally small in the CF model—it vanishes identically in the FP theory—and higher-loop effects are not negligible in comparison.

The perturbative calculations of the QCD propagators have recently been pushed up to two-loop order [BGPR21]. As in the quenched case, this allows one to really assess the reliability of the perturbative CF description. Again, we refer the reader to Ref. [BGPR21] for details and, here, we just show the quality of the results in Figs. 11 and 12. The two-loop corrections clearly improve the one-loop results, in particular, for what concerns the quark dressing function. One also observes that the quality of the perturbative description is better for larger quark (or pion) masses.<sup>25</sup> In fact, if one finds that the gluon, ghost and quark dressing functions seems always well-described by the two-loop perturbative results, this is not quite so for the quark mass function, in particular, for low pion masses. This is to be expected as the latter is directly sensitive to the dynamical breaking of the chiral symmetry in the chiral limit.

<sup>25</sup> It may seem, at first sight, that the quality of the fits are equally good for heavy and light quarks, Figs. 11 and 12, respectively. However, as explained below, the detailed analysis of the errors reveals that it is not the case.

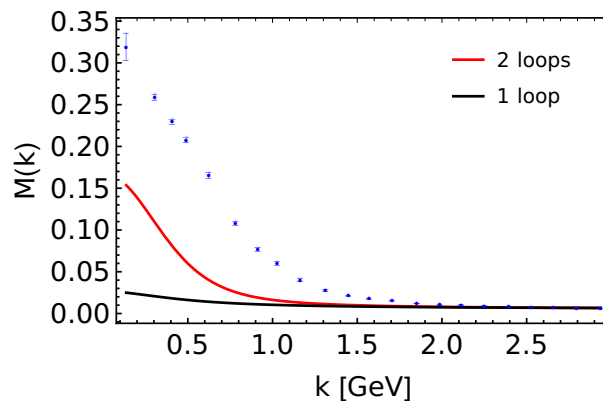


FIG. 13: The quark mass function at one and two-loop orders as compared to the lattice data of Ref. [OSSS19] for  $M_\pi = 150$  MeV. Here, the quark mass parameter  $M_0$  is not part of the fit but is fixed to the lattice value at the UV scale  $\mu_0 = 2.94$  GeV. Figure from Ref. [BGPR21].

This is clearly visible in Fig. 12, corresponding to a rather unfavourable case, with  $M_\pi = 150$  MeV—close to the experimental value  $m_\pi = 140$  MeV. Perturbative calculations give an accurate description of the data from the IR to the UV, except for the quark mass function. Indeed, the good fit of the quark mass in the IR is at the expense of a rather poor description in the UV, even at two-loop order. If one insists, instead, on correctly describing the UV for the quark mass function, the fit deteriorates in the IR, as shown in Fig. 13. Thus, although the two-loop corrections improve significantly the one-loop results, the perturbative results are not able to reproduce the dynamical generation of the quark mass in the IR. That is a manifestation of the fact that the phenomenon of spontaneous chiral symmetry breaking is not captured at any finite order in perturbation theory and thus requires a more involved approximation scheme. This is discussed in Section VIC below.

### B. The quark-gluon vertex

The quark-antiquark-gluon vertex has also been studied in lattice simulations [SBK<sup>+</sup>03, SBK<sup>+</sup>05, KLSW07, SBK<sup>+</sup>17, KOS<sup>+</sup>21, OFdPdM18] and can thus be used to further test the perturbative CF approach. This vertex has a rich Dirac structure, with twelve scalar functions of three momentum variables [SK02]. Only those which are transverse with respect to the gluon momentum are accessible to lattice simulations (in the Landau gauge) and only a restricted set (and for particular momentum configurations) have actually been measured. All have been computed at one-loop order in the CF model in Ref. [PTW15] and compared to lattice data, which we review here. One adjusts the parameters<sup>26</sup>  $g_0$ ,  $m_0$ , and  $M_0$  of the model by fitting the correlators as in the previous subsection, following a similar procedure as the one outlined in Sect. VB for the YM case. Once this is done, the results for the various components of the three-point function are pure predictions of the model, apart from a normalisation factor, similar to the case of the three-gluon vertex. Another remark is that the results of Refs. [SBK<sup>+</sup>03, SBK<sup>+</sup>05] are quenched ( $N_f = 0$ ) lattice data. The comparison with the perturbative expressions for the quark-antiquark-gluon vertex are still meaningful because there are no quark loop contributions at one-loop order. Flavour effects only enters through the RG running of the parameters so, in these comparisons, the quenched running was used.<sup>27</sup> We focus below on the particular configurations of momenta that have been studied in lattice simulations.

For vanishing gluon momentum, the vertex has the following form

$$\Gamma_\mu(p, -p, 0) = -ig_g \left[ \lambda_1(p) P_{\mu\nu}^\perp(p) + 4\tilde{\lambda}_2(p) P_{\mu\nu}^\parallel(p) \right] \gamma_\nu - 2g_g \lambda_3(p) p_\mu, \quad (48)$$

where, as before,  $P_{\mu\nu}^\perp(p) = \delta_{\mu\nu} - p_\mu p_\nu / p^2$  and  $P_{\mu\nu}^\parallel(p) = p_\mu p_\nu / p^2$ . The function  $\lambda_1(p)$  thus quantifies the renormalisation of the classical contribution  $\propto \gamma_\mu$  in units of the (running) coupling  $g_g$ , defined as the ghost-antighost-gluon coupling

<sup>26</sup> In the previous section, the quark mass parameter is included in the fit together with  $m_0$  and  $g_0$ . In the present and the next sections, instead, it is simply fixed to agree with the lattice value  $M(\mu_0)$  at the scale  $\mu_0$ .

<sup>27</sup> Since the work of [PTW15], new lattice data have been produced with dynamical quarks [SBK<sup>+</sup>17, KOS<sup>+</sup>21, OFdPdM18].

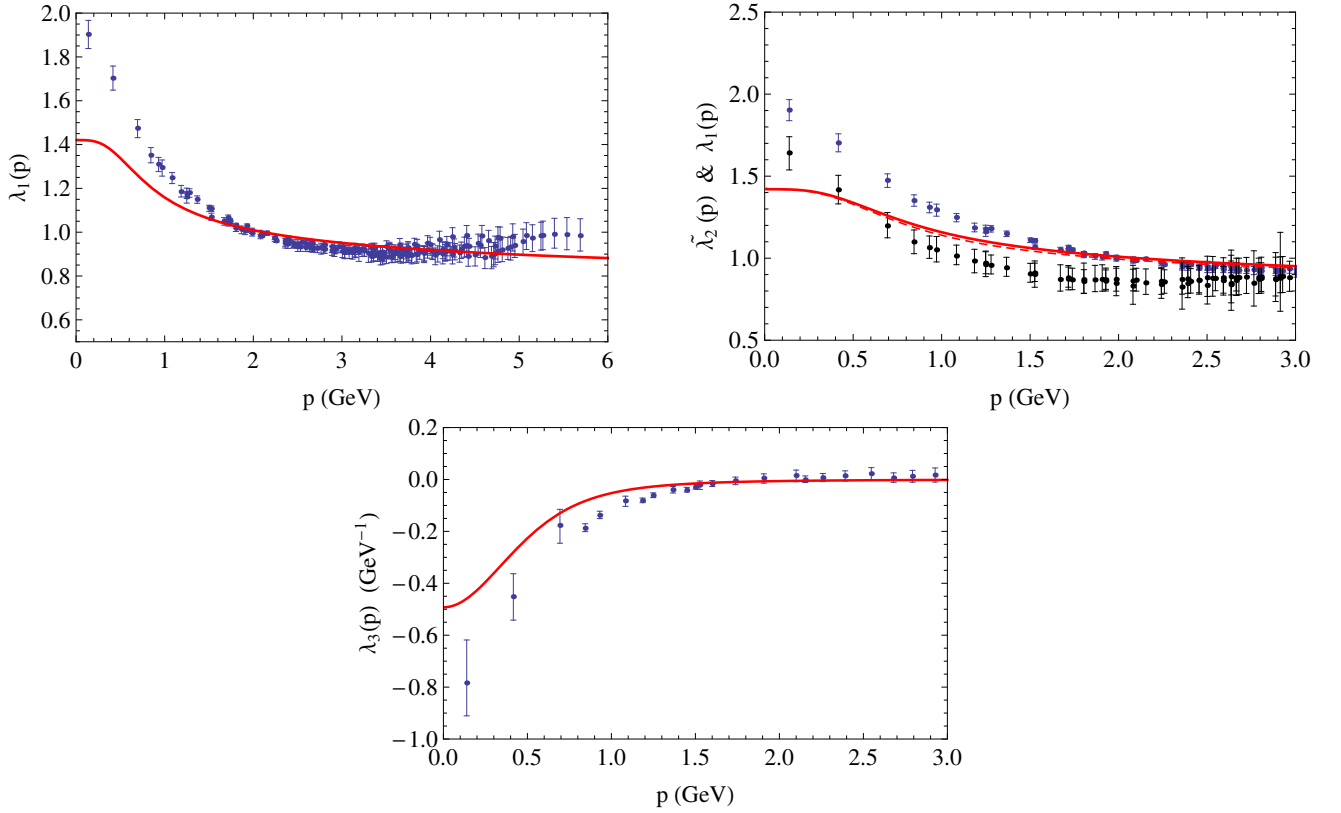


FIG. 14: Scalar functions of the quark-gluon vertex at vanishing gluon momentum,  $\lambda_1$ ,  $\tilde{\lambda}_2$ , and  $\lambda_3$ , as functions of the quark momentum. The lines are the one-loop results with  $M_0 = 0.2$  GeV,  $m_0 = 0.44$  GeV and  $g_0 = 4.2$  at the scale  $\mu_0 = 1$  GeV whereas the dots correspond to the lattice data of Ref. [SBK<sup>+</sup>03]. The second figure shows both  $\lambda_1$  (plain line, blue dots) and  $\tilde{\lambda}_2$  (dashed line, black dots). The one-loop curves are almost superimposed. Figures from Ref. [PTW15].

in the Taylor scheme. The functions  $\lambda_1(p)$ ,  $\tilde{\lambda}_2(p)$ , and  $\lambda_3(p)$  are shown in Fig. 14. The agreement between the one-loop results and the lattice data is very good given the simplicity of the approximation.

The quark-gluon vertex has also been measured in lattice simulations for equal quark and antiquark momenta  $p$  (so that the gluon momentum is  $k = -2p$ ), which involves two other scalar functions  $\tau_3$  and  $\tau_5$ :

$$\Gamma_\mu(p, p, -2p) = -ig_g [\lambda'_1(p)\gamma_\mu + 4\tau_3(p)\not{p}p_\mu - 2i\tau_5(p)\sigma_{\mu\nu}p_\nu], \quad (49)$$

where  $\sigma_{\mu\nu} = \frac{i}{2}[\gamma_\mu, \gamma_\nu]$  and  $\lambda'_1(p) = \lambda_1(p) - 4p^2\tau_3(p)$ . The functions  $\lambda'_1$  and  $\tau_5$  are shown in Fig. 15. The functions  $\lambda_1$  and  $\tau_3$  are also defined for other momentum configurations and comparisons of similar quality have been obtained between one-loop results and lattice data [PTW15].

Summarising, in all the investigated cases, the agreement is good in view of the fact that there is no adjustable parameter apart from an overall normalisation in this comparison. As in the pure gauge (quenched) theory, we thus conclude that part of the IR dynamics in the presence of dynamical quarks is well described by perturbative means in the CF model. The expected nonperturbative effects in the FP theory are partly taken into account in a simple gluon mass term. An important observation though is that the agreement between lattice data and one-loop results is generally less good at very low momenta. One explanation is that the quark-gluon coupling becomes too large in the IR for a reliable perturbative treatment. For instance, defining an effective quark-gluon coupling  $g_q$  as the coefficient of the classical structure  $\propto \gamma_\mu$  of the quark-antiquark-gluon vertex at vanishing gluon momentum, *i.e.*,  $g_q = g_g\lambda_1$ , we see, from the lattice data presented in Fig. 14 that the ratio between the couplings in the quark and in the pure gauge sectors  $g_q/g_g = \lambda_1$  can be as large as 2 in the deep IR. This implies that the perturbative expansion parameter in the quark sector  $\lambda_q = N_c g_q^2 / (16\pi^2)$  can reach up to four times that of the pure gauge sector. With the typical value  $g_g \sim 4$  for  $N_c = 3$ , that is,  $\lambda_g \sim 0.3$ , the parameter  $\lambda_q$  can reach up to 1.2 in the deep IR, a value for which a

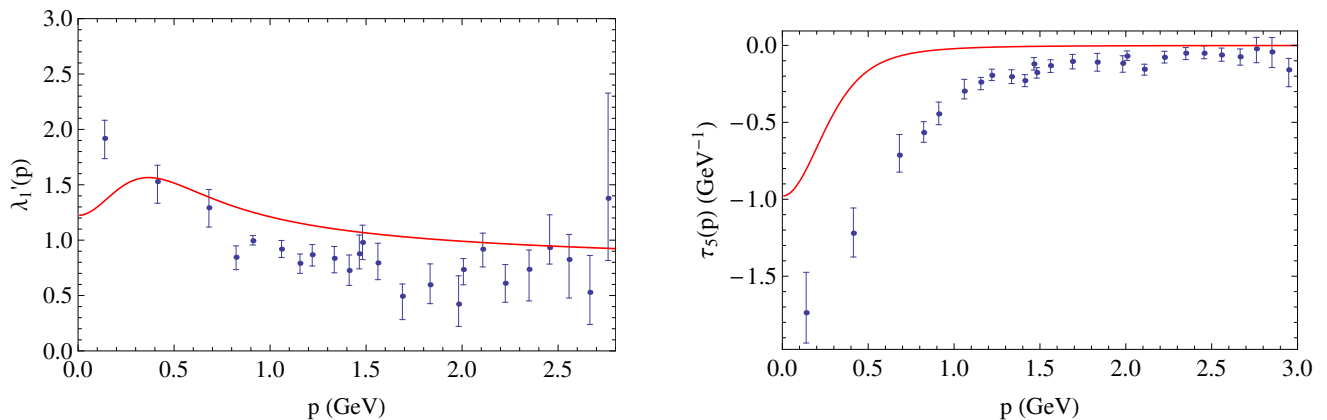


FIG. 15: The scalar components  $\lambda_1'$  and  $\tau_5$  of the quark-antiquark-gluon vertex for equal momentum  $p$  of the quark and antiquark; see Eq. (49). The parameters are  $M_0 = 0.2$  GeV,  $m_0 = 0.44$  GeV and  $g_0 = 4.2$  at the scale  $\mu_0 = 1$  GeV. Figure from Ref. [PTW15].

perturbative expansion is clearly invalid.<sup>28</sup>

### C. The rainbow-improved perturbative expansion and the spontaneous breaking of chiral symmetry.

The above observation that a straightforward coupling expansion is inadequate to treat the dynamics of light quarks goes along with the fact that the phenomenon of dynamical chiral symmetry breaking is not captured at any finite loop order in the CF—let alone in the FP—model. This, together with the fact that the coupling that governs the pure gauge sector remains small-to-moderate, motivates a perturbative expansion in the pure gauge coupling  $g_g$  alone, keeping all orders in the quark coupling  $g_q$ . One can further exploits another effectively small parameter in  $SU(N_c)$  gauge theories, namely  $1/N_c$ . Although  $N_c = 3$  in QCD, it is well-known that a  $1/N_c$  expansion successfully captures essential aspects of the dynamics [tH74, Wit79, DL16].

In Refs. [PRS<sup>+</sup>17, PRS<sup>+</sup>21], a controlled approximation scheme for IR QCD has been proposed, based on a double expansion of the CF model in the two parameters  $g_g$  and  $1/N_c$ . For instance, at leading order, the propagators in the gauge sector (ghost and gluon) are given by their tree-level expression whereas the quark self-energy includes the infinite set of so-called rainbow diagrams with a massive one-gluon exchange. This results in coupled integral equations for the quark renormalisation and mass functions which read, in terms of bare quantities,

$$Z^{-1}(p) = 1 - g_{q,b}^2 C_F \int_{\Lambda} \frac{d^4 q}{(2\pi)^4} \frac{Z(q)}{q^2 + M^2(q)} \frac{2\ell^4 - (p^2 + q^2)(p^2 + q^2 + \ell^2)}{p^2 \ell^2 (\ell^2 + m_b^2)} \quad (50)$$

$$Z^{-1}(p)M(p) = M_b + 3g_{q,b}^2 C_F \int_{\Lambda} \frac{d^4 q}{(2\pi)^4} \frac{Z(q)M(q)}{q^2 + M^2(q)} \frac{1}{\ell^2 + m_b^2} \quad (51)$$

where  $\ell = p + q$  and  $\int_{\Lambda}$  denotes an appropriately regulated momentum integral. Here,  $M_b$ ,  $m_b$ , and  $g_{q,b}$  are the (bare) quark mass, gluon mass, and quark gluon coupling, respectively, and  $C_F = (N_c^2 - 1)/(2N_c)$  is the Casimir of the fundamental representation of the  $SU(N_c)$  gauge group.

The rainbow resummation is known to capture the essential features of chiral symmetry breaking and the associated dynamical quark mass generation and has been widely used in the context of nonperturbative approaches to IR QCD (the bibliography on this topic is extremely large; for a review, see [MR03]). The benefit of the double expansion proposed in Refs. [PRS<sup>+</sup>17, PRS<sup>+</sup>21]—dubbed the rainbow-improved (RI) loop expansion—is that it avoids *ad hoc* modelling for the quark-gluon vertex and for the gluon propagator entering the rainbow diagrams. At leading order, these are simply given by their tree-level expressions in the CF model. Another asset is that the actual expansion in small parameters underlying the approximation scheme allows for a systematic implementation of RG improvement, which is crucial for a proper description of chiral symmetry breaking.

<sup>28</sup> This argument combines estimates from the heavy-quark limit for  $g_g$  and from the quenched limit for the quark-gluon vertex  $g_q$  and has to be updated when (light) quarks fluctuations are taken into account; see below.

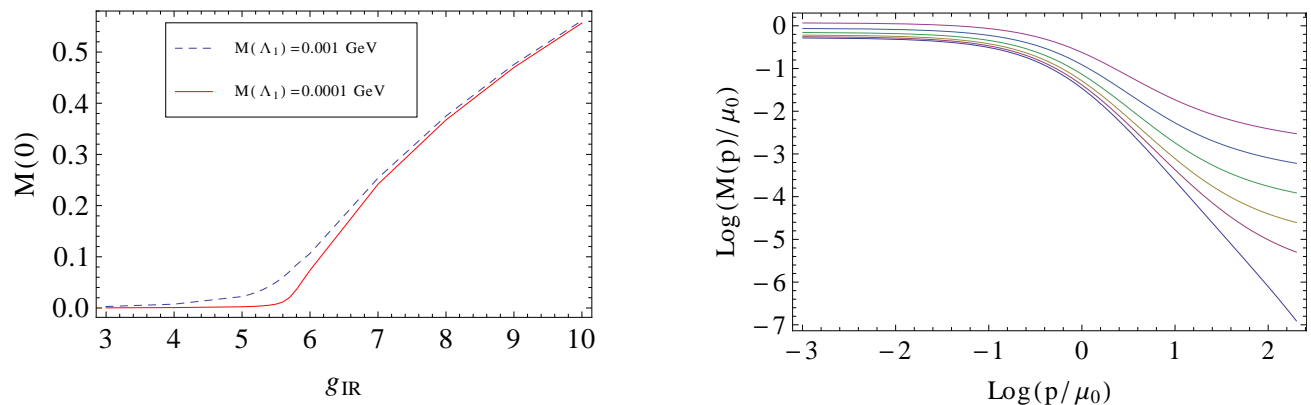


FIG. 16: Left: Constituent quark mass  $M(p=0)$  as a function of the coupling parameter  $g_{\text{IR}}$  (see text) for two values of the UV mass  $M(\Lambda_1)$ . The variation of  $g_{\text{IR}}$  is done by keeping  $\Lambda_{\text{QCD}}$  fixed. Right: Mass function  $M(p)$  in Log-Log scale for decreasing (from top to bottom) values of  $M(\Lambda_1)$  at the UV scale  $\Lambda_1 = 10$  GeV. We observe the onset of the power law behaviour at large momentum, characteristic of the spontaneous breaking of the chiral symmetry, as the chiral limit is approached. Figures from Ref. [PRS<sup>+</sup>17].

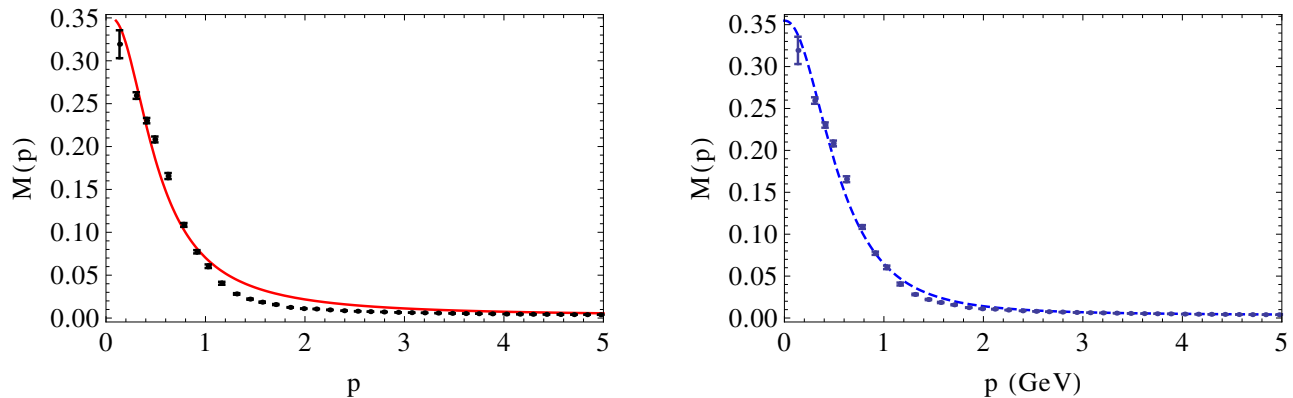


FIG. 17: Left: The quark mass function  $M(p)$  compared to the lattice data from Ref. [OSSS19]. The quark mass at the scale  $\Lambda_1 = 10$  GeV is fixed at its lattice value  $M(\Lambda_1) = 3$  MeV. The best fit parameters (see text) are  $m_0 = 0.12$  GeV, and  $g_0 = 2.42$  at  $\mu_0 = 1$  GeV. Right: The RG-improved one-loop expression of Ref. [PTW14] for  $M(p)$  is also able to describe well lattice data. This, however, necessitates artificially large values of the gluon mass and of the coupling, here,  $m_0 = 1.6$  GeV and  $g_0 = 13$  at  $\mu_0 = 1$  GeV. In particular, the one-loop approximation makes no sense. Figures from Ref. [PRS<sup>+</sup>21].

The RI loop expansion at first nontrivial order has been implemented in Ref. [PRS<sup>+</sup>17] using a toy-model RG running and in Ref. [PRS<sup>+</sup>21] using a consistent implementation of the RG running within the RI expansion. We refer the reader to these articles for the technical details and we review the main results here. Figure 16 illustrates some aspects of the chiral symmetry breaking phenomenon through the quark mass function  $M(p)$  [see Eq. (47)] using a toy model for the running quark-gluon coupling parametrized, in particular, by a finite IR value  $g_{\text{IR}}$ . A nonzero value  $M(p=0)$  is dynamically generated in the chiral limit—obtained by decreasing the value of  $M(\Lambda_1)$  at the UV scale  $\Lambda_1$ —above a critical value of  $g_{\text{IR}}$ . Also shown in Fig. 16 is the fact that the logarithmic UV tail of the theory with massive quarks turns into a power law in the chiral limit,  $M(p) \propto \langle \bar{\psi}\psi \rangle / p^2$  (up to calculable logarithmic corrections), controlled by the dynamically generated quark-antiquark condensate.

The results of the RI expansion for the quark and gluon propagators at next-to-leading order, using a self-consistent RG running, have been computed in Ref. [PRS<sup>+</sup>21] and compared to lattice data close to the chiral limit. At this order, the quark propagator is unchanged as compared to its leading-order expression, *i.e.*, it is given by the resummation of rainbow diagrams with tree-level one-gluon exchange, whereas the gluon propagator receives the usual perturbative one-loop corrections in the gauge sector and an effective quark-loop with rainbow-resummed quark propagators.

The comparison with lattice data is made by adjusting the various parameters, namely, the quark and gluon masses

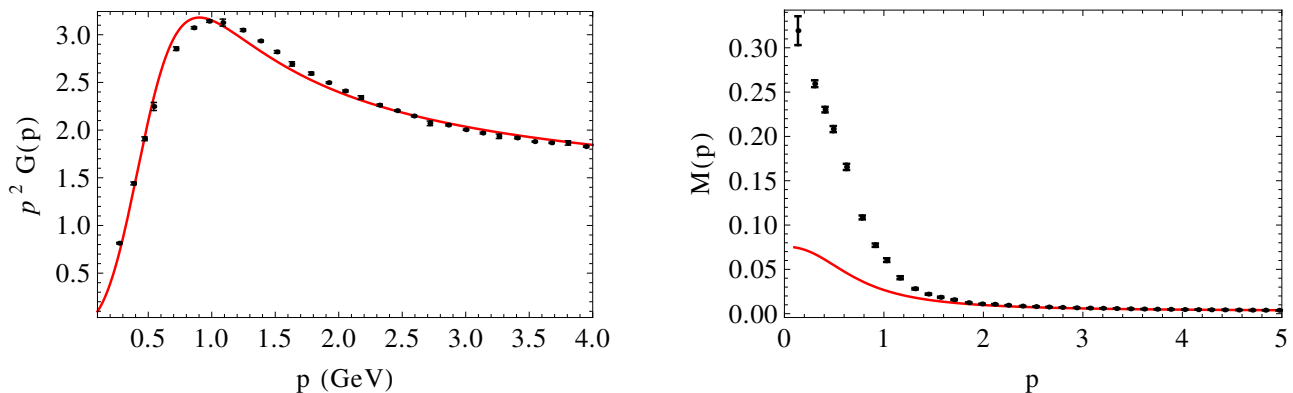


FIG. 18: The gluon dressing function  $p^2 G(p)$  (left) and the quark mass function  $M(p)$  (right) compared with lattice data from Ref. [SMMPvS12]. Here the fit is adjusted on the gluon dressing function alone and the best fit parameters (see text) are  $m_0 = 0.39$  GeV and  $g_0 = 4.67$  at  $\mu_0 = 1$  GeV. The quark mass at the scale  $\Lambda_1 = 10$  GeV is fixed at its lattice value  $M(\Lambda_1) = 3$  MeV. Figures from Ref. [PRS<sup>+</sup>21].

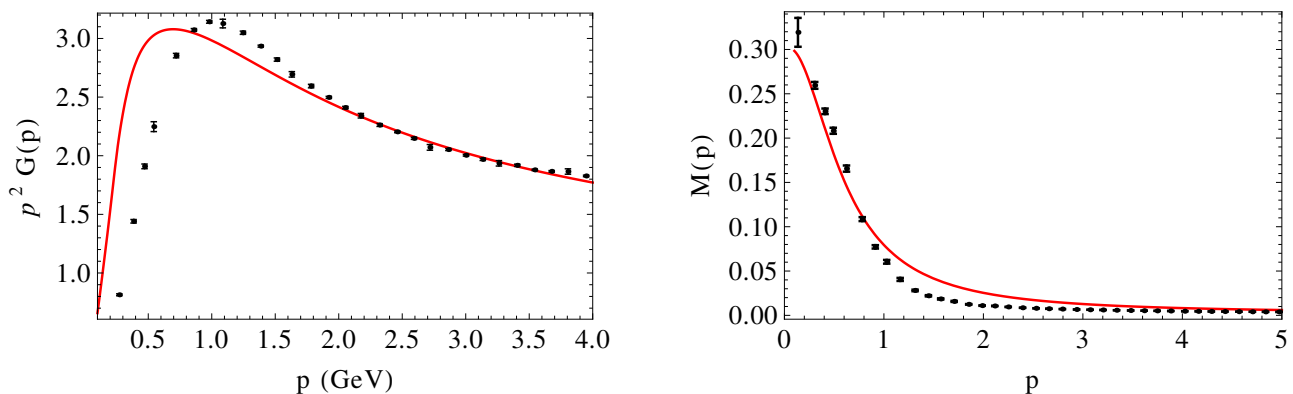


FIG. 19: Combined fit of the gluon dressing function  $p^2 G(p)$  (left) and the quark mass function  $M(p)$  (right) against the lattice results of Refs. [OSSS19] and [SMMPvS12], respectively. The quark mass at the scale  $\Lambda_1 = 10$  GeV is fixed at its lattice value  $M(\Lambda_1) = 3$  MeV. The best fit parameters (see text) are  $m_0 = 0.21$  GeV, and  $g_0 = 2.45$  at  $\mu_0 = 1$  GeV. Figures from Ref. [PRS<sup>+</sup>21].

and the coupling<sup>29</sup> at the scale  $\Lambda_1 = 10$  GeV. The gluon mass and the coupling are included as fit parameters and, in order to ease the comparison with the previous sections, we give their values  $m_0$  and  $g_0$  at the scale  $\mu_0 = 1$  GeV, obtained through the proper RG running. The quark mass is not included in the fits but is, instead, fixed to the lattice value at the scale  $\Lambda_1 = 10$  GeV, namely,  $M(\Lambda_1) = 3$  MeV in all the figures presented here. This corresponds to the (renormalised) current quark mass and plays the role of the control parameter for the chiral limit. The corresponding value  $M_0$  of the running quark mass at  $\mu_0 = 1$  GeV can be read off the plots of  $M(p)$  for each case under consideration. Fig. 17 shows that one can obtain an excellent agreement for the quark mass function alone. It was noticed that a similar agreement can be obtained from the one-loop calculation presented in the subsection VIA above, however, at the price of an uncomfortably large value of the gluon mass parameter. Good descriptions of the data with the RI expressions typically favour comparatively small values of the gluon mass parameter. Similarly, fitting the gluon propagator alone leads to very good agreement as shown in Fig. 18. This, however, favors relatively large values of the gluon mass parameter, which thus deteriorates the quality of the agreement for the quark mass function, as shown in the same figure.

As mentioned before in the one-loop analysis, fitting one function alone typically leads to artificially good fits,

<sup>29</sup> It is worth emphasising that, despite the different treatment of the (IR) couplings in the quark and in the pure glue sectors, there is, *in fine*, only one coupling parameter to specify in actual implementations of the RI loop expansion because both couplings are related by Slavnov-Taylor identities. In the UV, this relation is under perturbative control and one can fix the value of  $g_q$  in terms of  $g_g$ . In this section,  $g_0$  refers to the pure gauge coupling at the scale  $\mu_0$ :  $g_0 = g_g(\mu_0)$ .

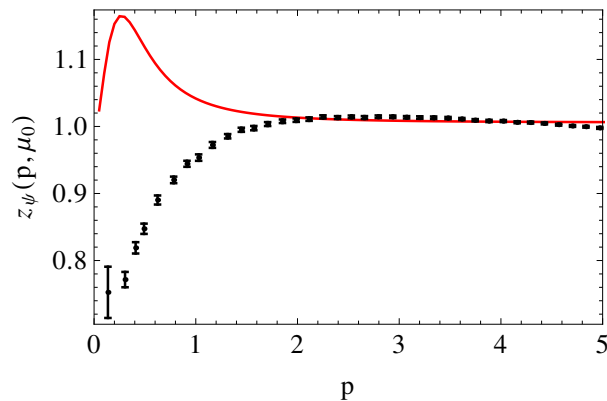


FIG. 20: The function  $z_\psi(p, \mu_0) = Z(p)/Z(\mu_0)$  normalised to  $z_\psi = 1$  at  $p = 2$  GeV against the lattice data of Ref. [OSSS19], for the set of parameters  $M(\Lambda_1) = 3$  MeV,  $m_0 = 0.21$  GeV, and  $g_0 = 2.45$  at  $\Lambda_1 = 10$  GeV and  $\mu_0 = 1$  GeV. Figure from Ref. [PRS<sup>+</sup>21].

not representative of the actual quality of the approximation. It is thus desirable to fit the quark mass function and the gluon propagator together, which, as just mentioned, are in tension with respect to the value of the gluon mass parameter. The best fit is presented in Fig. 19, which still shows a reasonably good agreement, at the 15% level [PRS<sup>+</sup>21]. Finally, the quark dressing function, shown in Fig. 20 is badly described as was already the case at one-loop order, see Figs. 11 and 12. Although the present approximation includes part of the two-loop contributions that are necessary for a proper description of this function, there remain significant two-loop corrections from the quark-gluon vertex corrections, that are not included. The difference between the complete two-loop result shown in Sect. VIA and the one shown in Fig. 20 gives a measure of the size of such vertex corrections.

We end this section with a comment on the order of magnitude of the expansion parameters used here. For the best fit values, the typical gluon coupling is at most  $\lambda_g = g_g^2 N_c / (16\pi^2) \approx 0.12$  for  $N_c = 3$ , whereas the running quark-gluon coupling reaches  $\lambda_q = g_q^2 N_c / (16\pi^2) \approx 0.68$  [PRS<sup>+</sup>21]. Although these values are slightly smaller than those obtained for heavy quarks in the previous Section, we see that a perturbative treatment of the quark-gluon coupling remains, *a posteriori*, questionable. Finally, it is interesting to note that the two expansion parameters that control the RI-loop expansion are roughly of the same order in the case  $N_c = 3$ , namely,  $1/N_c \approx 0.33$  and  $g_g \sqrt{N_c} / (4\pi) \lesssim 0.34$ .

#### D. Hadronic observables

The RI expansion can also be used for the calculation of physical observables in QCD. The simplest ones are the properties—masses and decay constants—of meson bound states, out of which the pion plays a particular role, being the Goldstone mode associated to the spontaneous breaking of the chiral symmetry. An important ingredient for this calculation using continuum approaches is the quark-antiquark-meson vertex. The latter can be consistently calculated in the RI loop expansion. At leading order, it is given by the infinite series of ladder diagrams with one-(massive)-gluon-exchange rungs and rainbow-resummed quark propagators [PRS<sup>+</sup>17]. This is not a surprise because this ladder resummation for the quark-antiquark-meson vertex in fact goes along with the rainbow resummation for the quark propagator to comply with the chiral symmetry constraints. The rainbow-ladder approximation is very well-known and is widely used for calculations of meson properties using nonperturbative continuum approaches [RW94, MT99, MR03, RBHW07, SAW15]. The benefit of the RI approach is that, as discussed above, the approximation is controlled by an expansion in terms of actual small parameters of the theory.

The rainbow-ladder equations have been studied for the case of the pion in the RI loop expansion [Ser20]. In the chiral limit, the relevant integral equation for the vertex can be greatly simplified and one ends up with a set of coupled one-dimensional integral equations which are easy to solve numerically. The pion decay constant  $f_\pi$  can then be systematically computed as a function of the parameters of the Lagrangian, namely, the gauge coupling and the gluon mass. Preliminary results show that there are regions of parameter space which give very good values of  $f_\pi$ . This is to be expected because, thanks to the chiral Ward identities, the value of  $f_\pi$  is, to a large extent, determined by the quark mass function [PS79] and, as described above, the CF model equipped with the RI expansion is clearly able to produce good fits of the latter.

Interestingly, we mention that the CF model can serve as a precise definition of a gluon mass (in the Landau gauge) which can be assigned a physically measurable value using, *e.g.*, the experimental value of  $f_\pi$ . The constraints on a

possible gluon mass in the particle data book [Z<sup>+</sup>20] refer to an outdated and, in fact, theoretically not precise definition of the gluon mass [Ynd95]. The work reported here brings the possibility of a precise, well-defined—necessarily gauge and scale dependent—gluon mass, similar to what is done for the quark masses [Z<sup>+</sup>20]. For discussions in this direction; see [Rob20].

## VII. NONZERO TEMPERATURE AND DENSITY: THE CONFINEMENT-DECONFINEMENT TRANSITION

Lattice simulations have established that YM theories undergo a confinement-deconfinement phase transition at nonzero temperature [Sve86, KKPZ02, LTW05, Gre12, SDPvS13]. The latter is controlled by the spontaneous breaking of a symmetry specific to the nonzero temperature problem, the center symmetry [Sve86, Gre, Pis02]. One possible order parameter for the latter is the Polyakov loop  $\ell$  [Pol78], defined as the average of a traced temporal Wilson loop:

$$\ell = \frac{1}{N_c} \text{tr} \left\langle P \exp \left\{ ig \int_0^\beta d\tau A_0(\tau, \mathbf{x}) \right\} \right\rangle. \quad (52)$$

Here, the inverse temperature  $\beta \equiv 1/T$  (the Boltzmann constant is set to  $k_B = 1$ ) sets the extent of the compact Euclidean time interval over which the fields are defined and the path ordering operator  $P$  orders the (matrix-valued) fields from left to right according to the decreasing value of their time argument. The gauge field is periodic in Euclidean time with period  $\beta$ —and so are the ghost and antighost fields in a gauge-fixed setting—whereas quark fields are antiperiodic. The Polyakov loop is directly related to the free energy  $F_q$  of the system in the presence of a static colour charge as [Pol78, Sve86]

$$\ell \propto e^{-\beta F_q}. \quad (53)$$

In particular, a phase with  $\ell = 0$  implies an infinite free-energy cost for the colour charge, characterising a confined phase. Clearly, the latter involves large field configurations with  $A_0 \sim 1/g$ , which are not captured at any finite order in perturbation theory around the trivial configuration  $A_0 = 0$ . One way to cope with this issue is to expand around a nontrivial background field configuration  $\langle A_0 \rangle \neq 0$ , to be determined dynamically. Doing so in the Landau gauge is, however, problematic because the latter explicitly breaks the center symmetry, which clearly plays a key role here. Convenient ways to encode both a nontrivial background and the essential aspects of the center symmetry have been put forward in Ref. [BGP10] and, more recently, in Ref. [VERST21], which uses background-field techniques [Abb81, Abb82] and, in particular, the background-field generalisation of the Landau gauge, the Landau-DeWitt (LDW) gauge [Wei96]. Similar to the massive extension of the former, discussed so far in this article, the massive extension of the latter or, in other words, the LDW version of the CF model has been worked out in Ref. [RSTW15b] and used as a starting point for a perturbative analysis of the nonzero temperature physics, in the presence of a nontrivial Polyakov loop.<sup>30</sup>

### A. The Landau-DeWitt gauge

The background field approach [Wei96] introduces an *a priori* arbitrary background field configuration  $\bar{A}_\mu$  through a modified gauge-fixing condition. In terms of  $a_\mu = A_\mu - \bar{A}_\mu$ , the LDW gauge condition reads

$$\bar{D}_\mu a_\mu^a = 0, \quad (54)$$

where  $\bar{D}_\mu \varphi^a \equiv \partial_\mu \varphi^a + g f^{abc} \bar{A}_\mu^b \varphi^c$ . One can construct the corresponding FP Lagrangian using standard techniques. One important property of the resulting gauge-fixed theory is a formal gauge invariance with respect to gauge transformations of the background field. The simplest background-field generalisation of the CF action which respects this essential property is [RSTW15b]

$$S_{\bar{A}} = \int_x \left\{ \frac{1}{4} F_{\mu\nu}^a F_{\mu\nu}^a + \frac{m^2}{2} a_\mu^a a_\mu^a + \bar{D}_\mu \bar{c}^a D_\mu c^a + ih^a \bar{D}_\mu a_\mu^a \right\}, \quad (55)$$

<sup>30</sup> We mention that a different approach to nonzero temperature physics has been pursued in the context of the screened perturbation theory, working directly in the Landau gauge with vanishing background [CS18].

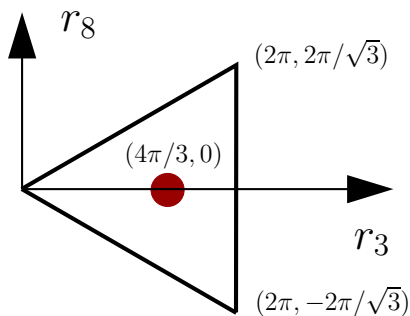


FIG. 21: Weil chamber for  $SU(3)$ . The red point corresponds to the center-symmetric background field configuration, see the text for details.

which is clearly invariant under the transformation  $\bar{A}_\mu^U \rightarrow \bar{A}_\mu = U\bar{A}_\mu U^{-1} + \frac{i}{g}U\partial_\mu U^{-1}$ ,  $\varphi \rightarrow U\varphi U^{-1}$ , with  $\varphi \equiv (a_\mu, c, \bar{c}, h)$  and where  $U$  is an element of the gauge group. This linear symmetry is inherited by the effective action,

$$\Gamma_{\bar{A}}[\varphi] = \Gamma_{\bar{A}^U}[U\varphi U^{-1}], \quad (56)$$

provided the transformation  $U$  preserves the periodic boundary conditions of the fields. Such transformations, which form a group denoted  $\mathcal{G}$ , do not need to be periodic themselves, however, but only periodic up to any element of the center of the gauge group,  $e^{i2\pi k/N_c}\mathbb{1}$  ( $k = 0, \dots, N_c - 1$ ) in the case of  $SU(N_c)$ . Their relevance is that they act by multiplying the Polyakov loop  $\ell$  by the corresponding center phase. In particular, this relates the confining phase, where  $\ell$  vanishes, to the phase where the symmetry group  $\mathcal{G}/\mathcal{G}_0$  is explicitly realised, where the subgroup  $\mathcal{G}_0$  of periodic transformations ( $k = 0$ ) needs to be quotiented away because it has no impact on (and is therefore not probed by) the Polyakov loop. The quotient group  $\mathcal{G}/\mathcal{G}_0$  is isomorphic to the center of the gauge group and is known as the center symmetry group [Pis02].

A convenient way to study the spontaneous breaking of  $\mathcal{G}/\mathcal{G}_0$ , and in turn the deconfinement transition, is from the functional

$$\tilde{\Gamma}[\bar{A}] = \Gamma_{\bar{A}}[\varphi = 0] \quad (57)$$

which is also invariant under the transformations  $U \in \mathcal{G}$ . A given state of the system is represented by a minimum of  $\tilde{\Gamma}[\bar{A}]$  denoted  $\bar{A}_{\min}$ , or by any other minimum obtained from it using a transformation  $U_0 \in \mathcal{G}_0$ . In other words, a physical state corresponds to a  $\mathcal{G}_0$ -orbit of minima [RSTW16, Rei20]. The center-symmetric states are those  $\mathcal{G}_0$ -orbits that are invariant under the action of  $\mathcal{G}/\mathcal{G}_0$  and the deconfinement transition occurs when the  $\mathcal{G}_0$ -orbit of minima of  $\tilde{\Gamma}[\bar{A}]$  moves away from its center-symmetric configuration.

The above considerations are greatly simplified if one restricts to constant temporal background fields along the diagonal or commuting part of the algebra  $\bar{A}_\mu(x) = \delta_{\mu 0}\bar{A}_0^j t^j$ , with  $[t^j, t^{j'}] = 0$ . In this case the functional  $\tilde{\Gamma}[\bar{A}]$  can be traded for the potential

$$V(r) = \frac{\tilde{\Gamma}[\bar{A}_0]}{\beta\Omega} - V_{\text{vac}}, \quad (58)$$

where  $\Omega$  is the spatial volume,  $V_{\text{vac}}$  the vacuum (zero temperature) contribution, and  $r \in \mathbb{R}^{N_c-1}$  is the vector of components  $r^j = \beta g \bar{A}_0^j$ . The transformations of  $\mathcal{G}_0$  divide  $\mathbb{R}^{N_c-1}$  into equivalent cells known as Weyl chambers and whose points can be seen as representatives of the various states ( $\mathcal{G}_0$ -orbits) of the system. A center transformation corresponds to an isometry of any of these cells whose fixed points are the invariant states under the considered transformation.<sup>31</sup> In the  $SU(2)$  case,  $r \in \mathbb{R}$  and the Weyl chambers are the segments  $[2\pi n, 2\pi(n+1)]$  each of which contains a center-symmetric point at its center. In the case of  $SU(3)$ , the Weyl chambers form a paving of  $\mathbb{R}^2$  by equilateral triangles. One representative is the fundamental triangle of edges  $(0,0)$ ,  $(2\pi, -2\pi/\sqrt{3})$  and  $(2\pi, 2\pi/\sqrt{3})$ , see Fig. 21. The center of any such triangle corresponds to the center-symmetric state (for instance  $(4\pi/3, 0)$  in the Weyl chamber shown in Fig. 21).

<sup>31</sup> The present considerations apply to other symmetries, such as charge conjugation [RSTW16].

The analysis of the confinement-deconfinement transition is then achieved by minimising the potential  $V(r)$  over a given Weyl chamber and monitoring, as a function of the temperature, whether the minimum  $r_{\min}$  is located at the center-symmetric points. In this sense, the corresponding background  $\bar{A}_{\min}$  plays the role of an order parameter, equivalent, in this gauge,<sup>32</sup> to the Polyakov loop [BGP10, RSTW16, Rei20]. From the minimum of the potential one can also access the thermodynamic pressure (and therefore any other thermodynamical observable) as

$$p = -V(r_{\min}) + p_{\text{vac}}, \quad (59)$$

whereas the Polyakov loop is obtained from a direct evaluation of the average (52) with the restriction that  $\langle A \rangle = \bar{A}_{\min}$ .

## B. The background-field effective potential in perturbation theory

The potential (58) has been computed at one-loop order in the (background-field-extended) CF model for a large variety of gauge groups [RSTW15b, RSTW16]. Two-loop corrections have also been computed for the SU(2) and SU(3) groups [RSTW15a, RSTW16]. We briefly describe the salient aspects of these calculations and we review the essential results here.

Calculations in the LDW gauge with a constant temporal background as specified above are greatly simplified if one switches from the usual Cartesian colour bases  $\{t^a\}$  to the Cartan-Weyl bases  $\{t^\kappa\}$  [RSTW16]. The labels  $\kappa$  are vectors that gather the adjoint colour charges  $\kappa^j$  of each colour mode such that  $[t^j, t^\kappa] = \kappa^j t^\kappa$ , where the generators  $t^j$  span the commuting part of the algebra, also known as the Cartan subalgebra. In the SU(2) case for instance, a Cartan-Weyl basis is  $\{t^0, t^+, t^-\}$ , where  $t^0 = \sigma_3/2$  and  $t^\pm = (\sigma_1 \pm i\sigma_2)/(2\sqrt{2})$  are the well-known raising and lowering operators, with  $\sigma_i$  the Pauli matrices. A convenient property of the Cartan-Weyl bases is that they allow for a one-to-one correspondence between the Feynman rules (and, consequently, of many calculation steps) with and without the background field. In particular, the only effect of the background is to shift the Euclidean four-momentum  $p$  of the propagator lines associated to a colour mode  $\kappa$  as  $p_\mu \rightarrow p_\mu^\kappa = p_\mu + T(r \cdot \kappa)\delta_{\mu 0}$ . This generalised momentum is conserved at vertices owing to momentum and colour conservation.

The calculation of the background-field potential  $V(r)$  at one-loop order is straightforward and yields [RSTW15b]

$$V_{\text{loop}}(r) = \frac{T}{2\pi^2} \sum_{\kappa} \int_0^\infty dq q^2 \left[ 3 \ln(1 - e^{-\beta\varepsilon_q + ir \cdot \kappa}) - \ln(1 - e^{-\beta q + ir \cdot \kappa}) \right], \quad (60)$$

with  $\varepsilon_q = \sqrt{q^2 + m^2}$ . By setting  $r$  to 0, one recognises the free-energy density of a gas of free massive gluons and massless ghosts. The factor of 3 relates to the fact that there are three massive transverse gluonic modes. The longitudinal gluonic mode is massless and cancels with one of the two ghost degrees of freedom. The background lifts the degeneracy between the various colour modes and shifts the dispersion relations by an imaginary amount  $i(r \cdot \kappa)T$  that can be interpreted as an imaginary chemical potential for the colour charge [FS17].

The essential features of the one-loop potential can be unveiled by looking at the two asymptotic regimes  $T \gg m$  and  $T \ll m$ . In the high temperature limit, all modes can be considered approximatively massless and, for each colour state, the ghost contribution in (60) cancels against one gluon mode, leaving only the two “physical” polarisations of the massless gluons. This results in the known Weiss deconfining potential [Wei81, PY80], which displays maxima at the confining points of the Weyl chambers. At low temperatures, instead, the massive gluon modes in (60) are exponentially suppressed and the potential is dominated by the (massless) ghost contribution. Because the latter contributes negatively, this leads to an inverted Weiss potential [BGP10], with minima at the confining points of the Weyl chambers. This is another example of the phenomenon of ghost dominance at IR (here, temperature) scales, mentioned in Sec. VD. As in the case of correlation functions, this phenomenon is not restricted to the CF approach but applies to a wide class of continuum approaches using background field techniques [BGP10, FLP15, QR17]. For pure YM theories, one finds an actual phase transition between the high and low temperature phases.

Fig. 22 shows the one-loop background-field potentials for the SU(2) and the SU(3) theories in  $d = 4$  in the relevant directions—along which the transition takes place—in the respective Weyl chambers. One finds a continuous transition in the SU(2) case and a first order transition for SU(3), in agreement with lattice simulations [Sve86] and other approaches [BGP10, QR17]. We find that the transitions for SU(2) and SU(3) occur, respectively, at

<sup>32</sup> The Polyakov loop remains more fundamental in a certain sense, as it is a gauge-invariant order parameter.

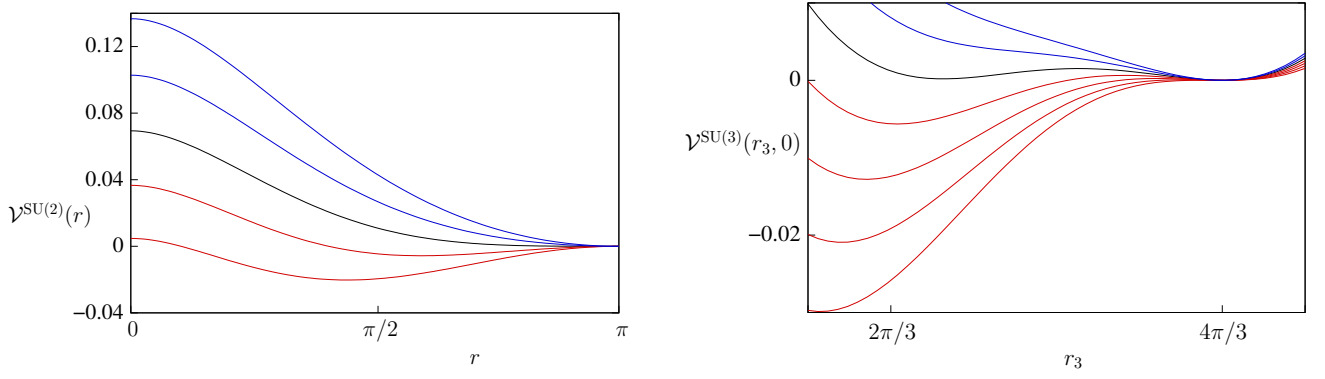


FIG. 22: The dimensionless background field potentials  $\mathcal{V}(r) = V(r)/T^4$  for the SU(2) and the SU(3) theories at one-loop order in the CF model, for temperatures  $T = T_c$  (black),  $T < T_c$  (blue), and  $T > T_c$  (red). The abscisses represent the charge conjugation invariant directions in the corresponding Weyl chambers, along which the confinement-deconfinement transition takes place. The confining point is located at  $r = \pi$  for SU(2) and at  $r_3 = 4\pi/3$  for SU(3). Figures from Ref. [RSTW15b].

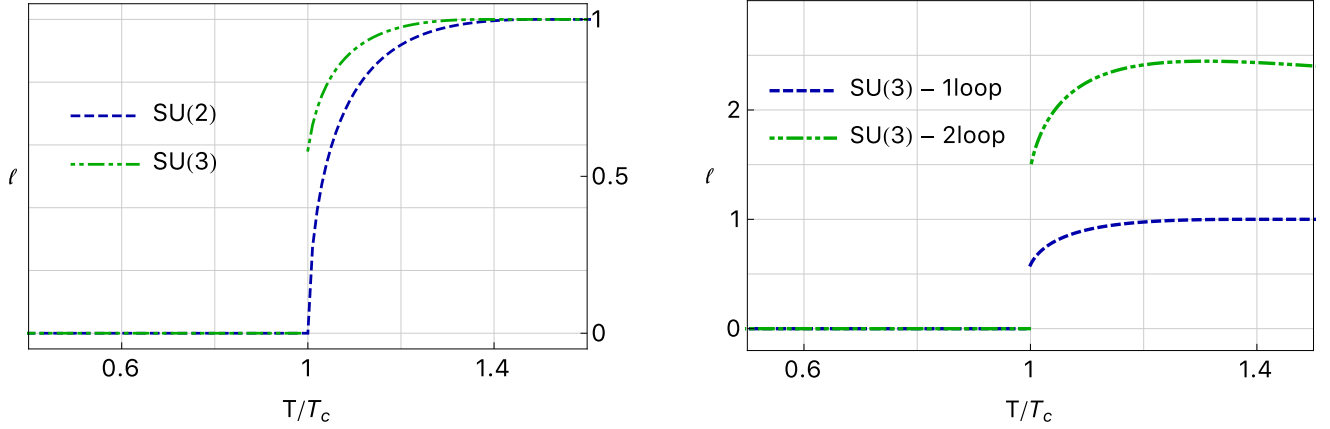


FIG. 23: The Polyakov loop (52) as a function of the temperature normalised to the transition temperature for the SU(2) and the SU(3) theories in the (background-extended) CF model at one-loop order (left) [RSTW15b] and including the two-loop corrections for the SU(3) case (right) [RSTW16]. Figures from Ref. [Rei20].

$T_c/m \simeq 0.336$  and  $T_c/m \simeq 0.364$ . Using the values fitted against the lattice propagators at zero temperature,<sup>33</sup> this translates to the transition temperatures reported in Tab. I, which are in remarkably good agreement with the lattice values [LP13] given the simplicity of the one-loop approximation. The inclusion of two-loop corrections, again, with parameters adjusted to reproduce the vacuum propagators at the relevant order, yields the values summarised in Tab. I. The improvement is clear.

<sup>33</sup> The evaluation of the potential is done by using the same zero-temperature renormalisation scheme as that used for the evaluation of the zero temperature propagators. More precisely, at one-loop order, the background dependent part of the potential is finite and the mass can be considered as the bare one, fixed by fitting tree-level expressions for the propagators to lattice data. At two-loop order, the background dependent part of the potential diverges and its renormalisation requires rescaling the mass parameter using one-loop renormalisation factors that should be taken equal to those used in the one-loop propagators.

$T_c$ (MeV)	lattice	one-loop CF <sup>(s)</sup>	two-loop CF <sup>(s)</sup>	one-loop CF <sup>(c)</sup>
SU(2)	295	237	284	265
SU(3)	270	185	254	267

TABLE I: Estimates for the confinement-deconfinement transition temperatures at one- and two-loop orders within the CF model with either the self-consistent (CF<sup>(s)</sup>) [RSTW15b, RSTW15a, RSTW16] or the center-symmetric (CF<sup>(c)</sup>) [VERST21] background field approaches—see text—and their comparison to the corresponding lattice results [LP13].

The corresponding Polyakov loops, at the same order of approximation, are shown in Fig. 23. As was also pointed out in Ref. [DGH<sup>+</sup>12] in the context of matrix model calculations, the rise of the Polyakov loop from its value right above the transition temperature to its maximum value is too fast as compared to lattice results. This compromises any direct comparison of this quantity to Monte-Carlo simulations. We shall come back to this below.

### C. The issue of massless unphysical modes in the confined phase

We have seen that the ghost dominance at low temperatures plays a pivotal role in the confinement-deconfinement mechanism described above. Although this mechanism is quite general and goes in fact beyond the particular case of the CF model considered in this review, it poses certain challenges that we now describe.

First, the fact that ghost degrees of freedom dominate in the low temperature phase may lead to inconsistent thermodynamics.<sup>34</sup> For instance, in the absence of the background, the ghost contribution results in a negative thermal pressure or a negative entropy in the low temperature limit [CS18, SR12]. Fortunately, the presence of the nontrivial background cures this pathological behaviour [RSTW16, QR17]. The reason is that, in the  $T \rightarrow 0$  regime, the confining gluonic background operates a transmutation of the ghost thermal distribution functions, such that the net contribution to the pressure or entropy density remains positive. As an illustration, consider the SU(2) pressure which, at low temperature, can be written

$$p_{\text{th}} \sim \frac{1}{6\pi^2} \int_0^\infty dq q^3 [-n_{q-i\pi T} - n_q - n_{q+i\pi T}], \quad (61)$$

where  $n_q \equiv 1/(e^{\beta q} - 1)$  is the Bose-Einstein distribution function. The bracket contains the three colour mode contributions, corresponding to  $\kappa \in \{-, 0, +\}$ . The neutral mode  $\kappa = 0$  is blind to the background and contributes negatively to the thermal pressure, as expected from a ghost degree of freedom. Were it not for the imaginary shift  $\pm i\pi T$  of their energies, the two other modes would give a similar negative contribution.<sup>35</sup> However, because of the presence of the confining background, these modes contribute instead with  $-n_{q\pm i\pi T} = 1/(e^{\beta q} + 1)$ , that is, a positive Fermi-Dirac distribution, leading eventually to a positive thermal pressure and a positive entropy at low temperature [RSTW15a]. These considerations extend to SU(3) [RSTW16].

The transmutation mechanism described here is also visible (but with the opposite effect) as one approaches the transition from below. In this limit, the gluon degrees of freedom are not exponentially suppressed, while the background remains confining, turning some of their positive distribution functions into negative ones, which tend to bring the thermal pressure or the entropy density down to a slightly negative value at one-loop order. This feature is clearly visible in the thermodynamical observables as illustrated in Fig. 24 for the entropy density. It has been shown, however, that the two-loop result corrects this unphysical feature [RSTW15a, RSTW16].

The low-temperature phase is plagued by yet another major problem. Namely, the dominant ghost degrees of freedom, be they surrounded or not by a confining gluonic background, remain massless. This leads to power law behaviour of the thermodynamical observables as  $T \rightarrow 0$ , at odds with the observations on the lattice. Again, it is worth emphasising that these issues are not restricted to the perturbative CF model and actually encompass all current continuum approaches to YM/QCD [QR17, SR12, CDJ<sup>+</sup>15]. This issue points to the inability (to date) of continuum approaches to provide a fully consistent picture of confinement.

<sup>34</sup> More generally, this is related to the question of the proper identification of the physical space of the model, discussed in Sec. IV C, over which thermal averages are to be taken. In the FP theory, the nilpotent BRST symmetry guarantees that states with negative (or null) norm do not contribute to thermal averages and thus to thermodynamic observables (except through loop effects). For instance, at one-loop order, the ghost contribution cancels that of the two “unphysical” gluon modes.

<sup>35</sup> The  $T \rightarrow 0$  expression in the absence of the background is given by Eq. (61) with  $q \pm i\pi T$  replaced by  $q$ . We recover here that the Landau gauge CF model predicts a negative pressure  $p = -\pi^2 T^4/30$  at low temperatures [RSTW15a, CS18].

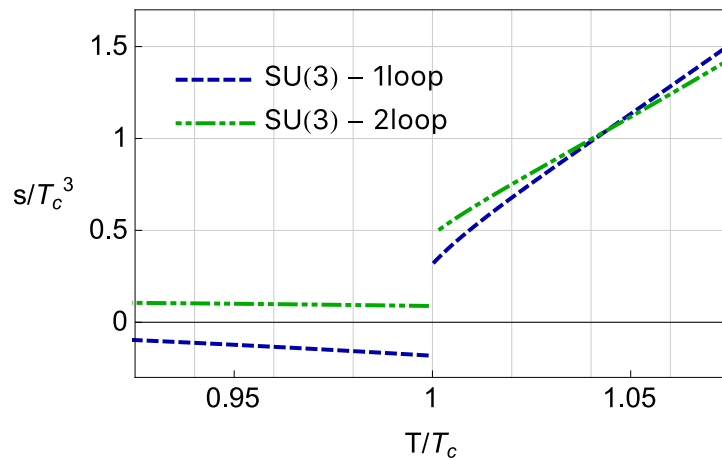


FIG. 24: The SU(3) entropy density in the vicinity of the phase transition at one- and two-loop orders in the LDW extension of the CF model [RSTW16, Rei20].

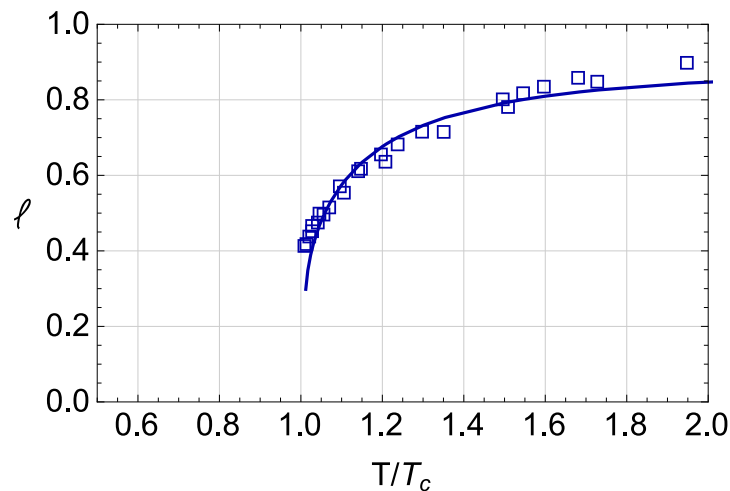


FIG. 25: The Polyakov loop for the SU(3) YM theory at one-loop order from the center-symmetric effective action proposal of Ref. [VERST21] as compared to the lattice data of Refs. [GHK08, LFK<sup>+</sup>13].

#### D. Center-symmetric background field approach

The results described above rely on the use of the background functional (57) [or the corresponding potential (58)], which involve self-consistent background fields defined as  $\bar{A} = \langle A \rangle_{\bar{A}}$ . It is to be emphasised that this quantity is not, strictly speaking, an effective action in the sense that it is not a standard Legendre transform and that it is a functional of the background field (which is a gauge-fixing device). Because of this, such a self-consistent background field approach suffers from various technical difficulties—not to be described here, see *e.g.* Ref. [RSTW16, Rei20, VERST21]—when approximations are involved and for its possible implementation in lattice simulations.

An alternative approach has been recently proposed, that avoids these difficulties [Rei20, VERST21]. It is based on using a fixed background field  $\bar{A}_c$  that is invariant under the action of  $\mathcal{G}/\mathcal{G}_0$ . The corresponding action  $\Gamma_{\bar{A}_c}[A]$  is a genuine gauge-fixed effective action which properly encodes the center symmetry and from which one directly obtains the gluon correlation functions. Also, it can be implemented in lattice simulations with techniques currently used for the Landau gauge. It has been evaluated at one-loop order in the CF model for constant, center-symmetric background field configurations in the temporal direction and in the Cartan subalgebra of the gauge group [VERST21]. This yields the correct phase structure for the SU(2) and SU(3) YM theories with transition temperatures reported in Tab. I, in remarkable agreement with lattice results, much better than the corresponding one-loop results in the previous self-consistent background field approach.

Another interesting improvement concerns the temperature dependence of the Polyakov loop. In particular, it

shows a moderate rise in the deconfined phase, as compared to the self-consistent background field approach, which compares well with lattice results [GHK08, LFK<sup>+</sup>13], see Fig. 25. Here, it is important to stress that the lattice data correspond to the renormalised Polyakov loop  $\ell_r(T)$ , related to the bare one computed here as  $\ell_r(T) = Z_\ell \ell(T)$ , where the renormalisation factor  $Z_\ell$  is a function of the coupling. At first sight, it might seem sufficient to simply normalise the perturbative results to the lattice data at a given temperature. Doing so, a rather good fit is obtained in the range  $[0, 2T_c]$ . The agreement deteriorates for larger temperatures, where important effects not taken into account in this simple one-loop calculation, such as the resummation of hard thermal loops [HBA<sup>+</sup>14] or the RG running [HLP15, KPR21], become important.

### E. Dynamical quarks

The success of the CF model in describing the finite temperature confinement-deconfinement transition in the pure YM case naturally leads one to investigate how well it can capture the phase structure in the presence of quarks. As in the vacuum case, two regimes must be distinguished, depending on the values of the quark masses. For large quark masses, the quark-gluon coupling does not differ substantially from the one in the pure gauge sector and one can rely on perturbation theory. Admittedly, this regime does not correspond to the physical QCD case. However, it possesses a rich phase structure which has been studied using various approaches in the literature. It should also be mentioned that, in this range of masses, the phase transition is still akin to a description in terms of the Polyakov loop or the self-consistent background.

At vanishing quark chemical potential, there exists a critical phase boundary in the space of quark masses, separating a region of first-order phase transitions for large quark masses (including the YM case) from a crossover region for lower quark masses (including the physical QCD point), see the left panel of Fig. 26. For  $N_f$  degenerate flavours, the boundary is characterised by the ratios  $R_{N_f} \equiv M_c(N_f)/T_c(N_f)$ , with  $M_c(N_f)$  and  $T_c(N_f)$  the critical quark mass and critical temperature respectively. Those have been computed at one- and two-loop orders in the CF model within the self-consistent background field approach described previously. The one-loop results, shown in the left panel of Tab. II, are in remarkable agreement with lattice estimates. It is important to notice that, at one-loop order, these dimensionless ratios do not involve the gluon mass parameter or the gauge coupling and are, therefore, a parameter-free prediction of the model.

$R_{N_f}(\mu = 0)$	$N_f = 1$	$N_f = 2$	$N_f = 3$	$R_{N_f}^{\text{tric}}$	$N_f = 1$	$N_f = 2$	$N_f = 3$	$K_3$
one-loop CF	6.74	7.59	8.07	one-loop CF	4.74	5.63	6.15	1.85
lattice	7.23	7.92	8.33	lattice	5.56	6.25	6.66	1.55

TABLE II: The dimensionless ratio  $R_{N_f} = M_c/T_c$  on the critical line of the Columbia plot for  $N_f = 1, 2$ , and 3 degenerate flavours at zero chemical potential (left) and at the tricritical point  $\mu/T = i\pi/3$  (right). In this case we also show the value of the coefficient  $K_{N_f=3}$  [see Eq. (63)], whose lattice value appears rather insensitive to the value of  $N_f$ . The one-loop results in the CF model [RST15] are compared to the lattice values [FLLP12]. [Ref. [FLLP12] only quotes the value of  $K_1$ . The  $N_f$  dependance of  $R_{N_f}$  is governed by the scaling law (3.6) of that reference, valid in the heavy-quark limit, which implies that  $R_{N_f} = R_1 + \ln N_f$  and, in turn, that  $K_{N_f} = K_1$ .] We stress that the one-loop CF results are independent of the parameters of the model.

We mention that for any model of the YM sector, such as the CF model considered here, the ratios  $R_{N_f}$  for different  $N_f$  at one loop are related by the universal relation [KPS12, MRS18b]

$$N_f R_{N_f}^2 K_2(R_{N_f}) = N'_f R_{N'_f}^2 K_2(R_{N'_f}), \quad (62)$$

with  $K_2$  the modified Bessel function of the second kind. Again, two-loop corrections have been computed [MRS18a]. Although small, their general tendency is to approach the lattice results. As explained in this reference, the ratios  $R_{N_f}$  cannot be directly compared with the lattice data beyond one loop because of the different meanings of the (regularisation and renormalisation dependent) quark masses. One way to (approximately) cope with this issue is to consider the ratios  $Y_{N_f} = (R_{N_f} - R_1)/(R_2 - R_1)$ , which compare pretty well with the lattice result, known for  $N_f = 3$  [MRS18a, MRS18b].

The phase structure of the theory has also been investigated in the presence of a quark chemical potential [RST15, MRS18a, MRS18b]. For SU(3), this requires considering backgrounds with two nonvanishing components  $r_3$  and  $r_8$ , a nonzero  $r_8$  component being dictated by the breaking of charge conjugation invariance due the presence of a chemical potential. For imaginary values of the chemical potential, one retrieves the Roberge-Weiss (RW) transition [RW86], characterised by a first order jump of the phase of the Polyakov loop at  $\mu/T = i\pi/3$  (and large enough temperatures). The RW transition is not disconnected from the phase boundary at  $\mu = 0$ . In fact, as the quark masses are decreased

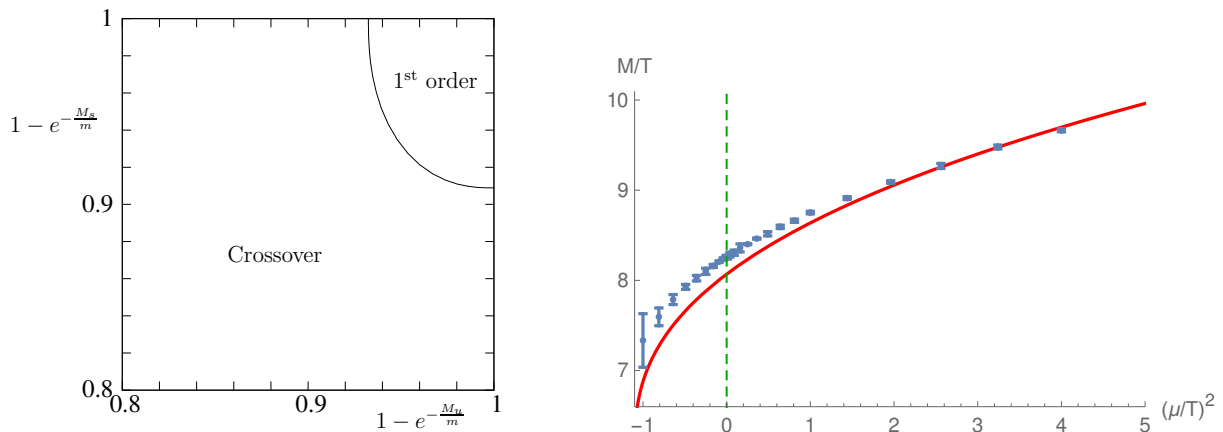


FIG. 26: Left: The critical phase boundary in the heavy quark corner of the Columbia plot, namely, the space of quark masses for the case with 2 + 1 degenerate quark normalis with masses  $M_u = M_d$  and  $M_s$ . The curve shown here is determined from the CF model at one-loop order [RST15]. The lines  $M_u \rightarrow \infty$ ,  $M_s \rightarrow \infty$ , and  $M_u = M_s$  correspond to the cases with, respectively,  $N_f = 1, 2$ , and 3 degenerate flavours. Right: The critical ratio  $R_{N_f}$  as a function of the chemical potential for  $N_f = 3$ . The CF model prediction at one-loop order [RST15] (plain line) is compared to the lattice data (dots) extracted from the results of Ref. [FLLP12] for  $R_1$  using the (lattice) relation  $R_{N_f} = R_1 + \ln N_f$ , valid in the heavy-quark limit.

below their critical values, the critical boundary enters the imaginary  $\mu$  region. As it reaches the particular value  $\mu/T = i\pi/3$  where the RW transition takes place, one finds a tricritical point characterised by the scaling law [dFP10]

$$R_{N_f} = R_{N_f}^{\text{tric}} + K_{N_f} \left[ \left( \frac{\pi}{3} \right)^2 + \left( \frac{\mu}{T} \right)^2 \right]^{2/5}, \quad (63)$$

for  $\mu/T \rightarrow i\pi/3$ . The (parameter-free) one-loop estimates of  $R_{N_f}^{\text{tric}} \equiv R_{N_f}(\mu/T = i\pi/3)$  and  $K_{N_f}$  in the CF model [RST15] are, again, in fairly good agreement with the lattice results [FLLP12]; see Tab. II and the right panel of Fig. 26. Also, as before, two-loop corrections tend to improve these values [MRS18a]. One also finds that the scaling law (63) extrapolates deep into the real chemical potential region  $\mu^2 > 0$ , as also seen in nonperturbative continuum approaches. Let us mention that a proper treatment of real chemical potentials requires the background  $r_8$  to be chosen purely imaginary. This surprising result relates to the QCD sign problem: for a real chemical potential, the QCD action is not real and there is a priori no reason to find real self-consistent backgrounds—*i.e.*, that solve the equation  $\bar{A} = \langle A \rangle_{\bar{A}}$ . On the other hand, it has been shown [RST15] that backgrounds of the form  $(r_3, r_8) \in \mathbb{R} \times i\mathbb{R}$  are compatible with the self-consistency assumption.

In the case of light quarks, the situation is not different from that in the vacuum: the quark-gluon coupling is a few times larger than the pure gauge coupling, thus preventing the use of perturbation theory. One can exploit the strategy developed in the vacuum based on the double expansion in powers of the inverse number of colours and the pure gauge coupling. As already explained above, this involves the resummation of rainbow diagrams in the quark propagator. Solving the corresponding equations can be done with present day technology [Fis19] but has not been attempted yet in the context of the CF model. Instead, as a first step in this direction, a drastically simplified version of the rainbow resummation at nonzero temperature and quark chemical potential has been implemented in Ref. [MRS20], which gives encouraging results.

## F. Propagators

The results presented in the previous subsections concern gauge-invariant quantities. As in the vacuum, lattice simulations also provide results for gauge-dependent correlation functions at nonzero temperature and density. In particular, many results have been produced for the YM and QCD propagators in the Landau gauge [HKR95, HKR98, CKP01a, CKP01b, CMM07, FMM10, CM10, CM11, ABI<sup>+</sup>12, MPvSS12, SOBC14, SO16, KS21, SBHK19, SK19].

The Landau gauge ghost and gluon propagators have been computed at one-loop order in the CF model—*i.e.*, with no background—at nonzero temperature and compared to lattice data for the SU(2) YM theory [RSTW14]. The

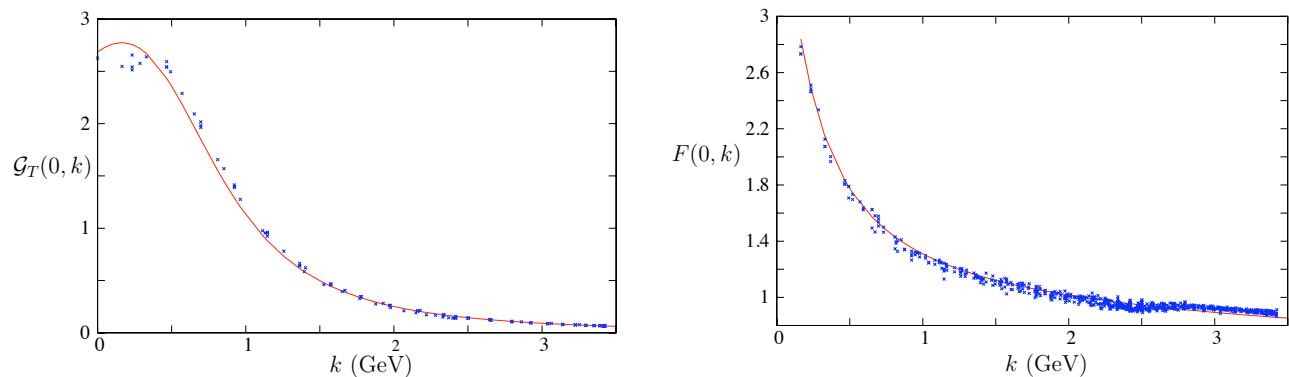


FIG. 27: The magnetic gluon (left) and the ghost (right) propagators at vanishing (Matsubara) frequency as a function of spatial momentum in the SU(2) YM theory at  $T = T_c$ , in the Landau gauge. The curves are the one-loop results (without RG improvement) in the CF model and the blue points are the data from Ref. [MPvSS12]. Figures from Ref. [RSTW14].

magnetic<sup>36</sup> gluon and ghost propagators are rather well reproduced, see Fig. 27. In contrast, the temperature dependence of the electric propagator differs substantially from the existing lattice data around the transition temperature [FMM10, MPvSS12]. We stress, however, that, first, this discrepancy is not specific to the perturbative CF approach, which produces in fact results very similar to those of nonperturbative continuum approaches [FP11] and, second, that the lattice results in the electric sector suffer from large uncertainties [MC14]. It has been suggested [FP11] that the discrepancy between continuum and lattice results may originate from the fact that the order parameter associated to the deconfinement transition is not properly accounted for in the perturbative Landau gauge calculations. Also, perturbative calculations in the CF model suggest that the limit of vanishing background field, corresponding to the Landau gauge, is unstable against small deviations [RSTW15b], which may explain the large numerical uncertainties mentioned here.

This has opened the way to the evaluation of correlation functions in background Landau gauges using the CF model [RSTT17, VERST21] with the idea that the proper inclusion of the order parameter may stabilize the comparison to lattice results. Although data for two-point functions in such gauges are not available yet, some interesting results have already been obtained within the CF model. In the self-consistent background gauge, the zero-momentum limit of the SU(2) electric propagator features a relatively sharp peak at the transition [RSTT17] which turns into a divergence in the case of the center-symmetric background gauge [VERST21]. In fact it has been argued that this divergence should also be there in the self-consistent approach [Rei20] were it not for the use of (inevitable) approximations that jeopardise certain properties of the gauge-fixing. In this sense, the results obtained with the center-symmetric background gauge, because they do not rely on these properties, should be more robust.

Similar one-loop calculations (without background) have been performed and compared to lattice calculations in the Landau gauge for two-colour QCD at nonzero quark chemical potential<sup>37</sup> [SK19, KS21]. In this case, the physics is that of a possible Bardeen-Cooper-Schieffer (BCS) phase with a nontrivial pairing between quarks. The mentioned references consider the effect of a phenomenological BCS gap  $\Delta$  on the electric and magnetic components of the gluon propagator through the quark loop contribution. As for the nonzero temperature case above, one allows for a variation of the CF parameters (coupling and gluon mass) with the chemical potential, to account for possible in-medium effects. In a nutshell—we refer the reader to these references for details—one obtains good agreement between the one-loop expressions and the lattice data, as illustrated in Fig. 28 for the electric propagator. A similar quality is achieved for the magnetic sector as well.

<sup>36</sup> In the Landau gauge, the gluon propagator is transverse with respect to the gluon four-momentum. In the vacuum, Lorentz invariance guarantees that there is only one possible scalar function. At nonzero temperature, however, the Lorentz symmetry group is explicitly broken into its rotation subgroup and there exist two independent  $3d$ -longitudinal (electric) and  $3d$ -transverse (magnetic) components.

<sup>37</sup> For  $N_c = 2$ , lattice simulations are possible at nonzero chemical potential because there is no sign problem: The integration measure under the Euclidean path integral is positive definite.

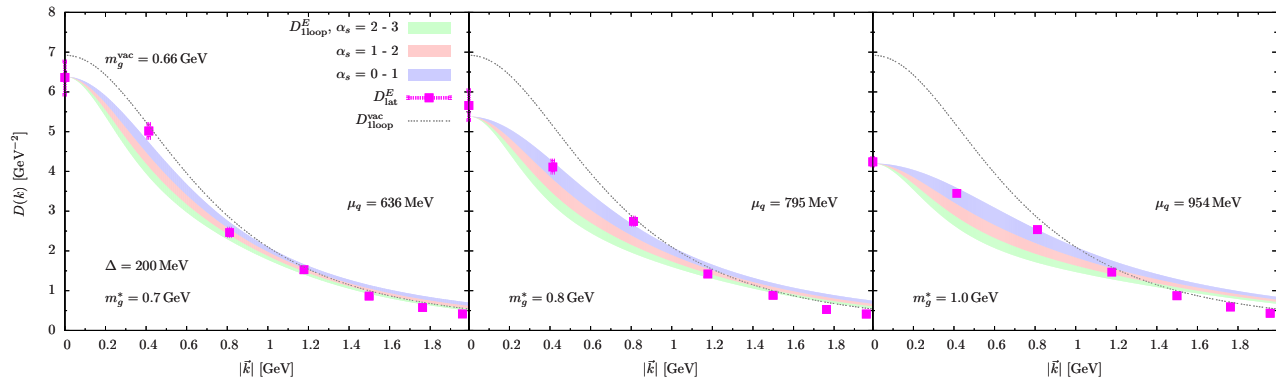


FIG. 28: The electric gluon propagator in two-colour QCD in the Landau gauge at zero temperature and nonzero quark chemical potential  $\mu_q$ . The various curves correspond to the one-loop result in the CF model (with no RG improvement) for different values of the coupling [SK19]. The chemical potential increases in the plots from left to right. The vacuum ( $\mu_q = 0$ ) result is also shown (dotted line) for reference. The quark gap  $\Delta$  is held fixed and the gluon mass parameter is adjusted by hand to obtain a good overall description of the lattice data (squares) of Ref. [BHMS19]. Figure from Ref. [SK19].

### VIII. RESULTS IN THE MINKOWSKIAN DOMAIN

So far, we have reviewed the large piece of evidences accumulated over the past decade which strongly support the idea of a valid perturbative description of (some aspects of) the IR dynamics of YM and QCD-like theories. The many successful comparisons to lattice data in the Euclidean domain encourage one to use the perturbative approach in situations where lattice techniques are not available. One example, described above, is the phase diagram of QCD at nonzero quark chemical potential. Another important example concerns the study of correlation functions in the Minkowskian domain.

The analytic structures of the gluon, ghost, and quark propagators in the complex momentum plane have been studied at one-loop order in the Landau gauge CF model [HK19, KWH<sup>+</sup>20, HK20, HK21] as well as in the screened perturbation theory approach [Sir16a, Sir17, SC21] in the vacuum and at nonzero temperature and density, with and without RG improvement. These studies are based on analytically continuing the Euclidean propagators<sup>38</sup> to the whole complex plane of square momentum  $s = -p^2$ . The most important results are that both the gluon and the quark propagator possess pairs of complex conjugate poles and that their spectral functions are not positive definite. The spectral functions mentioned here are defined as the imaginary parts of the corresponding propagators along the real  $s$  axis. They vanish identically in the Euclidean domain  $s \leq 0$  and are nonzero for Minkowskian momenta  $s \geq 0$ . It is worth emphasising that the spectral functions defined in this way are not exactly those entering the (assumed) spectral representations discussed in Sec. V C, due to the presence of poles away from the real  $s$  axis; see, *e.g.*, [HK20]. So, although related, the nonpositive spectral functions reported here are not to be put in one-to-one correspondence with the positivity violations mentioned in Sec. V C, observed in lattice calculations.

This being said, both the nonpositive spectral functions and the presence of pairs of complex-conjugate poles in the  $s$ -plane are in line with the fact that neither the massive gluon field nor the quark field correspond to actual asymptotic states. That is sometimes viewed as a sign of confinement although, as explained in Sect. III A, this interpretation is subject to caution. First, the nonzero imaginary part of the poles results in a finite lifetime of possible gluonic or quark excitations. Second, the nonpositive spectral functions show the absence of a proper Källén-Lehmann representation of asymptotic states with positive norm.

<sup>38</sup> Note that this is not quite the same thing, in general, as working with the Minkowskian version of the CF model. In particular, the presence of pairs of complex poles (see below) jeopardises the usual Wick rotation. It is not known to us whether a clear link exists between the (analytically continued) Euclidean CF model and its Minkowskian version beyond perturbation theory.

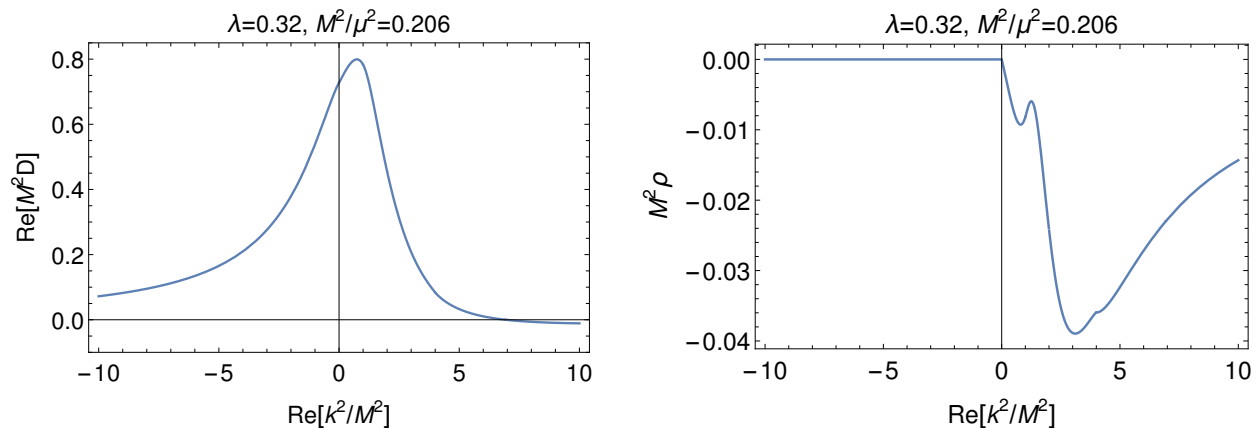


FIG. 29: Real (left) and imaginary (right) parts of the vacuum gluon propagator at one-loop order in the (pure gauge) CF model as a function of the square momentum. The calculation is done within the TW renormalisation scheme and does not include RG running. Here, the CF gluon mass is denoted  $M$  and  $\lambda = g^2 N_c / (16\pi^2)$ , with  $N_c = 3$ . The values of the parameters are chosen to provide a good fit of the lattice data for the real part in the Euclidean domain  $s = k^2 < 0$ . The imaginary part of the propagator, the so-called spectral function is negative, indicating that the (massive) gluon is not an asymptotic state in the theory, in line with the expectation from confinement. Figures from Ref. [KWH<sup>+</sup>20].

## IX. OPEN QUESTIONS

At this point, we hope to have convinced the reader that the CF model provides a very efficient framework for a valid description of many aspects of IR QCD based on controllable expansion schemes. Confronted to the many successful results reviewed here, a natural question that comes to mind is: how can such a simple model be so efficient? Can this be accidental? If one views the gluon mass parameter as a mere phenomenological IR deformation of the FP theory, the model works beyond expectations, almost unreasonably well. This calls one to wonder whether the CF model could have a deeper connection to (Landau gauge) IR QCD. This line of thought requires one to seriously address the various open problems of the CF model. Let us briefly mention—and speculate about—some of the most pressing issues.

One essential question is the status of the CF mass parameter. An interesting possibility is that it could be related to the issue of properly fixing the gauge in nonAbelian theories [ST12, KKSS15]. A recent proposal along these lines in the Landau gauge, exploiting the early ideas of Ref. [ST12] to handle the Gribov problem, has been shown to accommodate for a gluon mass term [RSTT21], although the resulting gauge-fixed action slightly differs from that of the CF model. Such gauge fixings do not exactly correspond to those realised in lattice simulations, but the successful comparisons described in this review suggest that the mass parameter can be adjusted to mimic the essential features of the latter [ST12, Maa12]. Another attractive possibility would be that the gluon mass is a dynamical consequence of the gauge-fixing procedure, whose value is fixed from the sole knowledge of the gauge coupling at a given scale, similar to what happens in the GZ approach [VZ12]. A concrete realisation of this scenario has been proposed in a general class of nonlinear gauges in Ref. [Tis18] which, unfortunately, does not survive the Landau gauge limit. Finally, it could also be that the gluon screening mass is an actual feature of the FP theory in the Landau gauge at a nonperturbative level. This has been investigated in the context of the screened perturbation theory, where the mass term is introduced as a variational parameter that must eventually be fixed by an extremisation procedure. A first interesting attempt in this direction has been worked out in Ref. [CS18] which, however, lacks the systematics of a genuine loop expansion and sometimes leads to unphysical results (like a spurious first order phase transition at nonzero temperature for the SU(2) YM theory. Finally, we mention that the hypothesis that the gluon mass is dynamically generated in the FP theory underlies all the studies based on nonperturbative continuum approaches.<sup>39</sup>

<sup>39</sup> As a side remark, it is interesting to note that this hypothesis actually supports the idea that the CF Lagrangian may be more than a mere phenomenological model and should perhaps be considered as a more fundamental realisation of Landau gauge QCD. Indeed, for technical reasons—not to be exposed here, see *e.g.*, [Hub20]—, these approaches (DSE, FRG, VHA) actually introduce a tree-level gluon mass parameter in one way or another [RSTW17] and are thus effectively based on the CF Lagrangian rather than on the FP one. The basic assumption of these approaches is that there exists a particular value of the CF mass which actually corresponds to the FP theory.

A more technical question is that of IR divergences in the Minkowskian domain. As mentioned in Sect. V, IR divergences in the Euclidian domain were studied in [TW11] and it was shown that, thanks to the presence of the gluon mass, there are no IR divergences for non-exceptional Euclidean momenta (for  $d > 2$ ). The case of exceptional Euclidean momenta is more delicate [TW11]. Also, the analysis of IR divergencies in the Minkowskian domain has not yet been carried out. This remains an open question because, as in QED, and despite the fact that the gluons are massive in the present model, the analysis of on-shell IR divergences is far from trivial due to the presence of massless modes in the CF model.

Other major issues are the construction of a proper physical space and the question of unitarity. As explained in Sec. IV C, and contrary to a widespread idea, this is still an open question within the CF model. In fact, it is important to stress that it is not even understood in the standard FP approach beyond perturbation theory. All continuum approaches have to face this issue, which directly affects the calculation of physical observables. A simple but generic example is the thermodynamic pressure at low temperatures. In all cases, the difficult task is the identification of the actual (confined) physical space.

An intricately related question, the mother of all, is that of confinement. The lack of perturbative unitarity in the CF model has led to its disproof as an alternative to the Higg's mechanism for a consistent theory of massive gauge bosons. However, it could very well be that the model is confining, which would completely change the game. Despite its importance, the precise definition of confinement has not been clearly established in the case of QCD (see *e.g.* the discussion in [Gre]). In the case of pure YM theory, the commonly accepted criterion for characterizing confinement corresponds to the Wilson loop area law. Although the Wilson loop is a perfectly well-defined quantity in the Euclidean domain, the area law corresponds to a linear behaviour for the static potential of a very distant quark-antiquark pair. In this limit, this potential is dominated by the behaviour of correlation functions with momenta out of the Euclidean domain near the singularities of various correlation functions. Accordingly, this behaviour is plagued by IR divergences that, at the moment, have not been put under control in the CF model. Controlling these IR divergences and reproducing the area law behaviour would clearly be of utmost importance.

## X. CONCLUSIONS

The CF model offers a promising avenue for investigating IR properties of continuum nonAbelian gauge theories in the Landau gauge beyond the textbook FP gauge-fixing prescription, which is limited to the UV. The systematic analysis of the two- and three-point vacuum correlation functions of the model and their comparison with results of *ab initio* lattice simulations in YM and QCD-like theories strongly support the idea that the inclusion of a gluon mass operator beyond the FP Landau gauge action suffices to capture most of the qualitative and many of the quantitative features of the Landau gauge correlations functions in the vacuum, from which one can extract physical observables.

The remarkable point is that many of these results (those for YM theory but also those for QCD with heavy quarks) rest on a purely perturbative approach within the CF model. For one thing, the model admits renormalisation group trajectories defined over the whole range of scales, in blatant contrast to the FP approach, which features an IR Landau pole, and in good agreement with lattice data. For another, the trajectories that allow one to best reproduce the results of simulations correspond to a running gauge coupling that never gets excessively large, thus justifying *a posteriori* the use of a perturbative approach. This, in turn, not only allows for a simple computational setup at leading order, in comparison to more demanding nonperturbative methods, but also offers the possibility to systematically investigate higher-order corrections and, thereby, the validity of the approach. Various two-loop corrections have been evaluated for YM and (heavy-quark) QCD two- and three-point correlation functions and have been found to be globally small while improving the quality of the comparison to the lattice data.

The perturbative approach is not a panacea, however, not even within the CF model, and certain questions require one to go beyond the simple coupling expansion. This is the case of the light quark sector of QCD controlled by the spontaneous breaking of chiral symmetry and characterized by an enhanced quark-gluon coupling in the IR, as compared to the typical couplings in the pure gauge sector. The perturbative nature of the pure gauge sector of the CF model allows nonetheless for the construction of a systematic expansion scheme that rests on two small parameters, the pure gauge coupling on the one side, and the inverse number of colours on the other side. Already the leading orders of this expansion scheme suffices to capture the general features of the spontaneous breaking of chiral symmetry while providing a consistent picture of the various two-point correlation functions. It would be interesting in the future to extend this analysis to the three-point correlators as well. The ultimate goal is of course to investigate low energy observables, within nonAbelian gauge theories in general, and within QCD in particular. A preliminary determination of the pion decay constant  $f_\pi$  within this approach is very encouraging and gives good confidence that other observables, such as the spectrum of low-lying hadrons are within reach.

Various relevant observables at nonzero temperature and chemical potential have also been evaluated, including transition temperatures and nontrivial order parameters involving nonperturbatively large field configurations. As

in the vacuum case, the perturbative CF model seems to capture most qualitative features of the phase structure such as the confinement-deconfinement transition in YM theories, the critical line in the heavy-quark region of the Columbia plot, as well as the RW transition for imaginary chemical potential. In most cases, the description is even quantitative, with, for instance, transition temperatures that gives results comparing well with simulations at one loop and improving, sometimes significantly, at two-loop order. Similar conclusions emerge from the evaluation of quark mass-to-temperature ratios along the upper critical line in the Columbia plot. In the case of QCD with light quarks, perturbation theory is again not enough but one can extend the approach mentioned above for the vacuum case at nonzero temperature and chemical potential. Preliminary results show that the CF model has the potential to access features of the phase structure in this case too, in particular the possible existence of a critical end point in the QCD phase diagram. This needs to be confirmed by more refined studies.

Of course, there are still many open questions concerning the CF model and its use as (part of) a nonperturbative completion of the gauge fixing beyond the FP construction. Its many successes should serve as an incentive to better understand the nonperturbative gauge-fixing procedure, with the potential reward of granting a relatively simple access to some of the low-energy observables of QCD.

To conclude, lattice simulations have firmly established (see Fig. 1) that at least part of the IR regime of QCD is governed by a coupling of perturbative size in the Landau gauge. Although it has remained largely unknown to a broad audience, this is an observation of paramount importance with far-reaching consequences. We believe that the work reviewed in this article clearly establishes that many facets of the IR QCD dynamics admit a perturbative description in the Landau gauge and that the CF model is an efficient framework for the latter, be it at a fundamental or at a more phenomenological level. We hope that the present article will convince the reader of the usefulness of a change of paradigm concerning the IR dynamics of nonAbelian theories and will motivate QCD practitioners to include the CF model as one serious option in their toolbox [HLP20, SBHK19].

### Acknowledgments

We thank B. Delamotte, N. Dupuis, and G. Tarjus for a careful reading of the manuscript. We acknowledge the financial support from PEDECIBA, from the "Institut Franco-Uruguayen de Physique", and from the ECOS program U17E01 and from the ANII-FCE-126412 project.

- 
- [AAJS16] Gert Aarts, Felipe Attanasio, Benjamin Jäger, and Dénes Sexty. The QCD phase diagram in the limit of heavy quarks using complex Langevin dynamics. *JHEP*, 09:087, 2016.
- [AB98] D. Atkinson and Jacques C.R. Bloch. QCD in the infrared with exact angular integrations. *Mod. Phys. Lett. A*, 13:1055–1062, 1998.
- [Abb81] L. F. Abbott. The Background Field Method Beyond One Loop. *Nucl. Phys. B*, 185:189–203, 1981.
- [Abb82] L. F. Abbott. Introduction to the Background Field Method. *Acta Phys. Polon. B*, 13:33, 1982.
- [ABB<sup>+</sup>12] A. Ayala, A. Bashir, D. Binosi, M. Cristoforetti, and J. Rodríguez-Quintero. Quark flavour effects on gluon and ghost propagators. *Phys.Rev.*, D86:074512, 2012.
- [ABB<sup>+</sup>16] A. Athenodorou, D. Binosi, Ph. Boucaud, F. De Soto, J. Papavassiliou, J. Rodríguez-Quintero, and S. Zafeiropoulos. On the zero crossing of the three-gluon vertex. *Phys. Lett. B*, 761:444–449, 2016.
- [ABI<sup>+</sup>12] R. Aouane, V.G. Bornyakov, E.M. Ilgenfritz, V.K. Mitrjushkin, M. Müller-Preussker, et al. Landau gauge gluon and ghost propagators at finite temperature from quenched lattice QCD. *Phys.Rev.*, D85:034501, 2012.
- [ABIP14] A.C. Aguilar, D. Binosi, D. Ibañez, and J. Papavassiliou. Effects of divergent ghost loops on the Green's functions of QCD. *Phys.Rev.*, D89:085008, 2014.
- [ABP08] A.C. Aguilar, D. Binosi, and J. Papavassiliou. Gluon and ghost propagators in the Landau gauge: Deriving lattice results from Schwinger-Dyson equations. *Phys.Rev.*, D78:025010, 2008.
- [ADSF<sup>+</sup>20] A.C. Aguilar, F. De Soto, M.N. Ferreira, J. Papavassiliou, J. Rodríguez-Quintero, and S. Zafeiropoulos. Gluon propagator and three-gluon vertex with dynamical quarks. *Eur. Phys. J. C*, 80(2):154, 2020.
- [ADSF<sup>+</sup>21] A. C. Aguilar, F. De Soto, M. N. Ferreira, J. Papavassiliou, and J. Rodríguez-Quintero. Infrared facets of the three-gluon vertex. *Phys. Lett. B*, 818:136352, 2021.
- [AJ88] D. Atkinson and P. W. Johnson. Chiral Symmetry Breaking in QCD. 1. The Infrared Domain. *Phys. Rev. D*, 37:2290–2295, 1988.
- [AN04] A.C. Aguilar and A.A. Natale. A Dynamical gluon mass solution in a coupled system of the Schwinger-Dyson equations. *JHEP*, 0408:057, 2004.
- [AP06] Arlene C. Aguilar and Joannis Papavassiliou. Gluon mass generation in the PT-BFM scheme. *JHEP*, 12:012, 2006.
- [AP08] Arlene C. Aguilar and Joannis Papavassiliou. Power-law running of the effective gluon mass. *Eur.Phys.J.*, A35:189–205, 2008.

- [AvS01] Reinhard Alkofer and Lorenz von Smekal. The Infrared behavior of QCD Green's functions: Confinement dynamical symmetry breaking, and hadrons as relativistic bound states. *Phys.Rept.*, 353:281, 2001.
- [B<sup>+</sup>14] A. Bazavov et al. Equation of state in (2+1)-flavor QCD. *Phys. Rev. D*, 90:094503, 2014.
- [BBC<sup>+</sup>15] P. Bicudo, D. Binosi, N. Cardoso, O. Oliveira, and P. J. Silva. Lattice gluon propagator in renormalizable  $\xi$  gauges. *Phys. Rev. D*, 92(11):114514, 2015.
- [BBDS<sup>+</sup>14] Ph. Boucaud, M. Brinet, F. De Soto, V. Morenas, O. Pène, K. Petrov, and J. Rodríguez-Quintero. Three-gluon running coupling from lattice QCD at  $N_f = 2 + 1 + 1$ : a consistency check of the OPE approach. *JHEP*, 04:086, 2014.
- [BBL<sup>+</sup>01] Frederic D.R. Bonnet, Patrick O. Bowman, Derek B. Leinweber, Anthony G. Williams, and James M. Zanotti. Infinite volume and continuum limits of the Landau gauge gluon propagator. *Phys. Rev. D*, 64:034501, 2001.
- [BBL<sup>+</sup>06] Philippe Boucaud, Th. Bruntjen, J.P. Leroy, A. Le Yaouanc, A.Y. Likhov, et al. Is the QCD ghost dressing function finite at zero momentum? *JHEP*, 0606:001, 2006.
- [BBLW00] Frederic D.R. Bonnet, Patrick O. Bowman, Derek B. Leinweber, and Anthony G. Williams. Infrared behavior of the gluon propagator on a large volume lattice. *Phys.Rev.*, D62:051501, 2000.
- [BC80] James S. Ball and Ting-Wai Chiu. Analytic Properties of the Vertex Function in Gauge Theories. 2. *Phys.Rev.*, D22:2550, 1980.
- [BDSRQZ17] Ph. Boucaud, F. De Soto, J. Rodríguez-Quintero, and S. Zafeiropoulos. Refining the detection of the zero crossing for the three-gluon vertex in symmetric and asymmetric momentum subtraction schemes. *Phys. Rev. D*, 95(11):114503, 2017.
- [BFH<sup>+</sup>14] Szabolcs Borsányi, Zoltan Fodor, Christian Hoelbling, Sandor D. Katz, Stefan Krieg, and Kalman K. Szabo. Full result for the QCD equation of state with 2+1 flavors. *Phys. Lett. B*, 730:99–104, 2014.
- [BG80] Uzi Bar-Gadda. Infrared Behavior of the Effective Coupling in Quantum Chromodynamics: A Nonperturbative Approach. *Nucl. Phys. B*, 163:312–332, 1980.
- [BG02] R.E. Browne and J.A. Gracey. The Curci-Ferrari model with massive quarks at two loops. *Phys.Lett.*, B540:68–74, 2002.
- [BGP10] Jens Braun, Holger Gies, and Jan M. Pawłowski. Quark Confinement from Color Confinement. *Phys. Lett. B*, 684:262–267, 2010.
- [BGPR21] Nahuel Barrios, John A. Gracey, Marcela Peláez, and Urko Reinosa. Precision QCD propagators with dynamical quarks from the Curci-Ferrari model. 2021. arXiv eprint: hep-th/2103.16218.
- [BHL<sup>+</sup>04] Patrick O. Bowman, Urs M. Heller, Derek B. Leinweber, Maria B. Parappilly, and Anthony G. Williams. Unquenched gluon propagator in Landau gauge. *Phys.Rev.*, D70:034509, 2004.
- [BHL<sup>+</sup>05] Patrick O. Bowman, Urs M. Heller, Derek B. Leinweber, Maria B. Parappilly, Anthony G. Williams, et al. Unquenched quark propagator in Landau gauge. *Phys.Rev.*, D71:054507, 2005.
- [BHL<sup>+</sup>07] Patrick O. Bowman, Urs M. Heller, Derek B. Leinweber, Maria B. Parappilly, Andre Sternbeck, et al. Scaling behavior and positivity violation of the gluon propagator in full QCD. *Phys.Rev.*, D76:094505, 2007.
- [BHMS19] Tamer Boz, Ouraman Hajizadeh, Axel Maas, and Jon-Ivar Skullerud. Finite-density gauge correlation functions in QC2D. *Phys. Rev. D*, 99(7):074514, 2019.
- [BHMvS14] Adrian Blum, Markus Q. Huber, Mario Mitter, and Lorenz von Smekal. Gluonic three-point correlations in pure Landau gauge QCD. *Phys.Rev.*, D89(6):061703, 2014.
- [BIMPS09] I.L. Bogolubsky, E.M. Ilgenfritz, M. Muller-Preussker, and A. Sternbeck. Lattice gluodynamics computation of Landau gauge Green's functions in the deep infrared. *Phys.Lett.*, B676:69–73, 2009.
- [BLLY<sup>+</sup>08] Philippe Boucaud, J.P. Leroy, A. Le Yaouanc, J. Micheli, O. Pene, et al. On the IR behaviour of the Landau-gauge ghost propagator. *JHEP*, 0806:099, 2008.
- [BLY<sup>+</sup>08] Philippe Boucaud, J-P. Leroy, A.Le Yaouanc, J. Micheli, O. Pene, and J. Rodriguez-Quintero. IR finiteness of the ghost dressing function from numerical resolution of the ghost SD equation. *JHEP*, 06:012, 2008.
- [BLY<sup>+</sup>12] Ph. Boucaud, J.P. Leroy, A.Le Yaouanc, J. Micheli, O. Pene, and J. Rodriguez-Quintero. The Infrared Behaviour of the Pure Yang-Mills Green Functions. *Few Body Syst.*, 53:387–436, 2012.
- [BMMP10] V.G. Bornyakov, V.K. Mitrjushkin, and M. Muller-Preussker. SU(2) lattice gluon propagator: Continuum limit, finite-volume effects and infrared mass scale  $m(\text{IR})$ . *Phys. Rev. D*, 81:054503, 2010.
- [BP88] Nicholas Brown and M.R. Pennington. Preludes to Confinement: Infrared Properties of the Gluon Propagator in the Landau Gauge. *Phys. Lett. B*, 202:257, 1988. [Erratum: Phys.Lett.B 205, 596 (1988)].
- [BP89] Nicholas Brown and M.R. Pennington. Studies of Confinement: How the Gluon Propagates. *Phys. Rev. D*, 39:2723, 1989.
- [BPRW20] Nahuel Barrios, Marcela Peláez, Urko Reinosa, and Nicolás Wschebor. The ghost-antighost-gluon vertex from the Curci-Ferrari model: Two-loop corrections. *Phys. Rev. D*, 102:114016, 2020. arXiv eprint: hep-th/2009.00875.
- [BRS75] C. Becchi, A. Rouet, and R. Stora. Renormalization of the Abelian Higgs-Kibble Model. *Commun.Math.Phys.*, 42:127–162, 1975.
- [BRS76] C. Becchi, A. Rouet, and R. Stora. Renormalization of Gauge Theories. *Annals Phys.*, 98:287–321, 1976.
- [CDJ<sup>+</sup>15] F. E. Canfora, D. Dudal, I. F. Justo, P. Pais, L. Rosa, and D. Vercauteren. Effect of the Gribov horizon on the Polyakov loop and vice versa. *Eur. Phys. J. C*, 75(7):326, 2015.
- [CDM<sup>+</sup>18] Attilio Cucchieri, David Dudal, Tereza Mendes, Orlando Oliveira, Martin Roelfs, and Paulo J. Silva. Faddeev-Popov Matrix in Linear Covariant Gauge: First Results. *Phys. Rev. D*, 98(9):091504, 2018.
- [CF76a] G. Curci and R. Ferrari. On a Class of Lagrangian Models for Massive and Massless Yang-Mills Fields. *Nuovo Cim.*, A32:151–168, 1976.
- [CF76b] G. Curci and R. Ferrari. Slavnov Transformations and Supersymmetry. *Phys. Lett. B*, 63:91–94, 1976.

- [CFM<sup>+</sup>16] Anton K. Cyrol, Leonard Fister, Mario Mitter, Jan M. Pawłowski, and Nils Strodthoff. Landau gauge Yang-Mills correlation functions. *Phys. Rev. D*, 94(5):054005, 2016.
- [CKP01a] A. Cucchieri, F. Karsch, and P. Petreczky. Magnetic screening in hot nonAbelian gauge theory. *Phys. Lett. B*, 497:80–84, 2001.
- [CKP01b] A. Cucchieri, F. Karsch, and P. Petreczky. Propagators and dimensional reduction of hot SU(2) gauge theory. *Phys. Rev. D*, 64:036001, 2001.
- [CM08a] A. Cucchieri and T. Mendes. Constraints on the IR behavior of the gluon propagator in Yang-Mills theories. *Phys.Rev.Lett.*, 100:241601, 2008.
- [CM08b] Attilio Cucchieri and Tereza Mendes. Constraints on the IR behavior of the ghost propagator in Yang-Mills theories. *Phys.Rev.*, D78:094503, 2008.
- [CM10] Attilio Cucchieri and Tereza Mendes. Electric and magnetic Landau-gauge gluon propagators in finite-temperature SU(2) gauge theory. *PoS, FACESQCD:007*, 2010.
- [CM11] Attilio Cucchieri and Tereza Mendes. Electric and Magnetic Screening Masses around the Deconfinement Transition. *PoS, LATTICE2011:206*, 2011.
- [CMM07] Attilio Cucchieri, Axel Maas, and Tereza Mendes. Infrared properties of propagators in Landau-gauge pure Yang-Mills theory at finite temperature. *Phys.Rev.*, D75:076003, 2007.
- [CMM08] Attilio Cucchieri, Axel Maas, and Tereza Mendes. Three-point vertices in Landau-gauge Yang-Mills theory. *Phys.Rev.*, D77:094510, 2008.
- [CMS09] Attilio Cucchieri, Tereza Mendes, and Elton M.S. Santos. Covariant gauge on the lattice: A New implementation. *Phys.Rev.Lett.*, 103:141602, 2009.
- [CMT03] Attilio Cucchieri, Tereza Mendes, and Andre R. Taurines. SU(2) Landau gluon propagator on a 140\*\*3 lattice. *Phys. Rev. D*, 67:091502, 2003.
- [CMT05] Attilio Cucchieri, Tereza Mendes, and Andre R. Taurines. Positivity violation for the lattice Landau gluon propagator. *Phys.Rev.*, D71:051902, 2005.
- [CS18] Giorgio Comitini and Fabio Siringo. Variational study of mass generation and deconfinement in Yang-Mills theory. *Phys. Rev. D*, 97(5):056013, 2018.
- [CS20] Giorgio Comitini and Fabio Siringo. One-loop RG improvement of the screened massive expansion in the Landau gauge. *Phys. Rev. D*, 102(9):094002, 2020.
- [CZB<sup>+</sup>20] Zhu-Fang Cui, Jin-Li Zhang, Daniele Binosi, Feliciano de Soto, Cédric Mezrag, Joannis Papavassiliou, Craig D Roberts, Jose Rodríguez-Quintero, Jorge Segovia, and Savvas Zafeiropoulos. Effective charge from lattice QCD. *Chin. Phys. C*, 44(8):083102, 2020.
- [D<sup>+</sup>14] Stephan Dürr et al. Lattice QCD at the physical point meets SU(2) chiral perturbation theory. *Phys. Rev. D*, 90(11):114504, 2014.
- [DBdT16] Alexandre Deur, Stanley J. Brodsky, and Guy F. de Teramond. The QCD Running Coupling. *Nucl. Phys.*, 90:1, 2016.
- [dBSvNW96] Jan de Boer, Kostas Skenderis, Peter van Nieuwenhuizen, and Andrew Waldron. On the renormalizability and unitarity of the Curci-Ferrari model for massive vector bosons. *Phys.Lett.*, B367:175–182, 1996.
- [dFP10] Philippe de Forcrand and Owe Philipsen. Constraining the QCD phase diagram by tricritical lines at imaginary chemical potential. *Phys. Rev. Lett.*, 105:152001, 2010.
- [DGH<sup>+</sup>12] Adrian Dumitru, Yun Guo, Yoshimasa Hidaka, Christiaan P. Korthals Altes, and Robert D. Pisarski. Effective Matrix Model for Deconfinement in Pure Gauge Theories. *Phys. Rev. D*, 86:105017, 2012.
- [DGS<sup>+</sup>08] David Dudal, John A. Gracey, Silvio Paolo Sorella, Nele Vandersickel, and Henri Verschelde. A Refinement of the Gribov-Zwanziger approach in the Landau gauge: Infrared propagators in harmony with the lattice results. *Phys.Rev.*, D78:065047, 2008.
- [DJ82] Robert Delbourgo and Peter D. Jarvis. Extended {BRS} Invariance and Osp(4/2) Supersymmetry. *J. Phys. A*, 15:611, 1982.
- [DL16] Thomas DeGrand and Yuzhi Liu. Lattice study of large  $N_c$  QCD. *Phys. Rev. D*, 94(3):034506, 2016. [Erratum: *Phys.Rev.D* 95, 019902 (2017)].
- [DOS16] Anthony G. Duarte, Orlando Oliveira, and Paulo J. Silva. Lattice Gluon and Ghost Propagators, and the Strong Coupling in Pure SU(3) Yang-Mills Theory: Finite Lattice Spacing and Volume Effects. *Phys. Rev. D*, 94(1):014502, 2016.
- [DOS17] Anthony G. Duarte, Orlando Oliveira, and Paulo J. Silva. Reply to “Comment on ‘Lattice gluon and ghost propagators and the strong coupling in pure SU(3) Yang-Mills theory: Finite lattice spacing and volume effects’ ”. *Phys. Rev. D*, 96(9):098502, 2017.
- [DOT96] Andrei I. Davydchev, P. Osland, and O.V. Tarasov. Three gluon vertex in arbitrary gauge and dimension. *Phys.Rev.*, D54:4087–4113, 1996.
- [DOT98] Andrei I. Davydchev, P. Osland, and O.V. Tarasov. Two loop three gluon vertex in zero momentum limit. *Phys.Rev.*, D58:036007, 1998.
- [DW20] Pietro Dall’Olio and Axel Weber. Exploiting the scheme dependence of the renormalization group improvement in infrared Yang-Mills theory. 2020. arXiv eprint: hep-th/2012.02389.
- [DZ89] G. Dell’Antonio and D. Zwanziger. Ellipsoidal Bound on the Gribov Horizon Contradicts the Perturbative Renormalization Group. *Nucl. Phys. B*, 326:333–350, 1989.
- [EHW98] Ulrich Ellwanger, Manfred Hirsch, and Axel Weber. The Heavy quark potential from Wilson’s exact renormalization group. *Eur. Phys. J. C*, 1:563–578, 1998.

- [EWAV14] Gernot Eichmann, Richard Williams, Reinhard Alkofer, and Milan Vujanovic. Three-gluon vertex in Landau gauge. *Phys.Rev.*, D89(10):105014, 2014.
- [FA02] C.S. Fischer and Reinhard Alkofer. Infrared exponents and running coupling of SU(N) Yang-Mills theories. *Phys. Lett. B*, 536:177–184, 2002.
- [FG04] Christian S. Fischer and Holger Gies. Renormalization flow of Yang-Mills propagators. *JHEP*, 10:048, 2004.
- [FH12] Zoltan Fodor and Christian Hoelbling. Light Hadron Masses from Lattice QCD. *Rev. Mod. Phys.*, 84:449, 2012.
- [Fis19] Christian S. Fischer. QCD at finite temperature and chemical potential from Dyson–Schwinger equations. *Prog. Part. Nucl. Phys.*, 105:1–60, 2019.
- [FLLP12] Michael Fromm, Jens Langelage, Stefano Lottini, and Owe Philipsen. The QCD deconfinement transition for heavy quarks and all baryon chemical potentials. *JHEP*, 01:042, 2012.
- [FLP15] Christian S. Fischer, Jan Luecker, and Jan M. Pawłowski. Phase structure of QCD for heavy quarks. *Phys. Rev. D*, 91(1):014024, 2015.
- [FMM10] Christian S. Fischer, Axel Maas, and Jens A. Müller. Chiral and deconfinement transition from correlation functions: SU(2) vs. SU(3). *Eur. Phys. J. C*, 68:165–181, 2010.
- [FMP09] Christian S. Fischer, Axel Maas, and Jan M. Pawłowski. On the infrared behavior of Landau gauge Yang-Mills theory. *Annals Phys.*, 324:2408–2437, 2009.
- [FP] F. Figueroa and M. Peláez. Unquenched three gluon vertex. In preparation.
- [FP67] L.D. Faddeev and V.N. Popov. Feynman Diagrams for the Yang-Mills Field. *Phys.Lett.*, B25:29–30, 1967.
- [FP91] Stefano Fachin and Claudio Parrinello. Global gauge fixing in lattice gauge theories. *Phys. Rev. D*, 44:2558–2564, 1991.
- [FP07] Christian S. Fischer and Jan M. Pawłowski. Uniqueness of infrared asymptotics in Landau gauge Yang-Mills theory. *Phys.Rev.*, D75:025012, 2007.
- [FP09] Christian S. Fischer and Jan M. Pawłowski. Uniqueness of infrared asymptotics in Landau gauge Yang-Mills theory II. *Phys. Rev. D*, 80:025023, 2009.
- [FP11] Leonard Fister and Jan M. Pawłowski. Yang-Mills correlation functions at finite temperature. 2011. arXiv eprint: hep-ph/1112.5440.
- [FS17] Kenji Fukushima and Vladimir Skokov. Polyakov loop modeling for hot QCD. *Prog. Part. Nucl. Phys.*, 96:154–199, 2017.
- [GHK08] Sourendu Gupta, Kay Huebner, and Olaf Kaczmarek. Renormalized Polyakov loops in many representations. *Phys. Rev. D*, 77:034503, 2008.
- [GL16] Christof Gattringer and Kurt Langfeld. Approaches to the sign problem in lattice field theory. *Int. J. Mod. Phys. A*, 31(22):1643007, 2016.
- [GPRT19] John A. Gracey, Marcela Peláez, Urko Reinoso, and Matthieu Tissier. Two loop calculation of Yang-Mills propagators in the Curci-Ferrari model. *Phys. Rev. D*, 100(3):034023, 2019.
- [Gra03] J.A. Gracey. Three loop MS-bar renormalization of the Curci-Ferrari model and the dimension two BRST invariant composite operator in QCD. *Phys.Lett.*, B552:101–110, 2003.
- [Gre] Jeff Greensite. *An introduction to the confinement problem*. Springer.
- [Gre12] Jeff Greensite. The potential of the effective Polyakov line action from the underlying lattice gauge theory. *Phys. Rev. D*, 86:114507, 2012.
- [Gri78] V.N. Gribov. Quantization of Nonabelian Gauge Theories. *Nucl.Phys.*, B139:1, 1978.
- [GW73] David J. Gross and Frank Wilczek. Ultraviolet Behavior of Nonabelian Gauge Theories. *Phys.Rev.Lett.*, 30:1343–1346, 1973.
- [HAFS08] Markus Q. Huber, Reinhard Alkofer, Christian S. Fischer, and Kai Schwenzer. The Infrared behavior of Landau gauge Yang-Mills theory in d=2, d=3 and d=4 dimensions. *Phys.Lett.*, B659:434–440, 2008.
- [HBA<sup>+</sup>14] Najmul Haque, Aritra Bandyopadhyay, Jens O. Andersen, Munshi G. Mustafa, Michael Strickland, and Nan Su. Three-loop HTLpt thermodynamics at finite temperature and chemical potential. *JHEP*, 05:027, 2014.
- [HK19] Yui Hayashi and Kei-Ichi Kondo. Complex poles and spectral function of Yang-Mills theory. *Phys. Rev. D*, 99(7):074001, 2019.
- [HK20] Yui Hayashi and Kei-Ichi Kondo. Complex poles and spectral functions of Landau gauge QCD and QCD-like theories. *Phys. Rev. D*, 101(7):074044, 2020.
- [HK21] Yui Hayashi and Kei-Ichi Kondo. Effects of a quark chemical potential on the analytic structure of the gluon propagator. *Phys. Rev. D*, 103(9):094006, 2021.
- [HKR95] Urs M. Heller, F. Karsch, and J. Rank. The Gluon propagator at high temperature. *Phys. Lett. B*, 355:511–517, 1995.
- [HKR98] Urs M. Heller, F. Karsch, and J. Rank. The Gluon propagator at high temperature: Screening, improvement and nonzero momenta. *Phys. Rev. D*, 57:1438–1448, 1998.
- [HLP15] Tina K. Herbst, Jan Luecker, and Jan M. Pawłowski. Confinement order parameters and fluctuations. 2015. arXiv eprint: hep-ph/1510.03830.
- [HLP20] D. Hadjimichef, E. G. S. Luna, and M. Peláez. QCD effective charges and the structure function  $F_2$  at small- $x$ : Higher twist effects. *Phys. Lett. B*, 804:135350, 2020.
- [HMvS12] Markus Q. Huber, Axel Maas, and Lorenz von Smekal. Two- and three-point functions in two-dimensional Landau-gauge Yang-Mills theory: Continuum results. *JHEP*, 11:035, 2012.
- [Hub16] Markus Q. Huber. Correlation functions of three-dimensional Yang-Mills theory from Dyson-Schwinger equations. *Phys. Rev. D*, 93(8):085033, 2016.
- [Hub20] Markus Q. Huber. Correlation functions of Landau gauge Yang-Mills theory. *Phys. Rev. D*, 101:114009, 2020.

- [HvS13] Markus Q. Huber and Lorenz von Smekal. On the influence of three-point functions on the propagators of Landau gauge Yang-Mills theory. *JHEP*, 1304:149, 2013.
- [IMPS<sup>+</sup>07] E.-M. Ilgenfritz, M. Muller-Preussker, A. Sternbeck, A. Schiller, and I.L. Bogolubsky. Landau gauge gluon and ghost propagators from lattice QCD. *Braz.J.Phys.*, 37:193–200, 2007.
- [ISI09] Takumi Iritani, Hideo Suganuma, and Hideaki Iida. Gluon-propagator functional form in the Landau gauge in SU(3) lattice QCD: Yukawa-type gluon propagator and anomalous gluon spectral function. *Phys. Rev. D*, 80:114505, 2009.
- [KKPZ02] O. Kaczmarek, F. Karsch, P. Petreczky, and F. Zantow. Heavy quark anti-quark free energy and the renormalized Polyakov loop. *Phys. Lett. B*, 543:41–47, 2002.
- [KKSS15] Kei-Ichi Kondo, Seikou Kato, Akihiro Shibata, and Toru Shinohara. Quark confinement: Dual superconductor picture based on a non-Abelian Stokes theorem and reformulations of Yang–Mills theory. *Phys. Rept.*, 579:1–226, 2015.
- [KLSW07] Ayse Kizilersu, Derek B. Leinweber, Jon-Ivar Skullerud, and Anthony G. Williams. Quark-gluon vertex in general kinematics. *Eur. Phys. J. C*, 50:871–875, 2007.
- [KO78a] Taichiro Kugo and Izumi Ojima. Manifestly Covariant Canonical Formulation of Yang-Mills Field Theories. 1. The Case of Yang-Mills Fields of Higgs-Kibble Type in Landau Gauge. *Prog. Theor. Phys.*, 60:1869, 1978.
- [KO78b] Taichiro Kugo and Izumi Ojima. Manifestly Covariant Canonical Formulation of Yang-Mills Field Theories: Physical State Subsidiary Conditions and Physical S Matrix Unitarity. *Phys.Lett.*, B73:459, 1978.
- [KO79a] Taichiro Kugo and Izumi Ojima. Local Covariant Operator Formalism of Nonabelian Gauge Theories and Quark Confinement Problem. *Prog.Theor.Phys.Suppl.*, 66:1–130, 1979.
- [KO79b] Taichiro Kugo and Izumi Ojima. Manifestly Covariant Canonical Formulation of Yang-Mills Field Theories. 2. The Case of Pure Yang-Mills Theories Without Spontaneous Symmetry Breaking in General Covariant Gauges. *Prog. Theor. Phys.*, 61:294, 1979.
- [Kon15] Kei-Ichi Kondo. Confinement–deconfinement phase transition and gauge-invariant gluonic mass in Yang-Mills theory. 2015. arXiv eprint: hep-th/1508.02656.
- [KOS<sup>+</sup>21] Ayşe Kizilersü, Orlando Oliveira, Paulo J. Silva, Jon-Ivar Skullerud, and André Sternbeck. Quark-gluon vertex from Nf=2 lattice QCD. 2021. arXiv eprint: hep-lat/2103.02945.
- [KPP97] F. Karsch, A. Patkos, and P. Petreczky. Screened perturbation theory. *Phys. Lett. B*, 401:69–73, 1997.
- [KPR21] Jean-Loïc Kneur, Marcus Benghi Pinto, and Tulio E. Restrepo. QCD pressure: renormalization group optimized perturbation theory confronts lattice. 2021. arXiv eprint: hep-ph/2101.02124.
- [KPS12] Kouji Kashiwa, Robert D. Pisarski, and Vladimir V. Skokov. Critical endpoint for deconfinement in matrix and other effective models. *Phys. Rev. D*, 85:114029, 2012.
- [KS21] Toru Kojo and Daiki Suenaga. Thermal quarks and gluon propagators in two-color dense QCD. 2021. arXiv eprint: hep-ph/2102.07231.
- [KWH<sup>+</sup>20] Kei-Ichi Kondo, Masaki Watanabe, Yui Hayashi, Ryutaro Matsudo, and Yutaro Suda. Reflection positivity and complex analysis of the Yang-Mills theory from a viewpoint of gluon confinement. *Eur. Phys. J. C*, 80(2):84, 2020.
- [LFK<sup>+</sup>13] Pok Man Lo, Bengt Friman, Olaf Kaczmarek, Krzysztof Redlich, and Chihiro Sasaki. Polyakov loop fluctuations in SU(3) lattice gauge theory and an effective gluon potential. *Phys. Rev. D*, 88:074502, 2013.
- [LP13] Biagio Lucini and Marco Panero. SU(N) gauge theories at large N. *Phys. Rept.*, 526:93–163, 2013.
- [LTW05] Biagio Lucini, Michael Teper, and Urs Wenger. Properties of the deconfining phase transition in SU(N) gauge theories. *JHEP*, 02:033, 2005.
- [LvS02] Christoph Lerche and Lorenz von Smekal. On the infrared exponent for gluon and ghost propagation in Landau gauge QCD. *Phys.Rev.*, D65:125006, 2002.
- [Maa07] Axel Maas. Two and three-point Green’s functions in two-dimensional Landau-gauge Yang-Mills theory. *Phys. Rev. D*, 75:116004, 2007.
- [Maa10] Axel Maas. Constructing non-perturbative gauges using correlation functions. *Phys. Lett. B*, 689:107–111, 2010.
- [Maa12] Axel Maas. Local and global gauge-fixing. *PoS, ConfinementX:034*, 2012.
- [Maa13] Axel Maas. Describing gauge bosons at zero and finite temperature. *Phys. Rept.*, 524:203–300, 2013.
- [Maa20] Axel Maas. Constraining the gauge-fixed Lagrangian in minimal Landau gauge. *SciPost Phys.*, 8(5):071, 2020.
- [Man79] S. Mandelstam. Approximation Scheme for QCD. *Phys.Rev.*, D20:3223, 1979.
- [MC14] Tereza Mendes and Attilio Cucchieri. Systematic Effects at Criticality for the SU(2)-Landau-Gauge Gluon Propagator. *PoS, LATTICE2013:456*, 2014.
- [MO87] J. E. Mandula and M. Ogilvie. The Gluon Is Massive: A Lattice Calculation of the Gluon Propagator in the Landau Gauge. *Phys. Lett. B*, 185:127–132, 1987.
- [MO90] Jeffrey E. Mandula and Michael Ogilvie. Efficient gauge fixing via overrelaxation. *Phys.Lett.*, B248:156–158, 1990.
- [MPvSS12] Axel Maas, Jan M. Pawłowski, Lorenz von Smekal, and Daniel Spielmann. The Gluon propagator close to criticality. *Phys. Rev. D*, 85:034037, 2012.
- [MR03] Pieter Maris and Craig D. Roberts. Dyson-Schwinger equations: A Tool for hadron physics. *Int. J. Mod. Phys. E*, 12:297–365, 2003.
- [MRS18a] J. Maelger, U. Reinosa, and J. Serreau. Perturbative study of the QCD phase diagram for heavy quarks at nonzero chemical potential: Two-loop corrections. *Phys. Rev. D*, 97(7):074027, 2018.
- [MRS18b] Jan Maelger, Urko Reinosa, and Julien Serreau. Universal aspects of the phase diagram of QCD with heavy quarks. *Phys. Rev. D*, 98(9):094020, 2018.
- [MRS20] J. Maelger, U. Reinosa, and J. Serreau. Localized rainbows in the QCD phase diagram. *Phys. Rev. D*, 101(1):014028, 2020.
- [MS14] Dhagash Mehta and Mario Schröck. Enumerating Copies in the First Gribov Region on the Lattice in up to four

- Dimensions. *Phys. Rev. D*, 89(9):094512, 2014.
- [MT99] Pieter Maris and Peter C. Tandy. Bethe-Salpeter study of vector meson masses and decay constants. *Phys.Rev.*, C60:055214, 1999.
- [MV20] Axel Maas and Milan Vujanović. More on the three-gluon vertex in SU(2) Yang-Mills theory in three and four dimensions. 2020. arXiv eprint: hep-lat/2006.08248.
- [Neu86] Herbert Neuberger. Nonperturbative BRS Invariance. *Phys.Lett.*, B175:69, 1986.
- [Neu87] Herbert Neuberger. Nonperturbative BRS Invariance and the Gribov Problem. *Phys.Lett.*, B183:337, 1987.
- [OFdPdM18] Orlando Oliveira, T. Frederico, W. de Paula, and J. P. B. C. de Melo. Exploring the Quark-Gluon Vertex with Slavnov-Taylor Identities and Lattice Simulations. *Eur. Phys. J. C*, 78(7):553, 2018.
- [Oji82] Izumi Ojima. Comments on Massive and Massless Yang-Mills Lagrangians With a Quartic Coupling of Faddeev-popov Ghosts. *Z.Phys.*, C13:173, 1982.
- [OS12] Orlando Oliveira and Paulo J. Silva. The lattice Landau gauge gluon propagator: lattice spacing and volume dependence. *Phys. Rev. D*, 86:114513, 2012.
- [OSSS19] Orlando Oliveira, Paulo J. Silva, Jon-Ivar Skullerud, and Andre Sternbeck. Quark propagator with two flavors of O(a)-improved Wilson fermions. *Phys. Rev. D*, 99(9):094506, 2019.
- [Pis02] Robert D. Pisarski. Notes on the deconfining phase transition. In *Cargese Summer School on QCD Perspectives on Hot and Dense Matter*, pages 353–384, 3 2002.
- [PJL90] C. Parrinello and G. Jona-Lasinio. A Modified Faddeev-Popov formula and the Gribov ambiguity. *Phys. Lett. B*, 251:175–180, 1990.
- [PLNvS04] Jan M. Pawłowski, Daniel F. Litim, Sergei Nedelko, and Lorenz von Smekal. Infrared behavior and fixed points in Landau gauge QCD. *Phys.Rev.Lett.*, 93:152002, 2004.
- [Pol73] H. David Politzer. Reliable Perturbative Results for Strong Interactions? *Phys.Rev.Lett.*, 30:1346–1349, 1973.
- [Pol78] Alexander M. Polyakov. Thermal Properties of Gauge Fields and Quark Liberation. *Phys. Lett. B*, 72:477–480, 1978.
- [PRS<sup>+</sup>17] Marcela Peláez, Urko Reinosa, Julien Serreau, Matthieu Tissier, and Nicolás Wschebor. Small parameters in infrared quantum chromodynamics. *Phys. Rev. D*, 96(11):114011, 2017.
- [PRS<sup>+</sup>21] Marcela Peláez, Urko Reinosa, Julien Serreau, Matthieu Tissier, and Nicolás Wschebor. Spontaneous chiral symmetry breaking in the massive Landau gauge: realistic running coupling. *Phys. Rev. D*, 103(9):094035, 2021.
- [PS79] Heinz Pagels and Saul Stokar. The Pion Decay Constant, Electromagnetic Form-Factor and Quark Electromagnetic Selfenergy in QCD. *Phys. Rev. D*, 20:2947, 1979.
- [PTW13] Marcela Peláez, Matthieu Tissier, and Nicolas Wschebor. Three-point correlation functions in Yang-Mills theory. *Phys.Rev.*, D88:125003, 2013.
- [PTW14] M. Peláez, M. Tissier, and N. Wschebor. Two-point correlation functions of QCD in the Landau gauge. *Phys.Rev.*, D90:065031, 2014.
- [PTW15] Marcela Peláez, Matthieu Tissier, and Nicolás Wschebor. Quark-gluon vertex from the Landau gauge Curci-Ferrari model. *Phys. Rev. D*, 92(4):045012, 2015.
- [PY80] R. D. Pisarski and L. G. Yaffe. The density of instantons at finite temperature. *Phys. Lett. B*, 97:110–112, 1980.
- [QR15] Markus Quandt and Hugo Reinhardt. A covariant variational approach to Yang-Mills Theory at finite temperatures. *Phys. Rev. D*, 92(2):025051, 2015.
- [QR17] Markus Quandt and Hugo Reinhardt. Covariant variational approach to Yang-Mills Theory: Thermodynamics. *Phys. Rev. D*, 96(5):054029, 2017.
- [QRH14] Markus Quandt, Hugo Reinhardt, and Jan Heffner. Covariant variational approach to Yang-Mills theory. *Phys. Rev. D*, 89(6):065037, 2014.
- [RBHW07] C.D. Roberts, M.S. Bhagwat, A. Holl, and S.V. Wright. Aspects of hadron physics. *Eur. Phys. J. ST*, 140:53–116, 2007.
- [Rei20] Urko Reinosa. Perturbative aspects of the deconfinement transition – Physics beyond the Faddeev-Popov model. Habilitation thesis, 2020. arXiv eprint: hep-th/2009.04933.
- [Rob20] Craig D Roberts. Empirical Consequences of Emergent Mass. *Symmetry*, 12(9):1468, 2020.
- [RST15] Urko Reinosa, Julien Serreau, and Matthieu Tissier. Perturbative study of the QCD phase diagram for heavy quarks at nonzero chemical potential. *Phys. Rev. D*, 92:025021, 2015.
- [RSTT17] U. Reinosa, J. Serreau, M. Tissier, and A. Tresmontant. Yang-Mills correlators across the deconfinement phase transition. *Phys. Rev. D*, 95(4):045014, 2017.
- [RSTT21] Urko Reinosa, Julien Serreau, Rodrigo Carmo Terin, and Matthieu Tissier. Symmetry restoration and the gluon mass in the Landau gauge. *SciPost Phys.*, 10:035, 2021.
- [RSTW14] U. Reinosa, J. Serreau, M. Tissier, and N. Wschebor. Yang-Mills correlators at finite temperature: A perturbative perspective. *Phys. Rev. D*, 89(10):105016, 2014.
- [RSTW15a] U. Reinosa, J. Serreau, M. Tissier, and N. Wschebor. Deconfinement transition in SU(2) Yang-Mills theory: A two-loop study. *Phys.Rev.*, D91(4):045035, 2015.
- [RSTW15b] U. Reinosa, J. Serreau, M. Tissier, and N. Wschebor. Deconfinement transition in SU(N) theories from perturbation theory. *Phys. Lett. B*, 742:61–68, 2015.
- [RSTW16] U. Reinosa, J. Serreau, M. Tissier, and N. Wschebor. Two-loop study of the deconfinement transition in Yang-Mills theories: SU(3) and beyond. *Phys. Rev. D*, 93(10):105002, 2016.
- [RSTW17] Urko Reinosa, Julien Serreau, Matthieu Tissier, and Nicolás Wschebor. How nonperturbative is the infrared regime of Landau gauge Yang-Mills correlators? *Phys. Rev. D*, 96(1):014005, 2017.
- [RW86] Andre Roberge and Nathan Weiss. Gauge Theories With Imaginary Chemical Potential and the Phases of {QCD}.

*Nucl. Phys. B*, 275:734–745, 1986.

- [RW94] Craig D. Roberts and Anthony G. Williams. Dyson-Schwinger equations and their application to hadronic physics. *Prog. Part. Nucl. Phys.*, 33:477–575, 1994.
- [SAW15] Helios Sanchis-Alepuz and Richard Williams. Hadronic Observables from Dyson-Schwinger and Bethe-Salpeter equations. *J. Phys. Conf. Ser.*, 631(1):012064, 2015.
- [SBHK19] Yifan Song, Gordon Baym, Tetsuo Hatsuda, and Toru Kojo. Effective repulsion in dense quark matter from non-perturbative gluon exchange. *Phys. Rev. D*, 100(3):034018, 2019.
- [SBK<sup>+</sup>03] Jonivar I. Skullerud, Patrick O. Bowman, Ayse Kizilersu, Derek B. Leinweber, and Anthony G. Williams. Nonperturbative structure of the quark gluon vertex. *JHEP*, 0304:047, 2003.
- [SBK<sup>+</sup>05] Jon-Ivar Skullerud, Patrick O. Bowman, Ayse Kizilersu, Derek B. Leinweber, and Anthony G. Williams. Quark-gluon vertex in arbitrary kinematics. *Nucl.Phys.Proc.Suppl.*, 141:244–249, 2005.
- [SBK<sup>+</sup>17] Andre Sternbeck, Paul-Hermann Balduf, Ayse Kizilersu, Orlando Oliveira, Paulo J. Silva, Jon-Ivar Skullerud, and Anthony G. Williams. Triple-gluon and quark-gluon vertex from lattice QCD in Landau gauge. *PoS, LATTICE2016:349*, 2017.
- [SC18] Fabio Siringo and Giorgio Comitini. Gluon propagator in linear covariant  $R\xi$  gauges. *Phys. Rev. D*, 98(3):034023, 2018.
- [SC21] Fabio Siringo and Giorgio Comitini. Thermal extension of the screened massive expansion in the Landau gauge. 2021. arXiv eprint: hep-th/2101.08341.
- [Sch99] Martin Schaden. Equivariant gauge fixing of SU(2) lattice gauge theory. *Phys. Rev. D*, 59:014508, 1999.
- [Sco16] Luigi Scorzato. The Lefschetz thimble and the sign problem. *PoS, LATTICE2015:016*, 2016.
- [SDPvS13] Dominik Smith, Adrian Dumitru, Robert Pisarski, and Lorenz von Smekal. Effective potential for SU(2) Polyakov loops and Wilson loop eigenvalues. *Phys. Rev. D*, 88(5):054020, 2013.
- [Ser20] Julien Serreau. The massive gluon and the massless pion. *PoS, LC2019:080*, 2020.
- [Sex14] Dénes Sexty. New algorithms for finite density QCD. *PoS, LATTICE2014:016*, 2014.
- [SIMPS05] A. Sternbeck, E. M. Ilgenfritz, M. Muller-Preussker, and A. Schiller. Towards the infrared limit in SU(3) Landau gauge lattice gluodynamics. *Phys. Rev. D*, 72:014507, 2005.
- [Sin78] I.M. Singer. Some Remarks on the Gribov Ambiguity. *Commun.Math.Phys.*, 60:7–12, 1978.
- [Sir15a] Fabio Siringo. Perturbation theory of non-perturbative QCD. 2015. arXiv eprint: hep-ph/1507.05543.
- [Sir15b] Fabio Siringo. Perturbative study of Yang-Mills theory in the infrared. 2015. arXiv eprint: hep-ph/1509.05891.
- [Sir16a] Fabio Siringo. Analytic structure of QCD propagators in Minkowski space. *Phys. Rev. D*, 94(11):114036, 2016.
- [Sir16b] Fabio Siringo. Analytical study of Yang–Mills theory in the infrared from first principles. *Nucl. Phys. B*, 907:572–596, 2016.
- [Sir17] Fabio Siringo. Quasigluon lifetime and confinement from first principles. *Phys. Rev. D*, 96(11):114020, 2017.
- [Sir19a] Fabio Siringo. Calculation of the nonperturbative strong coupling from first principles. *Phys. Rev. D*, 100(7):074014, 2019.
- [Sir19b] Fabio Siringo. Yang-Mills ghost propagator in linear covariant gauges. *Phys. Rev. D*, 99(9):094024, 2019.
- [SK02] Jonivar Skullerud and Ayse Kizilersu. Quark gluon vertex from lattice QCD. *JHEP*, 0209:013, 2002.
- [SK19] Daiki Suenaga and Toru Kojo. Gluon propagator in two-color dense QCD: Massive Yang-Mills approach at one-loop. *Phys. Rev. D*, 100(7):076017, 2019.
- [SKB<sup>+</sup>04] J.I. Skullerud, A. Kizilersu, P.O. Bowman, D.B. Leinweber, and A.G. Williams. Looking inside the quark-gluon vertex. *Nucl.Phys.Proc.Suppl.*, 128:117–124, 2004.
- [SLR06] W. Schleifenbaum, M. Leder, and H. Reinhardt. Infrared analysis of propagators and vertices of Yang-Mills theory in Landau and Coulomb gauge. *Phys. Rev. D*, 73:125019, 2006.
- [SMMPvS12] Andre Sternbeck, Kim Maltman, Michael Muller-Preussker, and Lorenz von Smekal. Determination of LambdaMS from the gluon and ghost propagators in Landau gauge. *PoS, LATTICE2012:243*, 2012.
- [Smo82] N.V. Smolyakov. Furry Theorem for Nonabelian Gauge Lagrangians. *Theor. Math. Phys.*, 50:225–228, 1982.
- [SO10] Paulo J. Silva and Orlando Oliveira. Unquenching the Landau Gauge Lattice Propagators and the Gribov Problem. *PoS, LATTICE2010:287*, 2010.
- [SO16] P. J. Silva and O. Oliveira. Gluon Dynamics, Center Symmetry and the deconfinement phase transition in SU(3) pure Yang-Mills theory. *Phys. Rev. D*, 93(11):114509, 2016.
- [SOBC14] P. J. Silva, O. Oliveira, P. Bicudo, and N. Cardoso. Gluon screening mass at finite temperature from the Landau gauge gluon propagator in lattice QCD. *Phys. Rev. D*, 89(7):074503, 2014.
- [SR12] Chihiro Sasaki and Krzysztof Redlich. An Effective gluon potential and hybrid approach to Yang-Mills thermodynamics. *Phys. Rev. D*, 86:014007, 2012.
- [ST12] J. Serreau and M. Tissier. Lifting the Gribov ambiguity in Yang-Mills theories. *Phys.Lett.*, B712:97–103, 2012.
- [Ste06] Andre Sternbeck. The Infrared behavior of lattice QCD Green’s functions. 2006. arXiv eprint: hep-lat/0609016.
- [STT14] Julien Serreau, Matthieu Tissier, and Andréas Tresmontant. Covariant gauges without Gribov ambiguities in Yang-Mills theories. *Phys. Rev. D*, 89:125019, 2014.
- [STT15] Julien Serreau, Matthieu Tissier, and Andréas Tresmontant. Influence of Gribov ambiguities in a class of nonlinear covariant gauges. *Phys. Rev. D*, 92:105003, 2015.
- [Sve86] Benjamin Svetitsky. Symmetry Aspects of Finite Temperature Confinement Transitions. *Phys. Rept.*, 132:1–53, 1986.
- [SZ14] Martin Schaden and Daniel Zwanziger. BRST Cohomology and Physical Space of the GZ Model. 2014. arXiv eprint: hep-ph/1412.4823.
- [Tay71] J.C. Taylor. Ward Identities and Charge Renormalization of the Yang-Mills Field. *Nucl.Phys.*, B33:436–444, 1971.
- [tH74] Gerard ’t Hooft. A Two-Dimensional Model for Mesons. *Nucl. Phys. B*, 75:461–470, 1974.

- [Tis18] Matthieu Tissier. Gribov copies, avalanches and dynamic generation of a gluon mass. *Phys. Lett. B*, 784:146–150, 2018.
- [TW09] Matthieu Tissier and Nicolas Wschebor. Gauged supersymmetries in Yang-Mills theory. *Phys.Rev.*, D79:065008, 2009.
- [TW10] Matthieu Tissier and Nicolas Wschebor. Infrared propagators of Yang-Mills theory from perturbation theory. *Phys.Rev.*, D82:101701, 2010.
- [TW11] Matthieu Tissier and Nicolas Wschebor. An Infrared Safe perturbative approach to Yang-Mills correlators. *Phys.Rev.*, D84:045018, 2011.
- [Tyu75] I.V. Tyutin. Gauge Invariance in Field Theory and Statistical Physics in Operator Formalism. 1975. LEBEDEV-75-39. arXiv eprint: hep-th/0812.0580.
- [vB92] Pierre van Baal. More (thoughts on) Gribov copies. *Nucl.Phys.*, B369:259–275, 1992.
- [VERST21] Duijje Maria Van Egmond, Urko Reinosa, Julien Serreau, and Matthieu Tissier. A novel background field approach to the confinement-deconfinement transition. 2021. arXiv eprint: hep-ph/2104.08974.
- [vSAH97] Lorenz von Smekal, Reinhard Alkofer, and Andreas Hauck. The Infrared behavior of gluon and ghost propagators in Landau gauge QCD. *Phys.Rev.Lett.*, 79:3591–3594, 1997.
- [vSGW08] Lorenz von Smekal, Marco Ghiotti, and Anthony G. Williams. Decontracted double BRST on the lattice. *Phys. Rev. D*, 78:085016, 2008.
- [VZ12] N. Vandersickel and Daniel Zwanziger. The Gribov problem and QCD dynamics. *Phys. Rept.*, 520:175–251, 2012.
- [Web12] Axel Weber. Epsilon Expansion for Infrared Yang-Mills theory in Landau Gauge. *Phys. Rev. D*, 85:125005, 2012.
- [Wei81] Nathan Weiss. The Effective Potential for the Order Parameter of Gauge Theories at Finite Temperature. *Phys. Rev. D*, 24:475, 1981.
- [Wei95] Steven Weinberg. *The quantum theory of fields. Vol. 1: Foundations*. Cambridge University Press, 1995.
- [Wei96] Steven Weinberg. *The quantum theory of fields. Vol. 2: Modern applications*. Cambridge University Press, 1996.
- [Wil80] Kenneth G. Wilson. *Monte-Carlo Calculations for the Lattice Gauge Theory*, pages 363–402. Springer US, Boston, MA, 1980.
- [Wit79] Edward Witten. Baryons in the  $1/n$  Expansion. *Nucl. Phys. B*, 160:57–115, 1979.
- [Wsc08] Nicolas Wschebor. Some non-renormalization theorems in Curci-Ferrari model. *Int.J.Mod.Phys.*, A23:2961–2973, 2008.
- [Ynd95] F. J. Yndurain. Limits on the mass of the gluon. *Phys. Lett. B*, 345:524–526, 1995.
- [Z<sup>+</sup>20] P. A. Zyla et al. Review of Particle Physics. *PTEP*, 2020(8):083C01, 2020.
- [ZBDS<sup>+</sup>19] S. Zafeiropoulos, P. Boucaud, F. De Soto, J. Rodríguez-Quintero, and J. Segovia. Strong Running Coupling from the Gauge Sector of Domain Wall Lattice QCD with Physical Quark Masses. *Phys. Rev. Lett.*, 122(16):162002, 2019.
- [ZJ75] Jean Zinn-Justin. Renormalization of Gauge Theories. *Lect. Notes Phys.*, 37:1–39, 1975.
- [Zwa89] D. Zwanziger. Local and Renormalizable Action From the Gribov Horizon. *Nucl.Phys.*, B323:513–544, 1989.
- [Zwa90] Daniel Zwanziger. Quantization of Gauge Fields, Classical Gauge Invariance and Gluon Confinement. *Nucl. Phys. B*, 345:461–471, 1990.
- [Zwa94] Daniel Zwanziger. Fundamental modular region, Boltzmann factor and area law in lattice gauge theory. *Nucl.Phys.*, B412:657–730, 1994.